Aus dem Bereich Immunphysiologie
Theoretische Medizin und Biowissenschaften bzw. Klinische Medizin
der Medizinischen Fakultät
der Universität des Saarlandes, Homburg/Saar

Alterations in the Composition of Lymph Node Stromal Cells Under Nutritional Challenge

Dissertation zur Erlangung des Grades eines Doktors der Medizin
der Medizinischen Fakultät
der UNIVERSITÄT DES SAARLANDES
2018

vorgelegt von:Niklas Klein
geb. am: 31.01.1992 in Trier

„Je suis de ceux qui pensent que la science est d'une grande beauté. Un scientifique dans son laboratoire est non seulement un technicien: il est aussi un enfant placé devant des phénomènes naturels qui l'impressionnent comme des contes de fées.“

- Prof. Dr. Marie Skłodowska-Curie

Index of contents

1. Abbreviations

ACC = acetyl-CoA carboxylase

AMPK = 5'adenosin monophosphate-activated protein kinase

APC = antigen presenting cell

Bcl-2 = B-cell CLL /lymphoma 2

BEC = blood endothelial cell

CD = cluster of differentiation

cDNA = complementary desoxyribonucleic acid

DAPI = 4'6-diamidin-2-phenylindol

DC = dendritic cell

DIO = diet induced obesity

DN = double negative cell

DNA = desoxyribonucleic acid

dsDNA = double stranded desoxyribonucleic acid

EDTA = ethyldiamintetraacetic acid

ERK1/2 = extracellular signal-regulated kinases 1/2

FACS = fluorescence assisted cell sorting

FBS = fetal bovine serum

FDC = follicular dendritic cell

FoxO1 = forkhead box O1

FRC = fibroblastic reticular cell

FSC = forward scatter

GAPDH = glyceraldehyde 3-phopshatase dehydrogenase

GLUT = glucose transporter

Grb2 = growth factor receptor-bound protein 2

HEPES = (4-(2-hydroxyethyl)-1-piperazineethanesulfonic acid)

HEV = high endothelial venule

ICAM-1 = intercellular adhesion molecule 1

IFN-γ = interferon-γ

IL-2 = interleukin-2

IL-4 = interleukin-4

IRS = insulin receptor substrate

JAK = Janus kinase

LEC = lymphatic endothelial cell

LepR = leptin receptor

LPS = lipopolysaccharide

Lti = lymphoid tissue inducer cells

LtO = lymphoid tissue organiser cell

MACS = magnetic cell sorting

MALT = mucosa associated lymphatic tissue

MAPK = mitogen-activated protein kinase

MHC = major histocompatibilty complex

MRC = marginal zone reticular cell

mRNA = messenger ribonucleic acid

MSC = mesenchymal stem cells

mTOR = mammalian target of rapamycin

NSCLC = non-small-cell lung cancer

P/S = penicillin/streptomycin

PBS = phosphate buffered saline

PCR = polymerase chain reaction

PDE3B = phosphodiesterase 3B

PECAM-1 = platelet/endothelial cell adhesion molecule-1

PI = propidium iodide

PI3K = phosphatidylinositol 3 kinase

POMC = propiomelanocortin

PTP1B = protein tyrosine phosphatase 1B

RFN = reticular fiber network

RNA = ribonucleic acid

SDS = sodium dodecyl sulfate

SG-buffer = Sammelgel buffer

SHP2 = SH2-containing protein tyrosin phosphatase 2

SLO = secondary lymphoid organ

SMA = smooth muscle actin

SOCS = suppressor of cytokine signaling

SSC = sideward scatter

ssDNA = single stranded desoxyribonucleic acid

STAT = signal transducers and activators of transcription

T-bet = T-box transcription factor TBX21

TAE-buffer = tris-acetat EDTA buffer

TBE-Buffer = tris-borat EDTA buffer

TBS = tris-buffered saline

TBST = tris-buffered saline tween

TCR = T-cell receptor

TEMED = tetramethylethylendiamin

TG-buffer = Trenngel buffer

Th1 = type-1-t-helper-cell

Th2 = type-2-t-helper-cell

TLR = toll-like receptor

TRC = T-cell zone fibroblastic reticular cell

Treg = regulatory T-cell

VLA2 = very late antigen 2

2. Abstract

Lymph nodes belong to the main actors in adaptive immunity, as they accommodate the cells of our acquired immunology, namely dendritic cells, T-cells and B-cells. Moreover they are its infrastructural and functional junction as immune cells, antigen and cytokines permanently flow through these secondary lymphatic organs. Therefore they are in need of cells which support as well as maintain the lymph node's structure and possess the ability to provide a proper immune response. This task is mainly fulfilled by so called fibroblastic reticular cells, which belong, next to lymphatic endothelial cells and blood endothelial cells, to mesenchymal stromal cells and are the main focus of research. This work focuses on how stromal cells in lymph nodes are influenced by diet. Since famine is not just an important issue in third world countries, but also in western countries, special diets and malnutrition caused by cancer are an every day epiphany. Hence it is an interesting question how diets impact the lymph node's cellular structure.

We have established an experimental system to study the effect of acute starvation in secondary lymphoid organs and to follow the alterations associated with the regression phase when food is again accessible. During short-term starvation and regression phase stromal cell populations decreased in lymph nodes. This change reflected the decrease of cell populations in absolute numbers, while the proportions in the frequency of stromal subpopulations remained the same. Additionally, the regression phase was associated with decreased podoplanin expression in stromal cells, in particular in FRCs. To identify possible mechanism for the decrease in stromal cell populations, we addressed leptin-leptin receptor pathway in SLOs. Indeed, we have identified leptin receptor variants in fibroblastic reticular cells (FRCs) where Western blot analysis revealed that next to an unfunctional knock-out receptor there is also the long functional LepRb isoform expressed. Addition of leptin during starvation is suspected to partially protect cell loss in lymph nodes. Yet more details about fibroblastic reticular cells' physiology have to be revealed in future studies regarding leptin signaling in lymph nodes as well as the return to status quo after the beginning of the regression phase.

Da Lymphknoten die angepasstesten Zellen des erworbenen Immunsystems beherbergen, nämlich dendritische Zellen, T-Zellen und B-Zellen, gehören sie zu den wichtigsten Schauplätzen der erworbenen Immunität. Sie sind als infrastrukturelle und funktionelle Knotenpunkte im immunologischen Geschehen zu bewerten: Antigene und Cytokine kommen ständig in Kontakt mit diesen sekundären lymphatischen Organen, daher werden spezialisierte Zellen benötigt, welche die Struktur des Lymphknotens erhalten, sowie die Befähigung besitzen, eine adäquate Immunantwort zu unterstützen. Diese Aufgabe wird vor Allem durch sogenannte fibroblastische retikuläre Zellen übernommen. Diese Zellen gehören neben lymphatischen Endothelzellen und Blutendothelzellen zu den sogenannten mesenchymalen Stromazellen. Auf sie wird in dieser Arbeit das Hauptaugenmerk gelegt, wobei der Fokus auf dem Einfluss bestimmter Ernährungszustände auf die im Lymphknoten ansässigen Stromazellen liegt. Entgegen der populären Meinung, Mangel- und Unterernährung sei nur eine Problematik die Drittweltländer betrifft, lässt sich kundtun, dass beide Formen durch spezielle Diäten oder malignomassoziierte Malnutrition auch als ein Phänomen westlicher Kulturkreise häufig angetroffen werden können. Daher ist die Klärung der Frage, inwiefern diese Ernährungsformen die Struktur von Lymphknoten auf zellulärer Ebene verändern von höchster Wichtigkeit.

Wir haben einen experimentellen Aufbau entwickelt mit dem wir die Auswirkungen, die eine akute Hungerphase sowie die darauffolgende Erholungsphase bei Renutrition auf den Lymphknoten hat, erforschen konnten. Während einer kurzfristigen Hungerphase und der darauffolgenden Erholung konnte beobachtet werden, dass die Populationen der verschiedenen Stromazellen untergehen. Dies zeigte sich in dem Abfall der absoluten Zellzahlen im Lymphknoten, wohingegen die Zusammensetzung der gesamten Stromazellpopulation unaffektiert blieb. Außerdem kam es in der Erholungsphase zu einer verminderten Podoplaninexpression der Stromazellen, insbesondere in FRC. Um einen möglichen Mechanismus für den Untergang von Stromazellpopulationen aufzudecken, untersuchten wir die Leptin-Leptinrezeptor Signalkaskade in SLO. Tatsächlich konnten wir veschiedene Varianten des Leptinrezeptors auf FRC feststellen: Western Blot Analysen ergaben, dass

neben einem knock-out-Rezeptor auch die lange, funktionstüchtige Isoform LepRb exprimiert wird. Die Zugabe von Leptin während der Hungerphase wird verdächtigt die Zellen im Lymphknoten teilweise vor zellulärem Untergang zu schützen. Es müssen jedoch noch weitere unklare Sachstände zu der Physiologie von FRC erörtert werden. Dazu gehört insbesondere die Signalkaskade des Leptinrezeptors und wann die Struktur des Lymphknotenstromas nach Beginn der Erholungsphase zum Status quo zurückkehrt.

3. Introduction

3.1 Characterization of the lymphatic system in general

To provide and ensure a proper function of the acquired immune system, lymph nodes are placed strategically in the whole body. Especially there where vessels build crossroads, one can find lymph nodes which in mammals finally drain towards the thoracic duct that discharges into the venous blood system. Lymph nodes are so called secondary lymphatic organs, often just called SLOs. In contrast to the primary lymphoid organs such as the thymus and the bone marrow, lymphocytes do not origin in SLOs, they migrate from their related primary lymphatic organ to the lymph node, MALT (mucosa associated lymphatic tissue, to which belong tonsills, Peyer's plaques, the Appendix vermiformis and all lymph follicles in mucosa) or spleen. Only non MALT lymph nodes are subject of this thesis. The lymph fluid, which passes all the lymphoid structures but the spleen, is a super filtrate of arterial blood that is first collected by lymph capillaries which begin cul-du-sac or as plexus and then drain towards the lymph nodes. As they reach the lymph node, they empty into the subcapsular zone that verges on the paracortical B-cell-zone which surrounds the cortical T-cell-zone. The T-cell-zone again encloses the medulla which faces towards the hilus and contains a high number of macrophages [196, 84, 117]. Lymph nodes all posses a characteristic structure, the scaffold of the lymph node is build by fibroblastic reticular cells that form an aqueduct-like system with their cell body extensions, which is crucial for the role of chemokine, dendritic cell, B- and T-cell transport through the lymph node. Since every T-cell only recognizes a specific antigen, it is crucial for the mounting of a immune response to ensure that they meet their related antigen presented by the dendritic cell in the lymph node, while they circulate between the secondary lymphoid organs [93, 107, 13, 14, 176, 26]. Marginal reticular cells in the subcapsular sinus and follicular dendritic cells (characterized by their surface markers gp38+, CD31-,ER-TR17-, CD35+ [32]) support B-cells via chemokines and provide survival factors for them such as APRIL and BAFF [32]. The structure of the B-cell-zone is different in primary and secondary follicles [107, 93, 100, 13, 153, 49, 71, 96]. Primary follicles only exist in lymph nodes which hadn't

encountered antigen yet and are characterized by a homogeneous dispersal of small lymphocytes. When first encountering an antigen by co-stimulation of T-helper-cells, germinal centers develop within the follicle. Secondary follicles posses a cortex of densely gathered emigrating and non-activated lymphocytes, which is asymmetrically formed around the follicle being smaller towards the T-cell-zone side. The germinal center is not as cell dense as the cortex, for it is build up by follicular dendritic cells, macrophages, B-cells, few T-helper-cells providing survival signals for positively selected B-cells and can again be subdivided under morphological aspects: a darker and a lighter region. In the darker region mitotic expansion of centroblasts, which have been stimulated by T-helper-cells, occurs after they moved there from the lighter region. The so-called somatic hypermutation of the genes encoding the V-region of the antigen receptor happens in this phase, resulting in stronger or weaker affinity for the corresponding antigen. Next to centroblasts, also centrocytes reexpressing the mutated surface markers appear and migrate to the basal lighter zone where they are being selected by antigen-presenting follicular dendritic cells and lots of centroblasts undergo apoptosis. The apoptotic bodies are then phagocyted by tingible-body macrophages. If positively selected they move towards the apical light zone in which they differentiate towards plasma cells or B-memory-cells and afterwards migrate out of the germinal center [59, 107]. Next to the B-cell-zone the T-cell-zone is located, which contains many high endothelial venules. The high endothelial venule allows cells via diapedesis to enter the lymph node from the blood system. Homing receptors on the T-cells and adressines on the endothel enable the possibility for hematopoetic cells to return to the lymph node [107]. The T-cell-zone is inhabited mostly by T-cells and dendritic cells. Upon inflammation, the lymph node increases in size as lymphocytes stream into the lymph node. Not just the number of cells changes in inflamed lymph node, but also its structure, known as lymph node remodeling: high endothelial venules proliferate as they reconstruct them, B-cell-follicles are enlarged, and the lymph node scaffold changes as stromal cells proliferate strongly and remodel the structure via their extracellular matrix production. When being infected by Lymphocytic Choriomeningitis Virus, FRCs are being attacked by cytotoxic T-lymphocytes as the FRCs are infected by the virus. The outcome of this is due to reduced FRC numbers: Their network is disrupted and

recruitment, survival and migration of lymphocytes is deranged, resulting in reduced immune defense [93, 206]. B-Cells develop in the bone marrow and each developmental stage of these cells can be identified by their surface markers. After they matured and became immune competent, they leave the bone marrow for the periphery. T-cells present in the thymus. The major part of T-cells though (ca. 95% to 98%) [107, 149], is being killed by apoptosis due to central tolerance. By somatic rearrangement of the genes which code for the recognition domain, both B- and T-cells gain a formidable variety of receptor variants which recognize a vast spectrum of antigen specificity. All lymphocytes carrying genetically and phenotypically the same receptor are called clones and they descend from one progenitor cell [107]. An important actor of the acquired immune system is the so called dendritic cell (DC). The first presentation of antigen after subcutaneous injection is mediated by lymph node resident DCs, a second antigen presentation happens 8 to 12h after injection by DCs which migrated from the periphery after antigen contact [172, 80, 81]. Sixt et al. have shown that around 60% of the resident CD11c positive DCs in the lymph node and 80% of the myeloid resident lymph node CD11b positive DCs of the T-cell area are directly connected to the fibers of the reticular network [172]. Surprisingly, mature dendritic cells that migrated to the lymph node are only in 19% associated with the reticular fiber network [172]. In order to recognize an antigen, B- and T-cells carry a different type of antigen receptor on their surface, B-cells posses an immune globulin as antigen receptor which is able to bind the antigen as a whole, whereas the T-cell-receptor is only capable of binding peptide fragments, whose precursor protein has already been processed in a cell and presented by MHC class II or MHC class I [107].

“The T-cell receptor (TCR) consists of a disulfide-linked heterodimer of the highly variable α and β chains expressed at the cell membrane as a complex with the invariant CD3 chains. T-cells carrying this type of receptor are often called α:β T cells. An alternative receptor made up of variable γ and δ chains is expressed with CD3 on a subset of T cells. Both of these receptors are expressed with a disulfide-linked homodimer of ζ chains.“ (Exact quote from Janeway et al.)[82]

T-cells can be subdivided generally in two classes: CD4+ T-helper-cells (which can further be distinguished into at least these four important subtypes: T1-helper-cells, T2-helper-cells, T17-helper-cells and regulatory T-cells) and CD8+ cytotoxic T-cells. Although being closely related, these cells vary in the composition of their surface markers and other translated proteins and consequently in their role in immunobiology from each other [107]. The defining surface molecules of the two classes are a co-receptor of the T-cell-receptor, only binding specifically to either MHC-class-I or MHC-class-II, namely CD4 binding specifically to MHC-class-II and CD8 binding specifically to MHC-class-I. While MHC-class-I is present on all cells with a nucleus, presenting processed protein, MHC-class-II is only present on B-cells, dendritic cells and macrophages. MHC-class-II is loaded in the endosome after phagocytosis of an antigen [149]. This explains the different roles of the T-lymphocytes and immunoactive cells. Whereas MHC-class-I triggers an immune response when presenting an antigen of its virus infected host cell or protein of an altered host cell and thus signaling for a cytotoxic T-cell [149]. Embryonic lymph node development is largely carried by lymphoid tissue inducer cells (LTi-cells) and stromal cells. Stromal cells are believed to be the first local cells in lymph node development, upon stimulation by retinoic acid they produce and release CXCL13 that recruit not just lymphoid tissue inducer cells but also their precursors [93, 58, 174]. When the present stromal cells' lymphotoxin beta receptors are stimulated by the lymphoid tissue inducer cells' lymphotoxin (LT)αβ, they differentiate into lymphoid tissue organizer cells which in addition to CXCL13 produce CCL21, CCL19, (VCAM)-1, (MadCAM)-1, VEGF-C, IL-17 and TRANCE that promote vascularization [203, 192, 93, 88]. Furthermore, more lymphoid tissue inducer cells and precursors are recruited to the place of action, providing further survival signals for them. The attracted lymphoid tissue inducer cells and the pre-lymphoid tissue inducer cells create a positive enhancement concerning the stimulation by mesenchymal stromal cells [192, *93*].

3.1.1 Characterization of fibroblastic reticular cells

Fibroblastic reticular cells (FRCs) are stromal cells which belong to mesenchymal stromal cells to which also marginal reticular cells (MRC) of the subcapsular sinus of the lymph node are counted [32]. FRCs inhabit secondary lymphoid organs [5] and their morphology covers fusiform, elongated and stellate phenotypes, which however is dependent on their location inside the lymph node [5, 40,48]. Cortical FRCs, situated next to the subcapsular sinus, posses a polarized or fusiform structure (some of those FRCs are orientated parallel to the sinus, others are oriented vertical to the sinus, having more of a polarized structure and reaching from the sinus far into the cortex) [5, 48]. T-cell-zone Fibroblastic Reticular Cells (TRCs) and Follicular Dendritic Cells (FDCs) are of a three dimensional stellate morphology [15, 13, 48, 38]. Fibroblastic reticular cells produce extracellular matrix, consisting of molecules such as ER-TR7 and collagens, which generates a three dimensional scaffold that ranges from the subcapsular and paracortical sinus to the blood vessels [28, 87, 191, 189, 71, 91, 7, 135]. This scaffold provides space for the migration of lymphocytes, dendritic cells, and also the conduit system that channels soluble molecules from the afferent lymph towards the high endothelial venules (see figure 2)[152, 26, 114, 172]. This cysternic system is called reticular fiber network by some authors [5], as it consists of cellular tails and both, fibrillar and collagen strands [48, 120, 134]. The reticular fiber network is structured as follows: The reticular fiber network consists of a collagen type 1 strand, being enveloped by basement membrane molecules, such as collagen type 4, laminins, perlecan, proteoglycan, and nidogen, which are again covered by smooth muscle actin and desmin [172]. Different than expected, the reticular fiber network is not entirely wrapped by fibroblastic reticular cells, even though this is the main cell type that covers it. Around 10% of the reticular fiber network is covered by either interdigitating DCs or macrophages to provide those cells with the molecules transported within [172, 77]. The reticular fiber network doesn't seem to be exclusively bound to the lymph node, Nolte et al. suggest that it is also abundant in the spleen where it fulfills similar tasks [172, 133]. To attract T-cells and dendritic cells which move along the reticular fiber network, fibroblastic reticular cells express CCL19, CCL21 (which both bind to their receptor CCR7 and CXCR4 on

T-cells) and IL7 [5, 9, 87, 13, 200, 114, 109, 13, 10, 201, 26]. As mentioned above, also dendritic cells move along the reticular network. After they enter the lymph node, they move from the subcapsular sinus towards the parenchyma where they connect to the reticular fiber network, to increase the odds to present a matching antigen to a T-cell. After all, the dendritic cell movement along the stromal surface is dependent on CLEC-2 binding to gp38 [26, 13, 162, 1, 2, 5]. By developing tubular and cysternic intracellular structures, FRCs create a network of tunnels which is connected to the conduit system and the abluminal cell surface by numerous stomata, ensuring an exchange between the conduit system and the interstitial space [5, 48]. FRCs which verge on each other are separated by space of ca. 20nm. The intra-cytoplasmic reticular system of these FRCs opens into this space via small orifices. The intra-cytoplasmic reticular system is suspected to be closely linked to the conduit system. FRCs located close to the subcapsular sinus collect antigen as well as lipids, cytokines, neuropeptides, microbial products and transport it through their conduit towards high endothelial venules [5, 48, 8]. HEVs are usually surrounded by FRCs, via CXCL12, CCL19 and CCL21, FRCs interact with lymphocytes that are located in the vessel, triggering their migration through the HEV [48, 62, 44, 114, 10, 188, 167]. Some FRCs not just envelop high endothelial venules with thin cytoplasmatic extensions and are connected to the reticular FRC network, but they also envelop vessels of the fenestrated type in the medulla (see figure 1) [48]. Apart from that, they also provide survival signals for T-lymphocytes and are able to present antigen in respect of self tolerance and limit autoreactivity by T-lymphocytes, hence being of utmost importance in immunologic events in contrast of former opinion [93, *98,* 130, 67, 113, 43, 61]. FRCs are believed to origin from mesenchymal precursor cells [93]. Stromal cells in the immunological sense are all cells that are not of hematopoetic origin and lack therefore exclusive leukocytic markers such as CD45. It is common to subdivide the stromal cells in murine lymph node into four populations, even if a more delicate subdivision is possible, but in case of our studies not relevant. The classification into four specimens is made by the help of the two surface markers CD31 and gp38. Both, blood endothelial cells, constructing ordinary blood vessels, high endothelial venules and lymphatic endothelial cells express CD31 also known as EndoCAM, whereas the double-negative fraction and FRCs are CD31 negative.

On the other hand, podoplanin (gp38) is expressed by only lymphatic endothelial cells and fibroblastic reticular cells, while double-negative cells as their name suggests and blood endothelial cells do not [32]. FRCs are also in possession of the intracellular marker ER-TR7 and CD140a [61], on which most of the authors are in agreement, while other intracellular markers are in discussion, such as VEGF, NOS2, IDO, INOS and RANKL, just to mention a selection which shows that FRC classification is still far from finite classification [5, 87, 172, 100, 32, 62, 63, 110, 166, 106, 78]. The composition of the stromal compartment is, as this study also shows, very dynamic. Fletcher at al. have shown that skin-draining and mesenteric lymph nodes have a significantly different composition of stromal cells, for mesenteric lymph nodes are less FRCs present than in skin-draining lymph nodes. In regard on the other stromal subsets however, no differences have been found. MRCs on the other hand appear in the FRC gate on flow cytometry also don't change in numbers making the difference exclusively for FRCs [62]. Under physiological conditions, the classic stromal cells, namely FRCs, LECs and BECs, carry Toll-like receptor 3 (TLR3) on their membrane, a receptor which binds and reacts to double-stranded RNA as it appears in many viruses, making it possible that they are able to react to viral infection. TLR7 and TLR8 are not expressed by either FRCs and LECs or BECs [61, 194]. Pericytes lack podoplanin on their surface, which is a classical FRC marker. They belong to the double negative cells. Marginal zone reticular cells in contrast do express gp38. They can only be differed from FRCs by their expression of MadCAM-1, CXCL13 and high levels of RANKL while FRCs in the T-cell-zone (TRCs) do not express above molecules but are positive for CD157 [5, 166, 110, 101, 124, 78]. The position of FDCs, who are resident in the B-cell-zone provide survival factors for B-cells such as BAFF, also express gp38 however can be distinguished from FRCs by their expression of CD35 [93, 16]. As mentioned above FRC and T-cell function are closely linked together since both provide survival signals for each other. Viral loss of FRCs also causes deterioration in antigen-specific T-cell priming and a loss in T-cells. This is due to the lack of IL-7, CCL19 and CCL21, which are produced by fibroblastic reticular cells to promote T-cell survival [5, 100, 160, 206, 26, 47]. Not only CD8+ T-cells interact with FRCs, also CD4+ T-cells interact with FRCs via MHC class II, since MHC II is produced by FRCs in low levels. The production of MHC II, which is

dependent on the PIV promoter region of CIITA, is increased during inflammation. Further evidence even suggests astonishingly, that MHC class II can even be transferred to fibroblastic reticular cells by dendritic cells via microsomes [26, 114, 56]. Apparently impairment of autoreactive T-cells by FRCs is also happening independently from antigen: freshly activated CD4+ and CD8+ T-cells are limited in their expansion by fibroblastic reticular cells, however in order to do so, a cell-cell-contact or at least aerial proximity between effector and receptor cells need to be established. The suppressive effect by FRCs is carried by inducible NO synthase (iNOS) [26, 106, 85, 166]. NO produced by fibroblastic reticular cells not only has suppressive effect on T-cells, apparently it is responsible for the genesis of CD4+ CD25+ Foxp3- regulatory T-cells (Tregs). But in order to do so, dendritic cells have to be present as depletion of DCs abolishes the ability of FRCs to induce Tregs [26, 2, 46, 131, 132]. It is believed that during inflammation stromal cells are recruited from mesenchymal stem cells, although this has not been unequivocally proven yet. Other than in steady state, mesenchymal stem cells appear in the blood in an ongoing inflammation and express adhesion molecules, suggesting that they are able to migrate from their place of origin to their destination to further differentiate [93, 20, 111, 125, 169, 156]. Another idea is that the FRC precursors originate directly from the lymph node, since there are also mesenchymal stromal cells present under physiological conditions [93, 169]. The last popular opinion includes the idea of stem cell recruitment from surrounding fat tissue, as it is possible to gather mesenchymal stromal cells from it, furthermore lymph nodes are usually embedded in fat tissue, thus, this idea has to be considered [93, 92, 144, 123, 21, 26]. The following differentiation of the mesenchymal stromal cells towards stromal cells triggered by lymphotoxin and TNF alpha is discussed in the field and remain to be elucidated in the future. [93, 138].

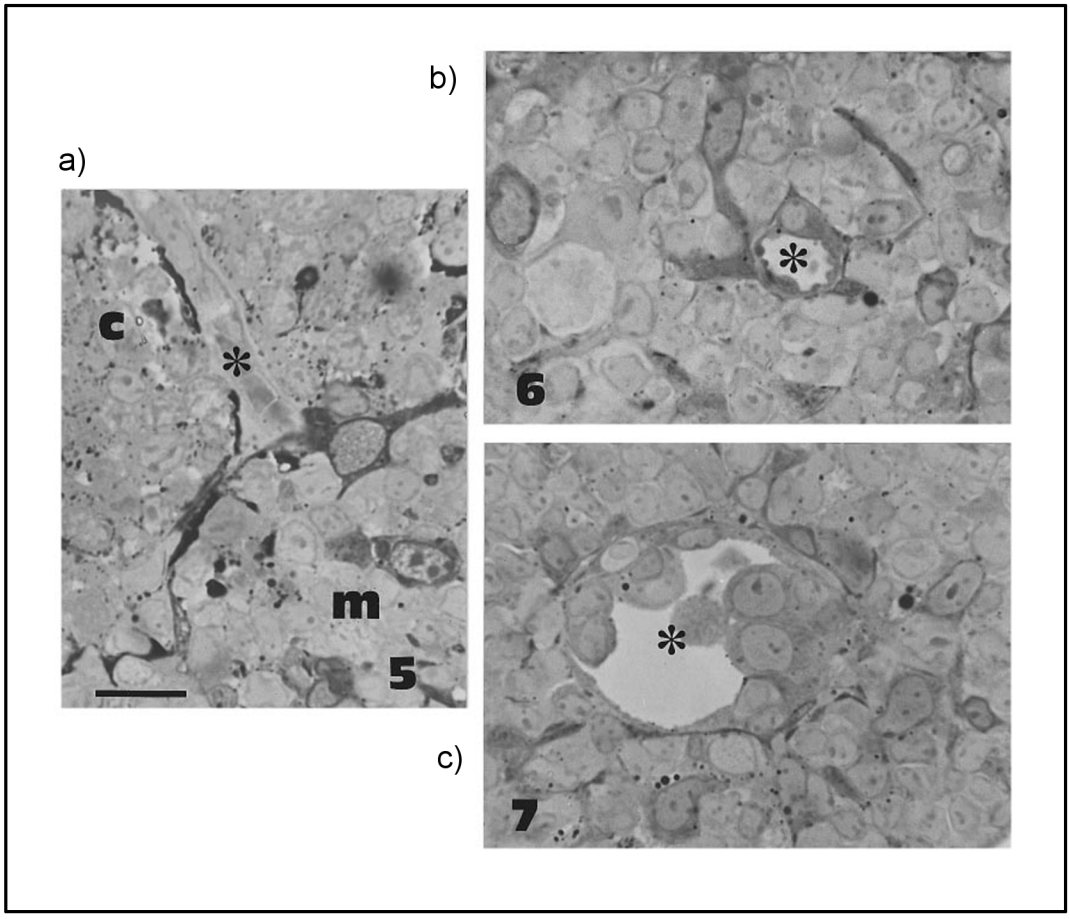

Figure 1: Display of lymph node structure via light microscopy: 1996, Crivellato et al. produced these light microscope images of lymph nodes. The samples have been fixated by using the zinc iodide-osmium method and are stained with toulidine blue. The bar represents a length of 15µm. FRCs can be identified in these exposures by their dark-grey coloring. These exposures show that FRCs which are resident in the medulla are of a stellate structure and posses 1 or 2 oval nuclei. The vessels (asterisk) shown in a) are ensheathed by FRC membranes, these membranes however do not ensheath the endothel cells continuously, creating a fenestrated hull for the vessel. Also fenestrated vessels (asterisk) are enveloped by cytoplasmic processes of FRCs (see b)). Next to fenestrated vessels, also high endothelial venules (asterisk) are wrapped by FRC structures (see c)).
(Figure by Crivellato et al. [48], rearranged by Niklas Klein)

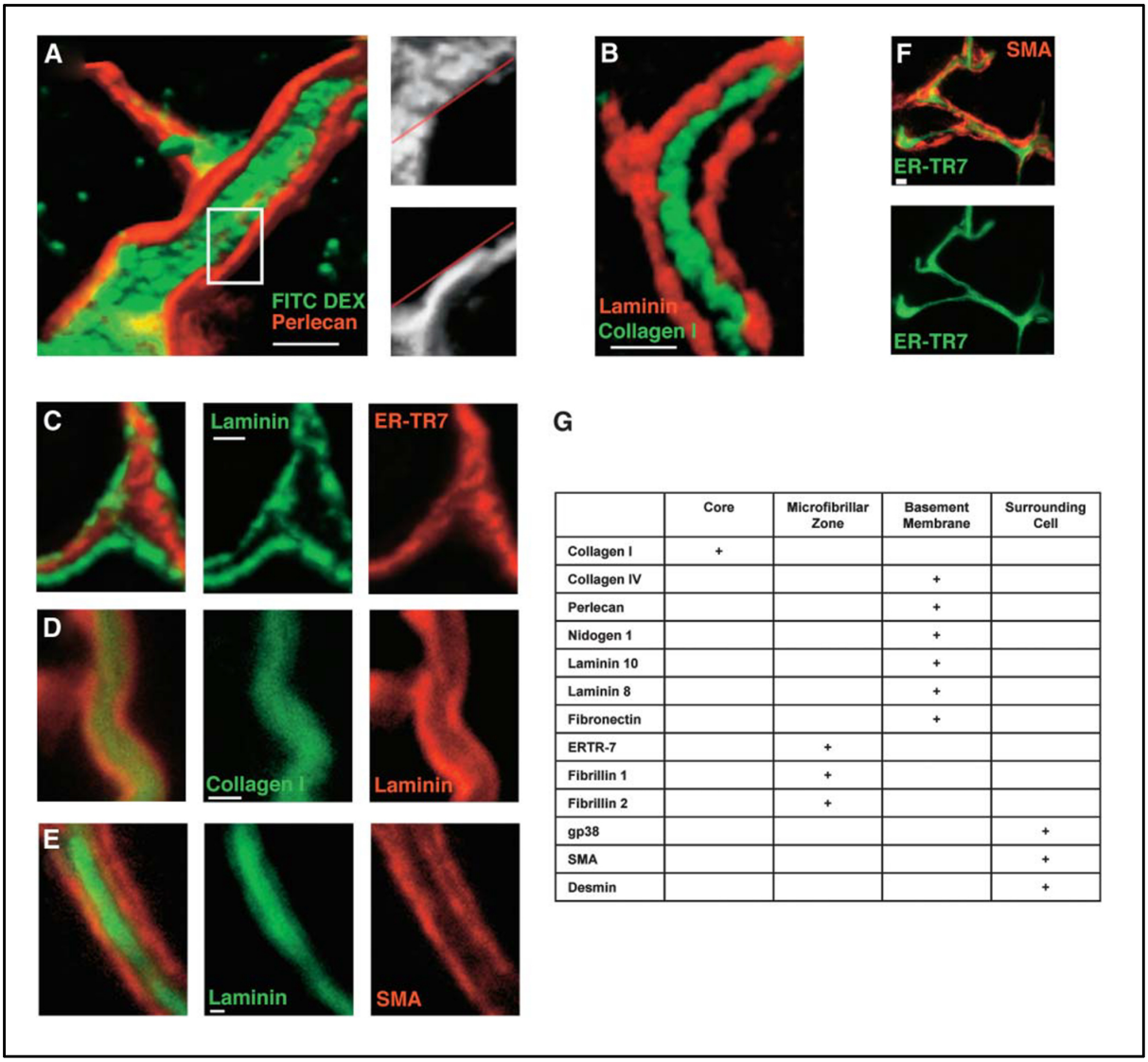

	Core	Microfibrillar Zone	Basement Membrane	Surrounding Cell
Collagen I	+			
Collagen IV			+	
Perlecan			+	
Nidogen 1			+	
Laminin 10			+	
Laminin 8			+	
Fibronectin			+	
ERTR-7		+		
Fibrillin 1		+		
Fibrillin 2		+		
gp38				+
SMA				+
Desmin				+

Figure 2: The three dimensional display of the conduit system of FRCs: This figure by Sixt et al. gives an excellent insight about how the reticular fiber network, or conduit system, looks like. It is a three dimensional reconstruction of an immune histochemical staining. The size bars measure 1µm. a) Shows a fiber in which 40kDa FITC-DEX (green) has been injected. One can clearly see that the lumen of the conduit is wrapped by the basement membrane molecule perlecan (red). The magnification box shows that perlecan does not overlap FITC-DEX, the red line marks the same static point in the upper and lower magnificated box. b) Shows a staining of pan-laminin and collagen 1 where one can see that the collagen 1 is surrounded by laminin. c) d) Also ER-TR7 antigen is ensheathing collagen 1. e) Reticular fibroblasts which express smooth muscle actin (SMA) wrap the basement membrane. f) Represents a double-staining for ER-TR7 and SMA. g) Reviews which molecules are present in which part of the reticular fiber network.
(Figure by Sixt et al. [172], rearranged by Niklas Klein.)

3.1.2 Characterization of lymphatic endothelial cells

Lymphatic endothelial cells, as their name suggests, build the lymphatic vessels, they origin from blood endothelial cells [195]. The vessels built by LECs transport the lymph fluid towards the lymph node and there the lymph fluid is spilled into the parenchyma, where it travels through the lymph node to reach again efferent lymphatic vessels in the medulla after the lymph fluid has been filtered through the paracortex and cortex [62, 117, 196]. Lymphatic endothelial cells are not just responsible for the transport of antigen towards the lymph node, they even seem to be able to enrich antigen under inflammatory conditions [32, 177]. CD31, EndoCAM or PECAM-1 is expressed not just on endothelial cells such as blood endothel or lymphatic endothel, but also on some macrophage subsets, granulocytes and platelets. It is thought to be crucial for angiogenesis, intercellular connections between endothelial cells and activation of leukocytic transendothelial migration [99]. Lymphatic endothelial cells have a special feature that is unique among all lymph node stromal cells: Those cells are the only stromal cells within the lymph node that express the melanocyte-associated enzyme tyrosinase. This is of high importance as this peripheral tissue antigen is recognized by certain T-cells which then have to go into apoptosis in order to prevent auto-immunity [61].

3.1.3 Characterization of blood endothelial cells

Blood endothelial cells (BECs), build up blood vessels and capillaries to which also high endothelial venules (HEV) belong that are specialized on the attraction of circulating naive T-cells and other immune cells [62, 117, 196]. In this work, blood endothelial cells present in the lymph node are characterized by the absence of CD45 and gp38 and presence of CD31.

3.2 Leptin and its receptors

3.2.1 Characterization of leptin

Leptin is a 16kDa heavy peptide hormone. It is mainly secreted by white adipocyte tissue and is most commonly known for its effects on the feeling of satiety, which takes place mostly but not exclusively in the hypothalamical region. Leptin is linked to secretion of hormones of the hypothalamus-hypophysis-adrenal axis. Moreover, it influences the reproductional behavior, angiogenesis, the hematopoetic system and also regulates the energy household through lipid and glucose metabolism [139, 74, 187, 52, 53, 202, 178, 64, 36, 168, 22]. Next to white adipocytes, leptin is also expressed in various other tissues, for instance lymphatic tissues, female sexual organs, such as placenta and ovary, but also in the pituary gland, skeletal muscle and immune cells, e.g. regulatory T-cells (Treg). As mentioned before, the hypothalamic region plays a crucial role in leptin signaling as leptin and its receptor are also expressed in this location, especially in the arcuate nucleus and ventrolateral hypothalamus where inhibition of fooduptake is mediated [139, 51, 202, 146, 145, 154]. The leptin level in blood is not constant, as it succumbs not just to a circadian rhythm, but is also dependent on other factors. It is secreted in a pulsatile mode influenced by calorie intake, namely high circulating leptin level in the condition of obesity and low levels in case of starvation. It also correlates in a linear manner with the amount of body fat [139, 50], as well as the gender: Levels of circulating leptin are higher in women [197, 76, 118]. Next to that, leptin levels are also changed under certain pathological conditions, such as reproductive diseases [39] and cardiovascular diseases [173, 193, 198, 150]. However, a high leptin level should result in a lower weight as its task is the reduction of food intake. However in obesity, higher leptin plasma levels over time lead to resistance against leptin. Various factors have been suspected to be in charge for central leptin resistance: The ongoing inflammation in obese individuals most certainly plays a crucial role, next to general factors such as autophagy and endoplasmic reticulum stress. Besides the disturbed leptin signaling in the hypothalamus mediated by inhibition via SOCS3 and PTP1B, there is an overall inhibition of the passage of leptin across the blood-brain barrier.

Moreover, there is a dysfunction in the skeletal muscle mitochondria that results the accumulation of lipids in the sceletal muscle cell. Normally, leptin has the ability to decrease the intramyocellular lipid level by induction of the mitochondrial fatty acid β-oxidation, in which skeletal muscle 5'adenosin monophosphate-activated protein kinase (AMPK) is believed to play a crucial role [139, 121, 128, 83, 178, 190, 165, 126, 75]. In contrast, Tanaka et al. generated transgenic skinny mice overexpressing leptin in the liver, which results in a high plasma leptin level that resembles obese humans. However, as in obese humans or mice with diet induced obesity (DIO), the leptin tolerance increases. This does not happen in the transgenic mice in which leptin stays metabolically active. Furthermore Tanaka et al. state that transgenic skinny mice have an increased sensitivity towards leptin, which augments skeletal muscle and liver insulin receptor signaling caused by chronic activity of AMPK, and thereby enhanced phosphorylation of acetyl CoA carboxylase (ACC) a target of AMPK, in skeletal muscle [178]. This provides a protective effect against diabetes according to Masuzaki et al. who hybridised transgenic skinny mice overexpressing leptin (Tg/+) with lethal yellow KKAy mice (Ay/+), an obesity-diabetes syndrome model. Six weeks after birth, Tg/+:Ay/+ mice showed higher plasma leptin levels than Ay/+, also insulin sensitivity and glucose tolerance was higher in the Tg/+:Ay/+ mice than in the Ay/+ mice. However, according to Masuzaki et al., the weight of the mice did not differ significantly between the models and compared to wild type mice. Yet at the age of 12 weeks, Tg/+:Ay/+ the mice's leptin level dropped to the level of that of Ay/+ mice and subsequently the Tg/+:Ay+ mice suffered from obesity-diabetes syndrome. Both groups then received a three-week food restriction treatment. The leptin level in Tg/+:Ay/+ mice however exceeded that of Ay/+ mice but dropped in Ay/+ mice and wild type mice. Interestingly, the weight, insulin sensitivity and glucose tolerance recovered in the Tg/+:Ay+ model, showing that higher leptin levels also during food restriction help to recover from diabetes [115]. Furthermore, transgenic skinny mice without the Ay allele lose their lean, insuline sensitive phenotype when being fed a high fat diet. When regaining the common diet, the transgenic skinny mice reduced their weight faster than their wildtype counterparts, and also their sensitivity for insulin recovered quickly. Tanaka et al. attribute this effect to the quick regeneration of leptin sensitivity [178]. Next to calorie intake, different hormones have

an impact on leptin expression: Catecholamines reduce the leptin level, while hormones such as glucocorticoids, insulin and pro-inflammatory cytokines stimulate the production of leptin [139, 4]. As mentioned above, females tend to have a higher level of circulating leptin than males, which may be caused by the higher quantity of female subcutaneous fat tissue. Additionally, estrogen and testosterone support this dimorphism, as testosterone lowers the leptin expression, while estrogen stimulates the production of leptin. Because of this, only female mice have been used in the process of the experiments [139, 121]. Experiments with leptin deficient or leptin receptor deficient mice show the importance of leptin as mice being subject to these conditions suffer from severe obesity, infertility and diminished linear growth as a consequence of missing leptin signaling triggered hyperphagia [139, 90]. As mentioned further above, leptin signaling has also a huge impact on the immune system. In both, the adaptive and the innate immune system, various cell types express the receptor for leptin and are directly influenced by that hormone. Both major T-cell populations, the CD4+ and the CD8+, carry LepR in their membrane. The function of leptin on CD8+ T cells, apart from a publication by Chen et. al. demonstrating an effect of leptin on T cell maintenance [37], remains poorly understood until today. On the other hand, their CD4+ counterpart is well researched. CD4+ T-cells express the long isoform of the leptin receptor. The binding of leptin on murine T-cells enhances proliferation via IL-2 mediated by MAPK and PI3K pathway and survival via enhancing the presence of GLUT1 and GLUT4 in the T-cell's membrane. Additionally, the migration mediated by ICAM-1 and very late antigen 2 (VLA2) is enhanced [146, 104, 105, 137, 171]. Also T-cell differentiation is affected by leptin, as ob/ob mice showed impaired development from naive T-cells towards helper cells compared to wild type mice. This could be attributed to lower amount of GATA-3 and T-bet, which are transcription factors for the differentiation to TH1 and TH2 helper cells [146, 19]. On regulatory T-cells, an inhibitory effect of leptin on their proliferation has been shown. Their frequencies are higher in both, ob/ob mice and db/db mice. mTOR plays a crucial role in this, as impairment of this pathway leads to increased numbers of Tregs in db/db mice [146, 147, 154]. In contrast, leptin promotes proliferation of TH17-cells. Mice with impaired leptin signaling, such as leptin or leptin receptor deficiency or obese mice, show a reduced frequency of TH17

cells. The low TH17 count can be compensated by exogenous leptin supply at least in obese mice [146, 151]. When looking at lymphocytes, leptin is not only a crucial participant in T-cell homeostasis, but also in the function of B-lymphocytes. A significant loss of B-cells and their precursors occurs in obese mice suffering from leptin deficiency. However a substitution of leptin over seven days could raise again the count of B-cells in the bone marrow. Tanaka et al. performed a starvation experiment which showed that also in starving mice B-cells were reduced in the same manner and that replenishment of leptin could prevented the B-cell drop [146, 41, 179]. Leptin prevents B-cell apoptosis by activation of B-cell CLL/lymphoma 2 (Bcl-2) and cyclin D1 causing cell cycle entry [146, 95]. Also cytokine secretion by B-cells is enhanced by leptin, such as IL-10, IL-6 and TNF-alpha. The boosted cytokine secretion is a result of the activation of STAT2/STAT3 and p38MAPK/ERK1/2 signaling cascade [146, 3]. When it comes to the innate immune system, leptin plays a key role as well. It influences the major key actors of innate immunity, such as macrophages, neutrophil, eosinophil, as well as basophil granulocytes, dendritic cells and natural killer cells [146]. First of all, the major phagocytic cell type, the marophages: Relatively early it became obvious that leptin is linked to these myeloid cells. Leptin deficiency leads to impaired ability to phagocytosis or excretion of inflammatory cytokines, whose excretion relates positively with the concentration of leptin. Accordingly, substitution of the peptide hormon reverses the impairing effect [146, 103, 66]. Moreover, activation, proliferation and migration of macrophages are regulated by leptin. Various surface molecules such as HLA-DR, CD11b and CD11c are upregulated and leptin serves as strong chemoattractant. The homing properties of leptin however are strictly linked to the presence of the long isoform leptin receptor on macrophages. As mentioned above, even macrophage phagocytosis is linked with leptin signaling. Gruen et al. demonstrated in mice that leptin causes enhanced calcium influx into the cell, resulting in the activation of JAK/STAT, MAPK and PI3K pathways which influence the macrophages' motility [146, 159, 72]. Next to macrophages, neutrophil granulocytes are also affected by leptin. They only express the short isoform of the leptin receptor and its activation results in the expression of CD11b and inhibition of apoptosis by impairment of mitochondrial cytochrome c release as well as the inhibition of caspase-3 and caspase-8, thus giving hints that

also the short isoform leptin receptor can mediate regulatory effects [146, 27, 205]. At least in humans, leptin enhances the intracellular hydrogen peroxidase resulting in a regulation of ROS production [146, 29]. Like in macrophages, leptin promotes phagocytosis also in case of neutrophils, as the ability to phagocyte klebsiella was impaired in ob/ob mice. [146, 122]. Also the granulocytic siblings of the neutrophil granulocyte, the eosinophil granulocytes succumb the influence of leptin signaling in a similar manner. Also in this case leptin impairs mitochondrial cytochrome c release and cleavage of Bax protein. Alike its influence on neutrophil granulocytes' surface proteins, leptin promotes the expression of several surface molecules such as CD18 and ICAM-1, however lowers the expression of L-selectin and ICAM-3. Another parallel to neutrophil granulocytes is the regulation of eosinophil cell migration in humans. Leptin enhances the secretion of inflammatory chemokines (e.g. monocyte chemotactic protein-1 and growth-related oncogene-alpha) and cytokines, such as IL-1beta and IL6 [146, 45, 199]. Different from neutrophil signaling, leptin in human eosinophil granulocytes is accountable for the fast phosphorylation of p38 MAPK and extracellular signal-regulated kinases 1/2 (ERK1/2), but seemingly does not influence the calcium household [146, 89]. Next to the already presented cells, there are the dendritic cells which are also regulated by leptin signaling. Dendritic cells are less potent antigen presenters and also their frequencies differ in leptin deficient animals compared to wild type controls [146, 112]

3.2.2 Characterization of the leptin receptor and signaling

The leptin receptor (LepR or OB-R) has various splice isoforms. LepR is counted to the class 1 cytokine receptor family and the signaling pathway is often mediated by janus kinases (JAKs) and so called “signal transducers and activators of transcription“ (STAT) [65]. LepR is mainly expressed in the brain, especially the hypothalamical region, where it triggers, as mentioned already above, anti-obese effects [139, 74]. Next to the brain, there are various other tissues and cells that bear the leptin receptor, for example on several immune cells [146, 145] and, as our work group showed, on fibroblastic reticular cells (see 5.2.1). The gene that codes for

these receptors, the OB-R gene, contains enough genetical information to provide the organism with at least five alternatively spliced isoforms (Ob-Ra, Ob-Rb, Ob-Rc, Ob-Rd, Ob-Re) [64, 180, 97]. Also a soluble isoform of LepR is described [94, 97]. Many sources state that only the long isoform, OB-Rb, is functional. However, several sources attribute a functionality also to short isoforms. Bruno et al. showed in their experiments with neutrophils, which only bear the short isoform of the leptin receptor, that leptin is able to trigger the JAK2/MAPK and the PI3K pathway and an anti-apoptotic effect in neutrophils. OB-Rb is the longest possible peptide chain translated by this gene and triggers pathways like JAK2/STAT3 and STAT5, AMPK/ACC, IRS/PI3K, SHP2/MAPK and SOCS3 [65, 139, 27]. Figure 3 gives an exemplary depiction of leptin/LepR singaling pathway. SOCS3 mediates an inhibition of the JAK2/STAT3 pathway and thereby creates a negative feedback loop. Next to SOCS3, also protein tyrosine phosphatase 1B (PTP1B) is involved in the inhibition of leptin signaling via dephosphorylation of phosphorylated JAK2 [139, 50, 121]. Usually, binding of leptin to its receptor, especially the long isoform LepRb, leads to a dimerization of the receptor. Thereafter the receptor dimer forms a complex with the Janus kinase 2 (LepRb/JAK2 complex) thus activating JAK2, which then phosphorylates itself and tyrosine molecules (Tyr 985, Tyr1007 and Tyr 1138) of the receptor dimer. Phospho-Tyr 1007 and phospho-Tyr 1138 again activate STAT3 and STAT5 by binding to it and phosphorylating it (phospho-Tyr 1007 binds to STAT3 andphospho-Tyr1138 binds to STAT5). So being phosphorylated, STAT3 and STAT5 move into the nucleus and follow their task as transcription factors. As mentioned before, a negative feedback mechanism is induced by SOCS3, as it is a product of the gene targeted by STAT3. Next to SOCS3, protein tyrosine phosphatase 1B is also a inhibitor of the signal cascade. The inhibitory effect is mediated by dephosphorylation of JAK2. However when JAK2 is phosphorylated, it induces the binding of SH2-containing protein tyrosine phosphatase (SHP2) and phopsho-Tyr985, which activate the adaptor protein growth factor receptor-bound protein 2 (Grb2). Grb2 can now activate the mitogen-activated protein kinase (MAPK). However, leptin-activated JAK2 is able to cut short the SHP2 cascade by directly activating MAPK. Another pathway induced by JAK2 is the downstream activation of phosphatidylinositol 3 kinase (PI3K) by phosphorylated insulin receptor substrate

(IRS). PI3K again will activate forkhead box O1 (FoxO1) (not shown in the figure), mammalian target of rapamycin (mTOR) and phopshodiesterase 3B (PDE3B) [139].

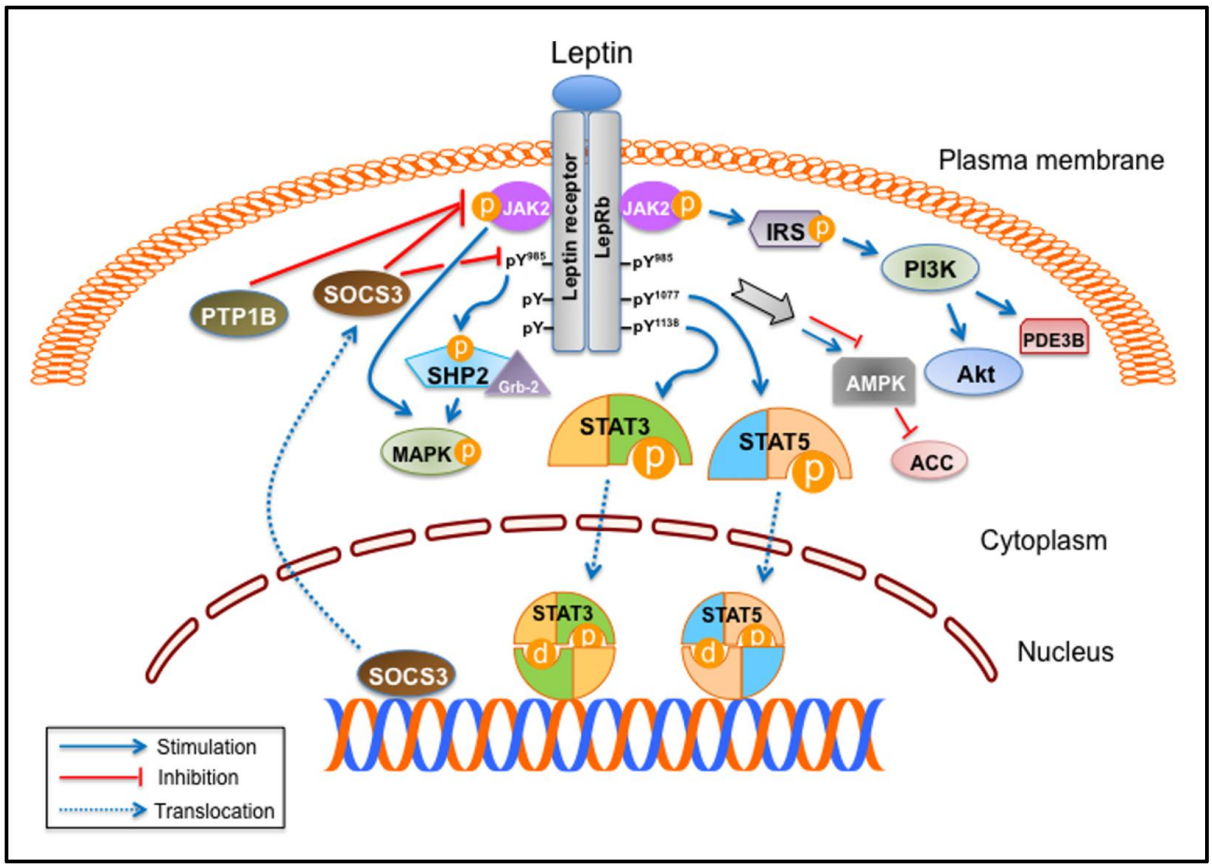

Figure 3: Exemplary depiction of the leptin/LepR singaling pathway: This figure by Park et al., gives a sublime overview about the signaling pathway of leptin binding to the long isoform of its receptor LepRb. When leptin binds to its receptor, two receptors form a dimer and configure to a complex with the Janus kinase 2 (LepRb/JAK2 complex), thereby activating Janus kinase 2 which subsequently phosphorylates not just itself, but also amino acids of the leptin receptor, namely Tyr985, Tyr1077 and Tyr1138. Phospho-Tyr 1138 and phospho-Tyr1077 are now bound by STAT3 and STAT5, which are again phosphorylated and therefore activated. Both STAT3 and STAT5 now shift to the cell core to initiate the transcription of their targeted genes. A negative feedback loop is created by the activation of SOCS3, which is also a target gene of STAT3, by phospho-Tyr985. It inhibits the JAK2/STAT3 pathway. Another inhibitor of the leptin signaling pathway is the protein tyrosine phosphatase 1B (PTP1B), it deploys its inhibitory effect by the dephosphorylation of JAK2. When JAK2 gets activated, SH2-containing protein tyrosin phosphatase 2 (SHP2) binds to phospho-Tyr985 of the LepRb, thus activating the adaptor protein growth factor receptor-bound protein 2 (Grb2), which again activates the mitogen-activated protein kinase (MAPK) signaling cascade. Independently from SHP2, MAPK is activated by leptin via JAK2. Furthermore it activates the phosphatidylinositol 3 kinase (PI3K) via a phosphorylation of insulin receptor substrate (IRS) which is again activated by JAK2. The targets of PI3K are forkhead box O1 (FoxO1), mammalian target of rapamycin (mTOR), and phosphodiesterase 3B (PDE3B). 5'adenosin monophosphate-activated protein kinase (AMPK) and acetyl-CoA carboxylase (ACC) regulate the metabolism and the feeling of satiety [139].
(Figure by Park et al. [139]).

4. Materials and Methods

4.1 Solutions, reagents and materials

Solutions and reagents that have been used are shown in table 1.

Table 1: Solutions and reagents: This table shows the solutions and reagents used in the experiments, as well as their suppliers.

Cell culture and flow cytometry		
Reagent	**Concentration**	**Supplier**
RPMI Culture Medium		Life technologies
Dulbecco's Phosphate Buffered Saline		Sigma Life Science
Hank's Balanced Salt Solution		Sigma
EDTA 0,5M pH 7,4	0,5M	Sigma
UltraPure EDTA	0,5M	Life technologies
Trypsin		Life technology
Heat Inactivated FBS		Life technologies
Penicillin/Streptomycin		Life technology
ACK Lysing Buffer		Life technologies
FACS-Buffer		Miltenyi Biotec
MACSquant Running Buffer		Miltenyi Biotec
AutoMACS Rinsing Buffer		Miltenyi Biotec
AutoMACS Running Buffer		Miltenyi Biotec
Collagenase P	100mg/ml	Roche
Dispase	100mg/ml	Roche
Dnase I	50mg/ml	Roche
Leptin		Biotechne
Fc-blocking-reagent		Miltenyi Biotech
4'6-Diamidin-2-phenylindol		Life technology
PI (Propidium Iodide)		Miltenyi Biotech
Ter119 antibody PeCy7	0,2mg/ml	Biolegend
CD45 antibody APC-Cy7	0,2mg/ml	Biolegend
gp38 antibody APC		Biolegend
CD31 antibody FITC	0,5mg/ml	BioLegend
Anti-goat antibody FITC		Life technologies
CD3e antibody A488	0,5mg/ml	BioLegend
CD19 antibody PE	02,mg/ml	BioLegend
CD11c antibody APC	0,2mg/ml	BioLegend
CD11b antibody PeCy7	0,2mg/ml	BioLegend
CD103 antibody PE	0,2mg/ml	BioLegend
CD35 antibody biotinylated	0,5mg/ml	Biosciences
Streptavidin PeCy7	0,2mg/ml	BioLegend

Streptavidin 405	**1mg/ml**	**Life technologies**
Goat IgG		**Biotechne**
Hamster IgG PE	**0,2mg/ml**	**BioLegend**
Rat IgG 2aκ PE		**Biolegend**
Rat IgG 2bκ PeCy7	**0,5mg/ml**	**BioLegemd**
Armenian hamster IgG APC	**0,2mg/dl**	**BioLegend**
Armenian hamster IgG PE		**Biolegend**
Leptin receptor antibody goat for flow cytometry	**0,2mg/ml**	**Sigma Aldrich**
Genetic analysis		
Reagent	**Concentration**	**Supplier**
Nuclease-Free Water		**Ambion**
cybergreen fast		**Life technologies**
cybergreen save		**Life technologies**
Agarose		**Biozym scientific**
Col1 primer		**Thermo Fisher Scientific**
CXCL-10 primer		**Thermo Fisher Scientific**
FLT-3 primer		**Thermo Fisher Scientific**
MCSF primer		**Thermo Fisher Scientific**
MMP2 primer		**Thermo Fisher Scientific**
MMP9 primer		**Thermo Fisher Scientific**
NOS-2 primer		**Thermo Fisher Scientific**
SMA primer		**Thermo Fisher Scientific**
TGF-β primer		**Thermo Fisher Scientific**
Buffer RLT Plus		**Qiagen**
Buffer RW1		**Qiagen**
Buffer RPE		**Qiagen**
Protein analysis		
Reagent	**Concentration**	**Supplier**
RIPA-buffer		**Thermo Fisher Scientific**
Protease inhibitor		**Thermo Fisher Scientific**
TAE-buffer	**0,04M Tris-acetat, 1mM EDTA**	**Biozym scientific**
TBE-Buffer	**0,89M Tris-borat, 0,02M EDTA**	**Biozym scientific**
Pre stained dual color marker		**Bio-Rad**
Laemmli buffer		**Bio-Rad**
Leptin receptor antibody rabbit Western Blot	**10mg/ml**	**Abcam**
ɣ-Tubulin antibody		**Cell Signaling Technology**

4.2 Cell culture

4.2.1 Cell line

To research basic functions of stromal cells, the use of a cell culture is essential. In this thesis several cell lines were utilized: FRC-T, FRC-TN, FRC-2 (FRCs of spleenic origin) and a bone marrow FRC cell line, namely CRL-2648™ by ATCC®, Manassas, Virginia, United States of America. After thawing, the cells are cultured, if not specified otherwise in a RPMI + 10% FBS + 1% Penicillin/Streptomycin medium (13ml in a cell culture flask with an cultivated area of 25 cm² and 25ml in a cell culture flask with a cultivated area of 175cm²). They are sterilely processed and kept at 37°C in a humidified incubator. Medium is changed every three days. After discarding the old medium, a flushing with PBS and then replacement of nutritional medium in the same concentration as mentioned above followed (see figure 4). Cell culture is monitored by light microscope in 40x magnification, regarding the shape of the cells, the density of their growth and amount of debris surrounding them. If required, cells are splitted and expanded. For this, the culture medium is taken away, the adherent cells are washed with PBS and were incubated for 2min at 37°C in 2 ml 0,05% trypsine solution, which will lyse adherent molecules. At the end of the incubation time, digestive function of trypsine is slowed down by diluting it with 8 ml RPMI and the sample is transferred into a 15ml tube which will be centrifuged (300g 5min 20°C). Supernatant will be discarded and the pallet will be resuspended in 13 ml medium and put back into a culture bottle. When cells are ready grown, they are harvested by first flushing them with PBS, then incubated in 5mM EDTA at 37°C until a single cell suspension is reached, if necessary, a cell scraper is used. The cells were monitored with light microscope.

4.2.2 Primary cell culture

4.2.2.1 Isolation of primary cells from mice

Mice were kept according to the regulations of the Landesamt für Verbraucherschutz, Saarbrücken Germany and are fostered under pathogen free conditions in a mouse cabinet. Mice were purchased from Charles River (Sulzfeld Germany). The animals were anesthetized with isoflurane and cervical dislocation was performed. Mice are dissected via median incision of the abdominal and thoracal skin, followed by a double T-cut to its extremities, then moving the skin flaps to the sides and fixed, which will reveal the inguinal, axillary and brachial subcutaneous lymph nodes which are used for the experiments. Lymph nodes are taken out with forceps and put in PBS on ice, adherent fat and other connective tissue is detached mechanically. To dissolve the lymph nodes the following protocol is used. When transferring into a 15ml Falcon Tube, the lymph nodes are crushed with a forceps to weaken the connective tissues of the lymph node. Now the lymph nodes are incubated in 1600µl of digestion buffer (50ml RPMI +100µl Collagenase C +100µl DNAse +400µl Dispase +5ml FBS) on 37°C in a water bath. In the first 10min, the sample will be shaken gently every 5min to ensure that the lymph nodes do not accumulate. On time mark 15min, the sample is resuspended by the help of a 1000µl pipette with its pipette tip cut off to mechanically dissolve the target. After additional 7,5min, this step is repeated. However supernatant, which contains the dissociated cells, will be collected and stored on ice. This step is now repeated every 7,5min but with an uncut pipette tip until time mark 45min, where the interval between the steps is reduced to 5min. After every second uptake of supernatant, the collected supernatant is centrifuged (1300g, 4min, 4°C), subsequently the supernatant is discarded and the pellet is filtered (100µm) and resuspended in collection buffer, consisting of RPMI + 1% FBS and 2mM EDTA. Digest is ceased when no particulate matter is left in the tube, latest after 90min of digest. Now the cells can be further processed to either flow cytometry analysis or cell culture.

4.2.2.2 Setup of a primary culture of lymph node stromal cells

In order to investigate further the fibroblastic reticular cells, the establishment of a primary cell culture was necessary. To do so, cells were isolated from C57BL/6J mice according to a previously published protocol [106]. Purified sample from lymph node digest is centrifuged (300g 5min 20°C) and resuspended in 2ml*number of wells in which cells are kept RPMI +10%FBS +1%P/S. 10^7 cells are assigned to one well of a six well plate, afterwards the cells are given 24h to rest. Now the cell medium is taken away and they are flushed strongly three times with 2 ml PBS, subsequently medium will be renewed. This is to make sure that non-adherent cells, namely T-cells, B-cells and erythrocytes are discarded from the culture. Adjacent further manipulation is ceased but change of nutrition medium is necessary until the cells are grown dense (see figure 4). This will ensure that double-negative and blood endothelial cells are absent and only macrophages, dendritic cells, lymphatic endothelial cells and fibroblastic reticular cells are left. Cells are now ready for further processing.

1. Carefully take away medium

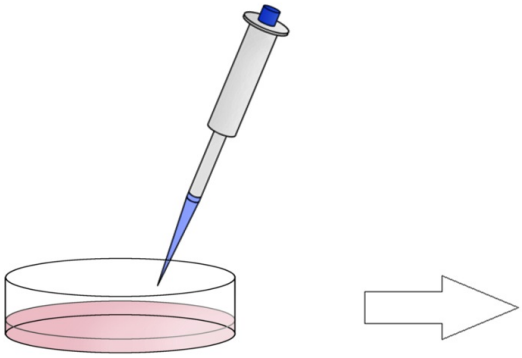

2. Refill with PBS

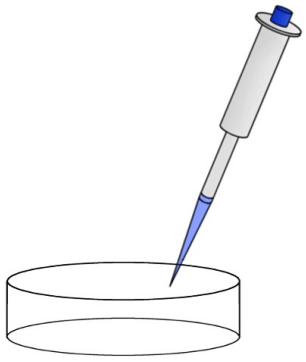

3. Gently shake and discard liquid

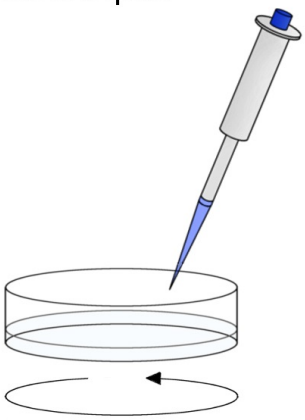

*repeat 3x

4. Refill with fresh nutrition medium

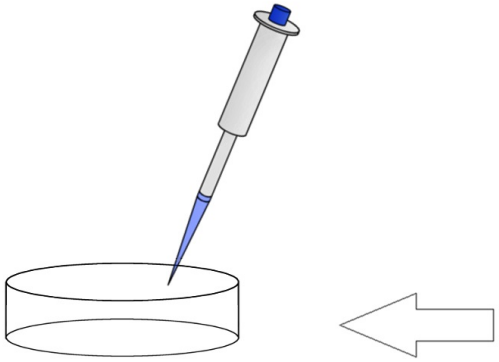

5. Put the culture back into incubator

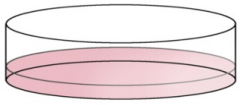

Figure 4: Washing of a cell culture: In order to cultivate a cell line and to ensure proper growth, the cells have to be washed periodically every three days. To do so, the culture dishes/ culture flasks are transported to a workbench where the work happens under sterile conditions. Before the first step, the culture plates or flasks are observed by the help of a microscope to ensure that the culture has not grown too densely. After placing the culture in the sterile working bench, all supernatant is taken off and discarded. If this happened, the discarded volume is replaced by 5 ml PBS. The culture dish/ culture flask will now be slewed gently a few times, then the supernatant is discarded. This step happens three times. After the last run, the initial volume of nutrition medium will be filled up again and the cells are brought back into the incubator.

4.3 Flow cytometry

To characterize cells by their size, their granulation and most important their surface and intracellular molecules, in this experiment flow cytometry was used (MACS Quant 10 Analyzer (Miltenyi)). Flow cytometry is a technique whose key instruments are white light and lasers of different wavelength, which, in case of the laser, activate the fluorochrome linked to the antibody. A blue laser (488nm) rays the cell and the deflected light is collected as forward scatter and sideward scatter. A high signal in the forward scatter will be caused by a bigger cell volume. Whereas high granulation of a cell will result in more dispersion of light, which is recognized by the sideward scatter. With its three lasers and eight filters, MACS Quant 10 Analyzer is capable of distinguishing between eight fluorescence channels additionally to the forward and sideward scatter (figure 8). Produced data was analyzed by using the software FlowJo 10.0.6 (Ashland, Oregon, USA). When gating the cell population, the procedure according to 5.1.1 was used.

4.4 Magnetic cell sorting

As there are multiple cell subsets left in a primary culture of lymph node stromal cells, obsolete cells are sorted out via magnetic cell sorting (MACS). This technique is based on antibodies linked to magnetic beads which will provide that the cells bound to those antibodies will stick in a magnetic field and can be released and thereby collected after turning off the magnetic field. In general there are two possibilities to magnetic sort of cells, the positve and negative MACS separation. In negative MACS separation, unwanted cells are bound to the magnetic beads and the flow through contains the targeted cells. In positive MACS separation, targeted cells are bound to magnetic beads and the first flow through is discarded, after moving the column out of the magnetic field, the flow-through with its containing cells is collected. Figure 5 complements the protocol. First of all, the sample is centrifuged (300g 5min 4°C), then the pellet is resuspended in 2ml MACS-buffer. Following the cells are counted via flow cytometry and again centrifuged (300g 5min 4°C). If done so, staining for

3*10^6 cells is as follows: Primary step consists of blocking of any Fc-Receptor with re-suspension in 290µl MACS-buffer + 10µl Fc-Block, which will be incubated on ice. After 5min 3µl of CD 45 biotinylated antibody and 6µl of CD 31 biotinylated antibody is given to the sample, which will now rest 10min on ice. Now the magnetic microbeads are given to the sample, in with 160µl MACS-buffer and 15µl anti-biotin-beads. Again the sample has to be incubated for 15min at 4°C. At time mark 7min the sample is gently mixed by shaking the tube. When 15min are over, the sample is filled up with MACS-buffer to a total sample volume of 5ml, and spinned down at 300g for 10min. Supernatant is taken away and the pellet is resuspended in 500µl MACS-buffer, the sample is now ready for MACS separation. In order to do so, the MACS device has to be installed (see figure 5). The column is prepared by attaching a 100µm filter to it after placing it in the magnetic field. To ensure that the inner part of the column is all wet, it is flushed with 3ml MACS-buffer. Finally the sample can be loaded on the column, which is now flushed with 3*3ml MACS-buffer, however it has to be taken care that the column must not run dry. In case of negative MACS separation, which is the case in the current work, target cells pass the column, and are collected in a tube. If aiming for positive MACS separation, it is necessary that the column is now moved out of the magnetic field and eluted with 5ml MACS-buffer. Target cells are now centrifuged (300g, 4min, 4°C), counted and can now be cultured. It is inevitable to let the cells rest for 24h and control their morphology via microscopy to control of the cell viability.

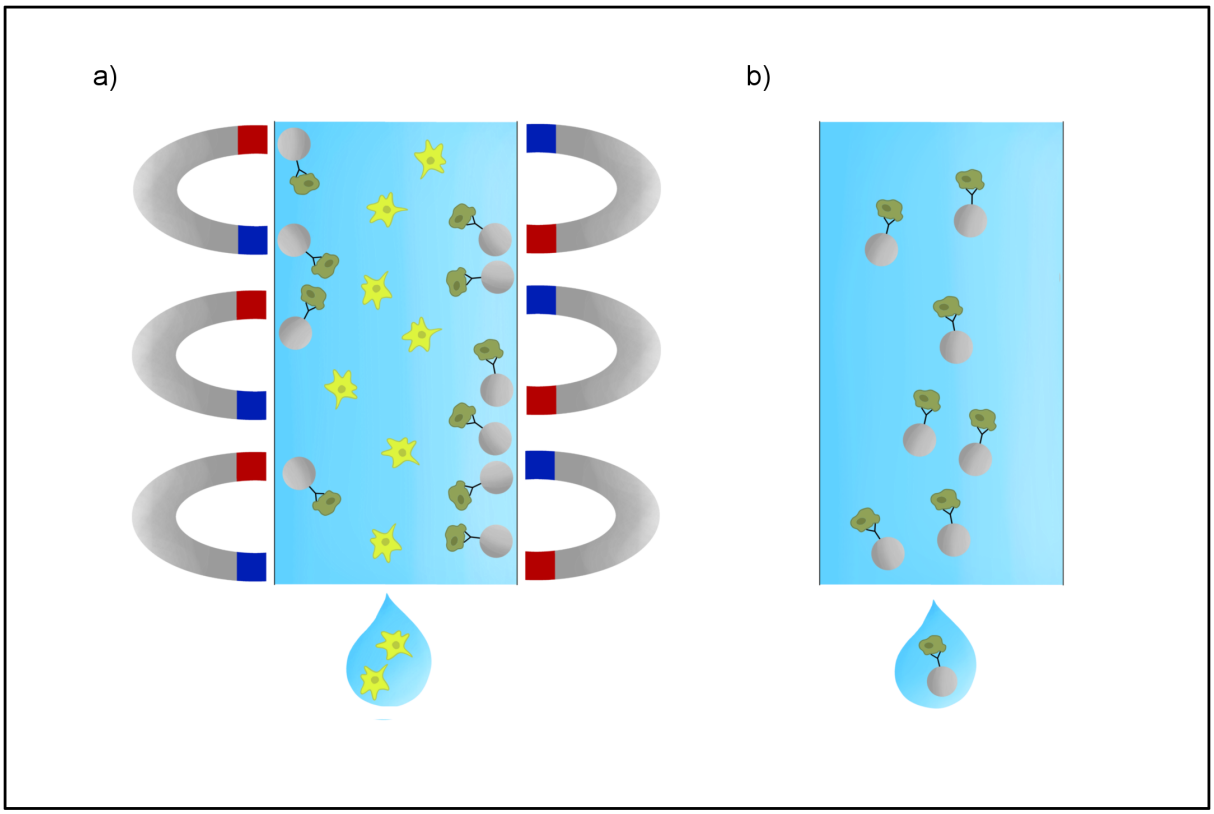

Figure 5: Principle of magnetic cell sorting: In this illustration, the principle of magnetic cell sorting is displayed in a highly simplified manner. After marking a certain cell population with magnetic beads, the sorting process may commence. Whether the target cells are marked or not is dependend on the general circumstances, e.g. the ratio between cell populations, the number of different populations in the probe, or even the availability of bead conjugated antibodies, in general it is possible to enrich the target cells by marking non-target cells. a) Shows the flow-through in a magnet field. The cells bound to magnetic beads conjugated antibodies will stick to metal spheres inside the column (not shown for simplification reasons) which are magnetized. Unmarked cells will be flushed out by the buffer flowing through the column, these cells can either be collected or discarded. b) When the column is taken out of the magnetic field, the metal spheres will lose their electromagnetic charge, releasing the magnetic-bead-antibody-cell-complex. These complexes can now be flushed out with buffer and, as the unmarked cells, either be collected or discarded. Due to further dilution of the cells in the process of culturing, the magnetic-bead-antibody-cell-complex dissolves and the cells are not inhibited in their growing behavior. However this whole process is extremely stressful for cells, so that a successful cultivation is not guaranteed.

4.5 Preparation of blood samples

To collect blood, the heart is punctured with a syringe from its apex towards the right atrium as fast as possible after sacrificing the mice to ensure that the blood is not already coagulating. 400µl blood are carefully removed. After 30min at room temperature the sample is centrifuged for 15min at 1500g at 4°C. When collecting serum, the supernatant can be carefully taken away and stored at -80°C.

4.6 Isolation of RNA

In order to generate cDNA that can be used to perform a PCR, the first step is to isolate the RNA from the cell population of interest. To do so, the Rneasy Plus Mini Kit by Qiagen has been used according to manufactural guidelines (Qiagen). As requested in the manual, after harvesting the cells, a maximum of 10^7 cells has been used per isolation. As the cell number was always lower than 5*10^6, 350µl of Buffer RLT Plus has been added to the tube after disrupting the cells. After doing so, the solution has been decanted to a gDNA Eliminator spin column which is placed inside a 2ml collection tube. The sample is now centrifuged for 30s at 3000g, during the centrifugation, the sample will pass the Eliminator spin column and accumulates in the collection tube, the Eliminator spin column may now be discarded. 350µl of 70% ethanol is now added to the flow-through and resuspended. The sample is now filled into a RNeasy spin column, which again is placed in a 2ml collection tube. The tubes are now centrifuged at 8000g for 15s. The flow-through has to be discarded. A volume of 700µl Buffer RW1 is added to the spin column, still placed inside of a 2ml collection tube, the centrifugation is repeated at 8000g for 15s, again, the flow-through is to be discarded. Now a volume of 500µl Buffer RPE is added to the spin column which has to be centrifuged with the same parameters as in the previous step, the flow-through is to be discarded. After this step, the same amount of Buffer RPE is added to the sample, this time however, the centrifugation is performed at 10000g for 2min. The spin column is now transferred to a 1,5ml collection tube and 30µl Rnase-free water is added on the spin column membrane without touching any

surroundings or the membrane with the pipette tip. The tube is again centrifuged at 8000g for 1min. After centrifugation, the RNA is inside of the 1,5ml collection tube.

4.7 Production of cDNA

Generating cDNA is a crucial step in the process of preparing a PCR. For this process, the QuantiNova Reverse Transcription Kit by Qiagen has been used. The method of operation is similar to that of retroviruses or hepadnaviruses, the key enzyme is reverse transcriptase. In order to transcribe RNA to cDNA, the reverse transcriptase needs two functions: First of all the ability of DNA-polymerase to synthesize complementary DNA, and second, the ability of RNAse-H which degradates the remaining RNA to oligonucleotides, so that the DNA-polymerase can again synthesize a complementary DNA-strand [149]. To start the process, the RNA samples, the gDNA removal mix and Reverse Transcription Enzyme is thawed on ice, while the Reverse Transcription mix and RNase-free water is thawed at room temperature. To remove possibly remaining genomic DNA, in the next step, the genomic DNA removal reagent is prepared. To do so, 2µl of gDNA removal mix is added to a sample volume up to 5µg of RNA, then, 1µl of Internal Control RNA is added. The reaction volume is now filled up with RNAse-free water to a total volume of 15µl, if done so, the samples are incubated for 2min at 45°C and put on ice. Now, the Reverse-transcription master mix is to be produced. To the previous sample with a total volume of 15µl is now added a 5µl mix consisting of 1µl of Reverse Transcription Enzyme and 4µl of Reverse transcription mix. The sample is now incubated for 3min at 25°C and again for 10min at 45°C, the sample eventually contains the cDNA. To inactivate the Reverse Transcriptase Enzyme, the sample is again incubated, this timer for 5min at 85°C. After diluting the sample 1:10, it can be frozen away at -30°C to -15°C before further use.

4.8 Polymerase chain reaction

To understand what physiological and biochemical changes undergo in a cell during the alteration of their surrounding environment, one key technique in order to check on the transcription of various genes is the polymerase chain reaction (PCR)(see figure 6). During PCR, DNA double strands are broken by high temperature into single strands and multiplied by DNA polymerases, theoretically multiplying DNA exponentially. In contrast to conventional PCR, during the real-time quantitative PCR (qPCR), produced DNA is measured at every cycle, allowing it to draw conclusions on the beginning DNA concentration and thereby directly on the mRNA concentration. As the beginning mRNA concentration of a certain gene as such is not utilizable, it has to be compared with the mRNA production of genes for crucial proteins which are necessitated in the cell at all times (housekeeping genes). As a control, the RNA for GAPDH is outstanding, as Glyceraldehyde 3-phopshatase dehydrogenase is a basic protein for every cell because it is produced at a constant level over time. To measure the amount of product each cycle, the fluorescent dye SYBR green, which intercalates double-stranded DNA, was utilized. As SYBR green only has fluorescent properties being activated by blue light when it intercalates double-stranded DNA, the signal of emitted light rises by the increase of dsDNA during subsequent cycles. Figure 6 shows the principle of PCR. Each cycle begins with the so called denaturation phase, in which dsDNA is melted to ssDNA (in this case we worked with cDNA which was transcribed from mRNA) at around 95°C. Thanks to the used taq polymerase, working with such high temperatures is possible, as it won't denature at 95°C. During the next phase, the annealing, the primers hybridize. The working temperature is oriented on the melting temperature of the primers. The cycle ends with the extension phase, in which the taq polymerase extends the DNA strand. If the amplicon is short enough, often the extension phase is combined with the annealing phase at a working temperature of circa 60°C [185]. In this study, only cDNA-samples made from corresponding mRNA have been processed. The cDNA-sample is diluted 1/10 (27µl distilled and sterile water + 3µl cDNA). The forward- and reverse primers are diluted 1/10. A master mix is now produced for every gene which has to be examined: for 10µl volume/wells, 50µl

SYBR green fast (Life technologies) + 22µl distilled and sterile water + 4µl forward-primer + 4µl reverse-primer. Every master mix is transferred in triplets on a PCR-plate (8µl master mix/well). Finally the cDNA-sample can be given to the wells containing their related master mix (2µl/well; 10µl total volume in each well). To ensure that there are no air bubbles in the sample, the plate is centrifuged briefly, consequently it can be processed by the thermo cycler (7500 Fast Real-Time PCR System by ThermoFisher Scientific). The thermo cycler first runs one cycle for 2min at 95°C, then 40 cycles 5s each at 95°C. If done so it runs another 40 cycles, this time 30 seconds each at 60°C. Thermo cycler finishes its program by performing 5s cycles reducing the temperature for every cycle by 0,5°C from 95°C to 65°C.

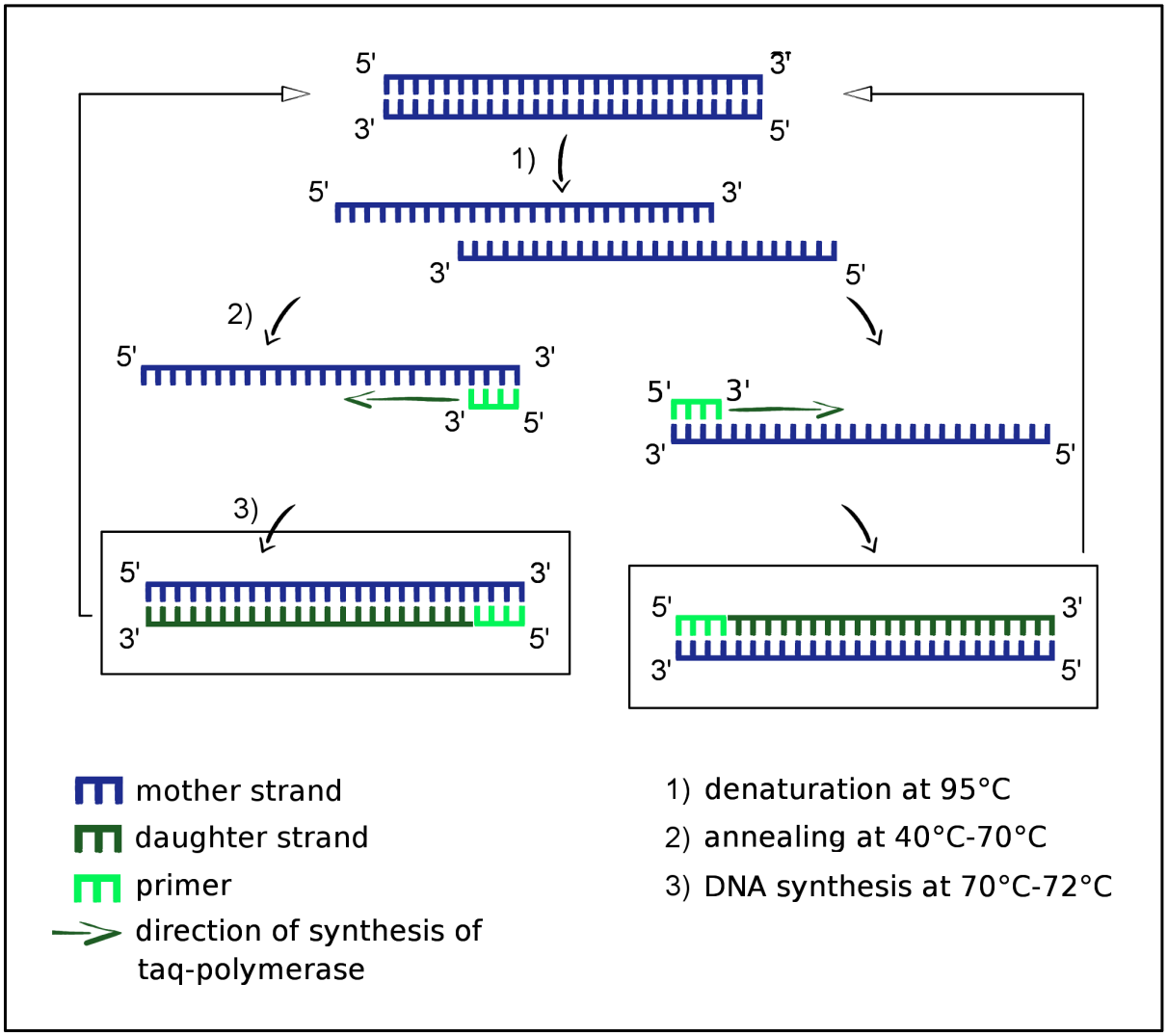

Figure 6: The principle of PCR. Polymerase chain reaction is a crucial technique to detect e.g. the cell's production of various gene products. By multiplying existing DNA or cDNA strands, the activity of certain genes can be estimated. As control, so called housekeeping genes are also part of any qPCR. These genes are obligatory to maintain the functionality of a cell and are usually expressed at a constantly high level. In our examination, the gene for GAPDH served as a housekeeping gene. The educts needed for PCR are DNA or cDNA, primers, nucleotides and taq-polymerases. During the process of PCR, DNA is multiplied exponentially according to the scheme. Before initializing the reaction, the dsDNA mother strand has to be denatured, thereby creating ssDNA. This is usually done by thermic energy. The commonly used temperature lies approximately at 95°C. The primers now can bind at 40°C – 70°C to their specific locus in the ssDNA, so called annealing, enabling taq-polymerase to lengthen the daughter strand in 5'-3' direction at 70°C – 72°C. When taq-polymerase reaches the 5' end of the mother strand, DNA synthesis comes to a halt, dsDNA has been generated. With dsDNA being present, the cycle can start over.

4.9 Protein isolation

After harvesting and counting of the cells, samples are centrifuged (300g, 4min, 4°C) and resuspended in 300µl of lysis solution (1ml RIPA-buffer + 50µl protease inhibitor, provided by ThermoFisher Scientific). The sample is vortexed shortly and put 10min on ice before it's again vortexed and put for another 10min on ice. Then the sample is centrifuged for 20min at 14000g at 4°C and afterwards the supernatant, which contains the proteins, is collected. In order to determine the amount and concentration of protein that has been isolated, we performed a protein concentration measurement by using a protein assay kit (Thermo Scientific Pierce BCA Protein Assay Kit): To calculate the total working reagent, the number of standards (BSA in the following concentrations: 2000µg/ml; 1500µg/ml; 1000µg/ml; 750µg/ml; 500µg/ml; 250µg/ml; 125µg/ml, 25µg/ml; 0µg/ml) is added to number of unknown samples, then multiplied by the number of replicates and again multiplied by the volume of working reagent per sample (200µl). The working reagent is then prepared by mixing reagent A (50 parts) with reagent B (1 part). We proceeded with the microplate procedure. To do so, 25µl of each standard or unknown replicate is transferred into a microplate well, subsequently we added 200µl of the working reagent and mixed the sample for 30s. Afterwards, the plate is incubated at 37°C for 30min. After cooling down the plate to room temperature, the spectrometric measurement at 562nm is undertaken. To calibrate the instrument, the absorbance of a cuvette with water is measured by a spectrophotometer. The resulting absorbance is subtracted from the absorbance of all other samples, which are measured now. Afterward a standard curve is generated by plotting the absorbance of the BSA standard solutions against their concentration. This standard curve is then used to calculate the unknown protein concentration [184].

4.10 cDNA-gel

4% agarose gel was prepared as follows: 4g agarose (standard gelling/melting temperature Agarose by Biozym scientific D31840 Oldendorf) is solved in 100ml 1x

TAE-buffer. The solution is heated up in a microwave and mixed until there is no particulate matter left and the solution is clear. While gently shaking the reagent to prevent the agarose from precipitating, the liquid is cooled down to room temperature. Then 10µl 1/10000 cybergreen safe is added and subsequently the material is poured into the gel chamber to let it harden. 2µl loading buffer is added to the cDNA-sample (10µl; total volume of sample 12µl) and samples can be gently transferred to the pockets in the now hardened gel. For each row there will be inserted 5µl marker as control in an extra pocket. A current is applied and the gel is run until the samples have traveled a sufficient distance through the gel. If this is ensured, the gel block can now be viewed by ultra violet light.

4.11 Western Blot

A Western Blot starts with the production of the separation gel, in this case a 7% separation gel. To do so, one starts with 2,5ml TG-buffer (1,5M Tris base, 4% SDS, pH 8,8) to which 5,66ml water and 1,75ml acrylamide are given. Subsequently to this is added 75µl APS and 15µl TEMED. The liquid is poured into a form and given time to harden. Now the sample is prepared by putting together 75µl of the sample (1,202mg protein/ml) and 2x Laemmlie buffer (reduced). This is incubated for 5min at 95°C to disrupt the superstructure of the proteins. At this point the collection gel of 4% has to be prepared, starting with 1,25ml 4x SG-buffer (0,5M Tris base, 4% SDS, pH 6,8) to which is added 3,21ml water, 500µl acrylamide, then 37,5µl 10% APS and 7,5µl TEMED. This reagent is now poured into its form. Finally the sample and marker are put into the pockets of the gel which is placed in an electrophoresis chamber that is filled with 10' SDS electrophoresis buffer (1% SDS, 250mM Tris-HCl, 1,92%M Glycin) and a voltage of 100V is applied for 1 to 2h, dependent on the distance the sample traveled through the gel. After blotting the membrane, it can be developed. First of all the membrane is blocked for 1h at room temperature in skim milk in TBST. After blocking the membrane, the antibody is applied to the membrane, which is then incubated over night at 4°C. After incubation, the sample is washed 3 times for 5min in TBST. Now the secondary antibody may be applied, the antibody

has to be incubated for 1h at room temperature in skim milk. If done so, the membrane is washed again 2 times for 10min with TBST, and then washed again once with TBS for 10min. 1Ml of luminol and 1ml of enhancer is added to the membrane, again an incubation step of 1 minute follows. The sample can now be measured.

4.12 Mice

All performed experiments in which animals were used have been approved by the Landesamt für Verbraucherschutz, Saarbrücken, Germany. Upon arrival, the animals were at least allowed 72h of rest to recover from the transport as they were held in a pathogen free environment (mouse cabinet purchased from Bioscape). The mice used in this work were female C57BL/6 mice, a commonly used wild type, purchased from Charles River (Sulzfeld, Germany), aged around 7 to 8 weeks at the time of the experiments. If not otherwise mentioned, the mice had access to food and water at will. Food and water have been monitored daily and cages were exchanged at least once a week. Mice in the starvation group were denied food for 48h (starvation phase) but had free access to water. In the regression phase group: After 48h starvation period food was given back to the animals for another 72h. The mice have been processed according to 4.2.2.1.

4.13 Calculation, analysis and software

Data collected with flow cytometry has been analyzed with FlowJo (10.0.8) by the company FlowJo, LCC. Statistical analysis has been performed with the help of PRISM 5.03, provided by the company GraphPad Software Inc. La Jolla, CA , USA and Microsoft Excel by Microsoft Corporation, One Microsoft Way, Redmond, USA. Figures made by the autor have been generated with PRISM and GIMP 2.10.0 by The GIMP Team.

5. Results

5.1 Analysis of the lymph node structure

5.1.1 Establishment of a staining scheme

To differentiate the various hematopoietic cell populations within the lymph node, such as macrophages, dendritic cells, T-cells, B-cells and stromal cells like fat cells, progenitor cells, blood endothelial cells, lymphoid endothelial cells and fibroblastic reticular cells, a complex gating strategy is crucial. The first step in gating stained digested lymph node tissue consists of gating out cell debris, as debris can give a false positive signal in fluorochrome-related channels. Another similar negative effect on the purity of the result is caused by dead cells that can bind to dye-linked antibodies and can appear unspecifically in any channel. As figure 7 shows, the biggest contingent of cells in lymph node are undoubtedly leukocytes, in this case more than 99% of the lymph node's cell population (erythrocytes already excluded), which can be differentiated from stromal cells mainly by their carried surface marker CD45. This surface protein belongs to the family of protein tyrosine phosphatases and has a crucial role in terms of cell growth and development [148]. The cells which are not in the CD45 positive gate are known as stromal cells. They only make a small amount of the total cell composition of the lymph node. Nevertheless the stromal compartment consists of multiple populations as mentioned above. To distinguish them, fluorescence-labeled antibodies against CD31 and gp38 are necessary. By using both of these antibodies, one can clearly see a separation between the four stromal populations (as shown in figure 7): Blood endothelial cells are only CD31 positive and fibroblastic reticular cells are only gp38 positive, while lymphatic endothelial cells carry both of these markers on their surface. When intended to prove whether FRCs posses leptin receptor in their cell membrane, a leptin receptor staining is added and checked in a last gate on FRCs.

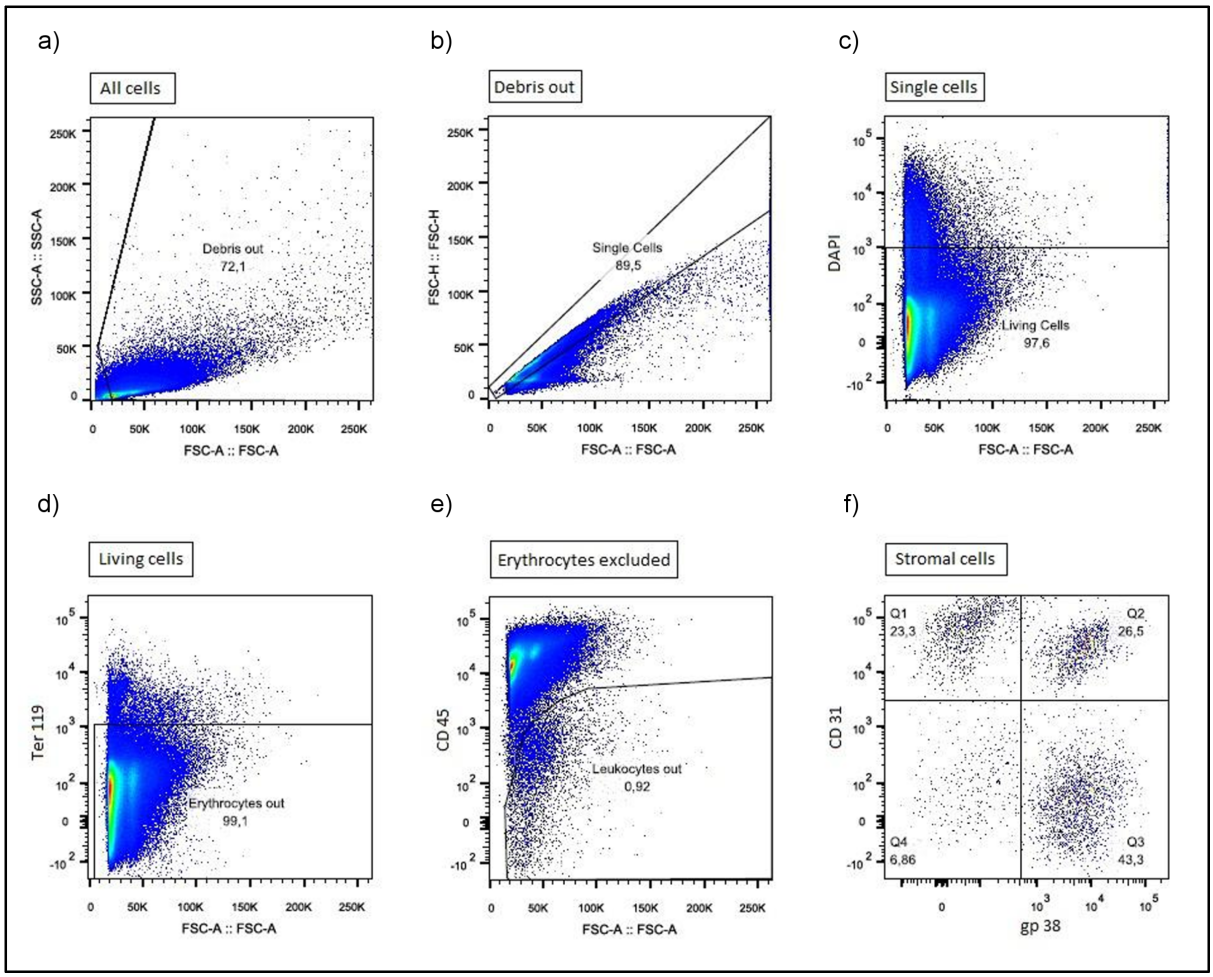

Figure 7: Exemplary gating of stromal cell populations: An exemplary gating for most experiments is displayed in this figure, the subfigures will be explained in the following part. a) As small cell-like bodies like microparticles, extracellulary vesicles, microsomes, apoptotic bodies and cell debris are not focus of the investigation in this work, they are ruled out by using forward and sideward scatter given that these cell-like bodies are as a rule smaller than regular cells. b) Doublets, triplets etc. can, dependent on the target of research, falsify the result. In the aspect of differentiation within the stromal cell department however, it is not always necessary to exclude cell agglomerates since these populations can be clearly distinguished by the help of their markers. To see whether a signal comes from a cell cluster or from a single cell, one compares forward scatter width and forward scatter height and all single cells should be within a certain range around a linear line which is determined by extrapolation of the beginning slope of the signal. The more volume a single cell gains, the more rises its signal from forward scatter width and forward scatter height, a cell doublet of the same volume is more likely to just have an increased signal in the forward scatter width. Because of that, every event not in this range is likely to be a cell cluster and therefore excluded from further gating. c) Dead cells are excluded by gating out DAPI positive signals (provided by Miltenyi Biotec, Bergisch Gladbach), hence dead cells can't transport this molecule out of their cell core in the extracellular space and so they appear positive in the corresponding channel [182]. PI (provided by Miltenyi Biotec, Bergisch

Gladbach) on the other hand is not able to pass the membrane of living cells, so dead cells stained with PI show a positive signal in the corresponding channel [183]. d) Ter 119 is used to rule out erythrocytes, while Ter 119 positive cells are classified as erythrocytes, all Ter 119 negative cells are not and therefore further gated [108, 70]. e) Leukocytes are characterized by the surface marker CD45 [18]. If leukocytes were target of the examination, all CD 45 positive cells have been gated and further characterized with specific antibody combinations. Stromal cells however do not carry CD45 on their surface and are therefore contained in the CD 45 negative gate. f) Whereas both endothelial cell types, the lymphatic and blood endothelial cells carry CD31, only lymphatic endothelial cells carry gp38. On the other side fibroblastic reticular cells are also in possession of gp38 but one does not find CD31 in their membrane, allowing to distinctively distinguish these three populations [61].

5.1.1.1 Outgating of cell debris

As small cell-like bodies like microparticles, extracellular vesicles, microsomes, apoptotic bodies and cell debris are not focus of the investigation in this part of the experiment, they are ruled out by using forward and sideward scatter, given that these cell-like bodies are smaller than regular cells, see figure 7a).

5.1.1.2 Doublet exclusion

Similar to cell debris, doublets, triplets etc. can falsify the result. In the aspect of differentiation within the stromal cell department however, it is not always necessary to exclude cell agglomerates since these populations can be clearly distinguished by the help of their markers. To see whether a signal comes from a cell cluster or from a single cell, one compares forward scatter area and forward scatter height. All single cells should be within a certain range around a linear line which is determined by extrapolation of the beginning slope of the signal. The more volume a single cell gains, the more rises its signal from forward scatter area and forward scatter height, a cell doublet of the same volume is more likely to just have either an increased signal in the forward scatter area, or in the forward scatter height, dependent on the steric orientation of the cell cluster. Because of that every event which has either a

strong signal on either of both detectors is likely to be a cell cluster and therefore excluded from further gating (see figure 8).

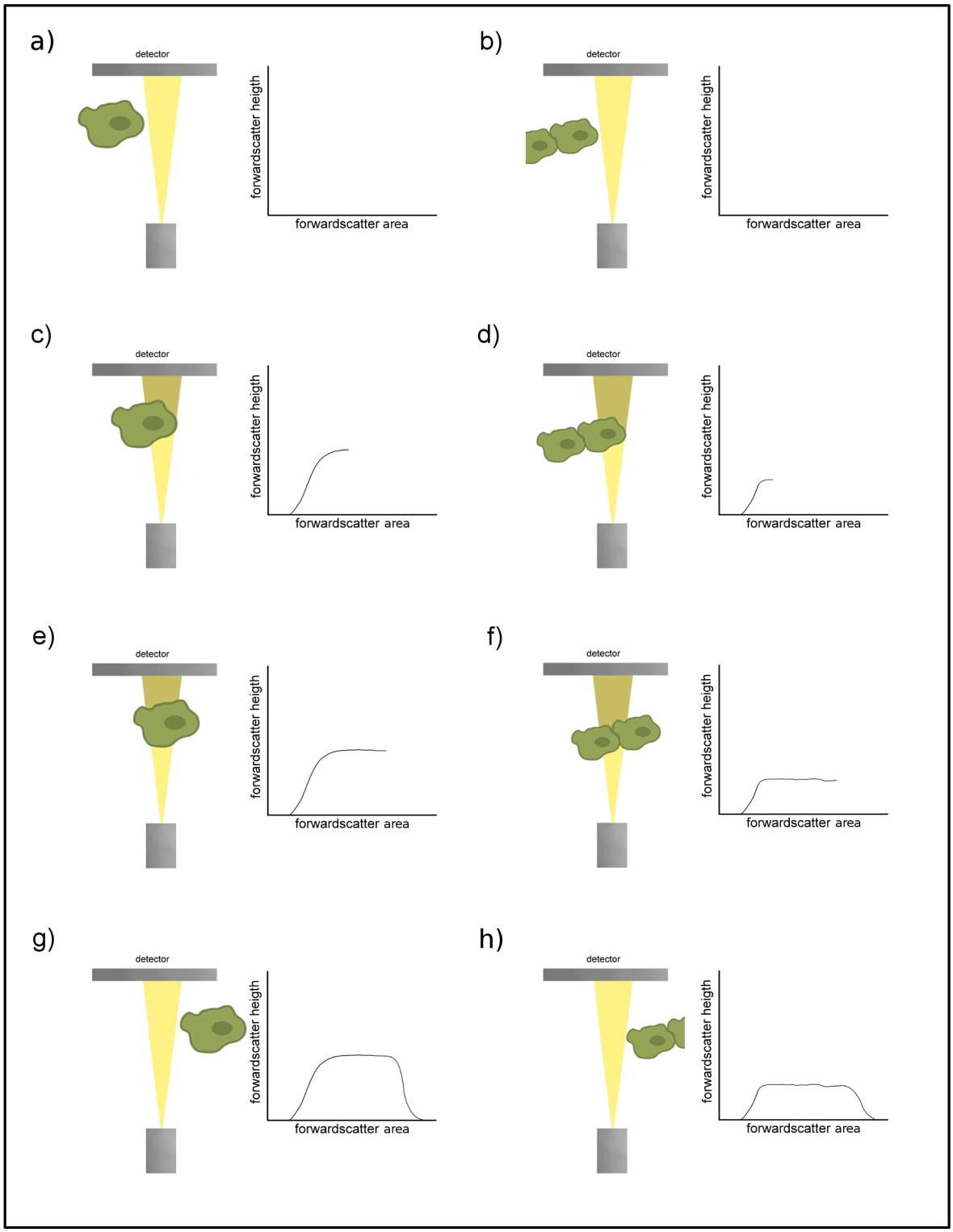

Figure 8: Differentiation between single cells and cell clusters: This illustration shows how forward scatter height and forward scatter area react to different cell constellations and how the resulting data can be interpreted. Whereas the image shows on the left side a big cell with the dimensions width=a and height=a, which will move through the light beam in the following subimages,

on the right side it shows two smaller adherent cells, a so called doublet, with the dimensions width=a and height=a/2, is moving through the light beam. Next to the cells, the related signal of the forward scatter height on the y-axis and the signal of the forward scatter area on the x-axis is shown. a) The single cell moves towards the light beam, as it does not cross the laser beam, no signal is triggered. b) The cell doublet moves towards the laser beam, as it does not cross the laser beam, no signal is triggered. c) The single cell enters the laser beam, its bigger diameter results in a higher signal of the forward scatter height. d) the doublet enters the laser beam, since its diameter is smaller than the bigger cell's, the signal of the forward scatter height is also smaller. e) The single cell moves through the laser beam, as its maximum diameter is reached, the forward scatter height signal does not increase, whereas the forward scatter area signal still ascends. f) The doublet moves through the laser beam, as its maximum diameter is reached, the forward scatter height signal does not increase, whereas the forward scatter area signal still ascends. g) The single cell leaves the laser beam, the forward scatter height and area signals decline and reach zero. h) The doublet leaves the laser beam, the forward scatter height and area signals decline and reach zero. This illustration shows that the relation of forward scatter height and area when measuring single cells is always close to 1, while the relation of forward scatter height and area drops the more cells are chained together. This explains the structure of the gate to rule out cell agglomerations, since it is by approximation the bisectrix of the y- and x-axis.

5.1.1.3 Dead cell exclusion

As a dead cell dye 4'6-Diamidin-2-phenylindol (DAPI) and propidium iodide (PI) have been used. The use of either of these dyes was dependent on additional fluorochromes in the staining mix. If these were detected in the V1-channel of the flow cytometer, PI instead of DAPI has been used since DAPI is also detected in the V1-channel, whereas PI is detected in the channel B3 (480 nm laser, 655-730 filter). Along with their different detection channel, the staining mechanism of these two dead cell dyes is different. DAPI passes the cell and core membrane of both, dead as well as living cells and binds to the AT region of dsDNA. The living cell entry is less efficient and appears lower than the dead cells, additionally, living cells transport DAPI to the extracellular space. DAPI positive cells appear positive in the corresponding channel when excited by light of a wavelength of 405 nm [182]. PI on the other hand is not able to pass the membrane of living cells so that it is commonly used to for dead cell stains. When this compound is in solution it has its excitation

peak at 493 nm and its emission peak at 636 nm, once bound, the fluorescence enhances by 20 to 30 fold and the excitation and emission spectrum changes to 535 nm for excitation and 617 nm for emission [183]. As shown in figure 7**,** dead cells are excluded by gating on the DAPI and PI negative section.

5.1.1.4 Exclusion of erythrocytes

During the course of preparation, erythrocytes are enriched as by-product of the digest. Erythrocytes carry neither CD45 nor CD31 or gp38 and therefore appear in the double negative gate of the stromal cell compartment. Ter119 was used to rule out erythrocytes. This surface marker is present on the red blood cell development line from proerythroblasts up to adult erythrocytes [186]. Ter 119 antibody's conjugate PE-Cy 7 is detectable by showing a signal in the channel B4 (laser 488 nm; filter 750 nm LP) and therefore can be outgated unambiguously.

5.1.1.5 Leukocyte gating

Leukocytes are with approximately more than 99% of the total lymph node's cells the biggest population of this secondary lymphoid organ. Therefore it is of most importance to gate on leukocytes precisely because they can easily derange the results of the analysis. The leukocytic surface marker CD45 belongs to the protein tyrosine phosphatase family, which is known to modulate cell development like mitosis, growth, differentiation and oncogenic transformation. CD45 also regulates T- and B-cell antigen receptor signaling. CD45 has an extracellular domain, one transmembrane chain and an intracellular catalytic domain which is composed of two tandem chains [34, 148]. If leukocytes were target of the examination, all CD45 positive cells have been gated and further characterized with specific antibody combinations.

5.1.1.6 Differentiation of the stromal cell compartment

In order to identify stromal subpopulations, in this study, two main markers were utilized: CD31 and gp38 also known as podoplanin. EndoCAM, PECAM1 or CD31 is, as its first abbreviation suggests, a protein which is strongly represented in endothelial cell types such as blood endothelial cells and lymphatic endothelial cells. Furthermore it is also translated within the cells of the hematopoetic line, such as certain macrophage populations. CD31 is related to immunoglobulins and plays probably a role in leukocyte migration, intercellular connections between endothelial cells, activation of integrins and angiogenesis [33]. The other important marker is podoplanin, which is a type-1 integral membrane glycoprotein that can help to further discriminate within the stromal cell compartment [35]. While both endothelial cell types, the lymphatic and blood endothelial cells, carry CD31, only lymphatic endothelial cells carry gp38. On the other hand, fibroblastic reticular cells are also in possession of gp38 but do not express CD31 in their membrane, allowing distinguishing these three populations as seen in figure 7. CD31 with its FITC dye appears positive in the channel B1 (laser 488 nm; filter 525/50 nm) whereas podoplanin with its APC-Cy 7 conjugate is detectable in the channel R2 (laser 635 nm; filter 750 nm LP).

5.1.2 Lymph node structure in mice

The main target of this research was to rule out how the structure of lymph nodes in respect of their cellular composition is affected by periods of starvation and recovering from it. This is relevant not just in sight on today's popular diets but also in respect of unregular food uptake or famine and related immunodefiency as well as cancer cachexia. In this study, the focus lays on the contribution of distinct lymph node cellular populations. Special emphasis was put on dendritic cells and fibroblastic reticular cells, as these have been shown to interact in order to adapt lymph node size and structure to external stimuli [11], thus contributing to an environment in which immune response can be initiated and controlled properly. To

investigate this, mice were separated into three groups: One group with ad libitum acces to food and water, one group with ad libitum acces to water but not to food for 48h (so called starvation group). And a third group, which after treatment like in starvation group was granted access to food and water for 72h (so called regression group). The following section describes the results determined by these experiments.

5.1.2.1 Distribution of FRCs

FRCs, or fibroblastic reticular cells are a stromal subset which is characterized as CD31 negative and gp38 positive. They build up the lymph node's scaffold and reticular fiber network, in which soluble molecules such as cytokines and antigens are transported. Furthermore they are able to modulate T-cells and are therefore important actors in the immune system. The following section deals with the dispersion of fibroblastic reticular cells in subcutaneous lymph nodes during steady-state, starvation and regression from starvation. Analyzing the data of our experiment, we estimate around 2163,36 fibroblastic reticular cells to be averagely present in one subcutaneous lymph node of a C57Bl/C57Bl/6 mouse. The values however range from 558 FRCs per lymph node up to 4382 FRCs per lymph node (see figure 9a). If it comes to starvation, the average amount of fibroblastic reticular cells counts 1830,83 per subcutaneous lymph node, ranging from 267 FRCs per lymph node up to 2838 FRCs per lymph node. This difference however is not significant (p=0,5881; unpaired t-test; n(control)=11; n(starvation)=6; figure 9a). Surprisingly, in the regression group, a heavy drop in fibroblastic reticular cell numbers happens, which we detected 72h after the starvation phase ended (see figure 9b). The average count of fibroblastic reticular cells after 48h of starvation and the subsequent 72h regression phase is 719,333 per subcutaneous lymph node. The individual values ranged from 252 cells per lymph node up to 1492 cells per lymph node. These values monitor a significant decrease in cell numbers compared to the control group (p=0,0164; unpaired t-test; n(control)=11; n(regression)=6; figure 9b). Not just compared to the control group, but also compared to the starvation group this change in numbers was significant (see figure 9c), as the number of FRCs in the

regression group was obviously lower than those in the starvation group (p=0,0459; unpaired t-test; n(starvation)=6; n(regression)=6; figure 9c). To check on the composition of the stromal subsets, also the distribution of cellular frequency and not just the absolute numbers of these cells were examined. Figure 16 illustrates the cellular frequencies within the stromal compartment. Double negative cells have not been included in the percentages due to technical reasons. In the control group, the biggest portion with an average percentage of 43,398% of all stromal cells is build up by FRCs (n=11), followed by LECs (n=11) with 32,754%. BECs represent an average percentage of 23,848% (n=11). These differences however are not significant (p>0,05). A different, yet not significant difference is presented by the dispersal of FRCs in the starvation group (p>0,05). Averagely 36.509% of the stromal cells are made up by fibroblastic reticular cells (n=6), whereas the biggest population in the starvation group, exhibited around 39.720%, is formed by lymphatic endothelial cells (n=6). Again, the smallest population are the blood endothelial cells, contributing 23,771% to the stromal species (n=6). The last group, the regression group, shows again a slightly different picture. There average values of the three cell types lie more closely together than in the other groups. The largest population is, like in the control group, represented by fibroblastic reticular cells, with an average value of 38,275%. This time, the smallest population are the LECs, with an average portion of 29,794%. Surprisingly, the centre span is represented by blood endothelial cells, as average 31,931% of the stromal subsets. As it was the case in the control group and in the starvation group, these differences are not significant as well (p>0,05; 2way ANOVA; n=6 mice/group). There are no other significant alterations detectable among the populations. A synopsis of the absolute numbers and relations between all three models is given in figure 10, where also representative gates of the cells are shown. Figure 15 a)-e) illustrates the position of FRCs within the stromal cell compartment.

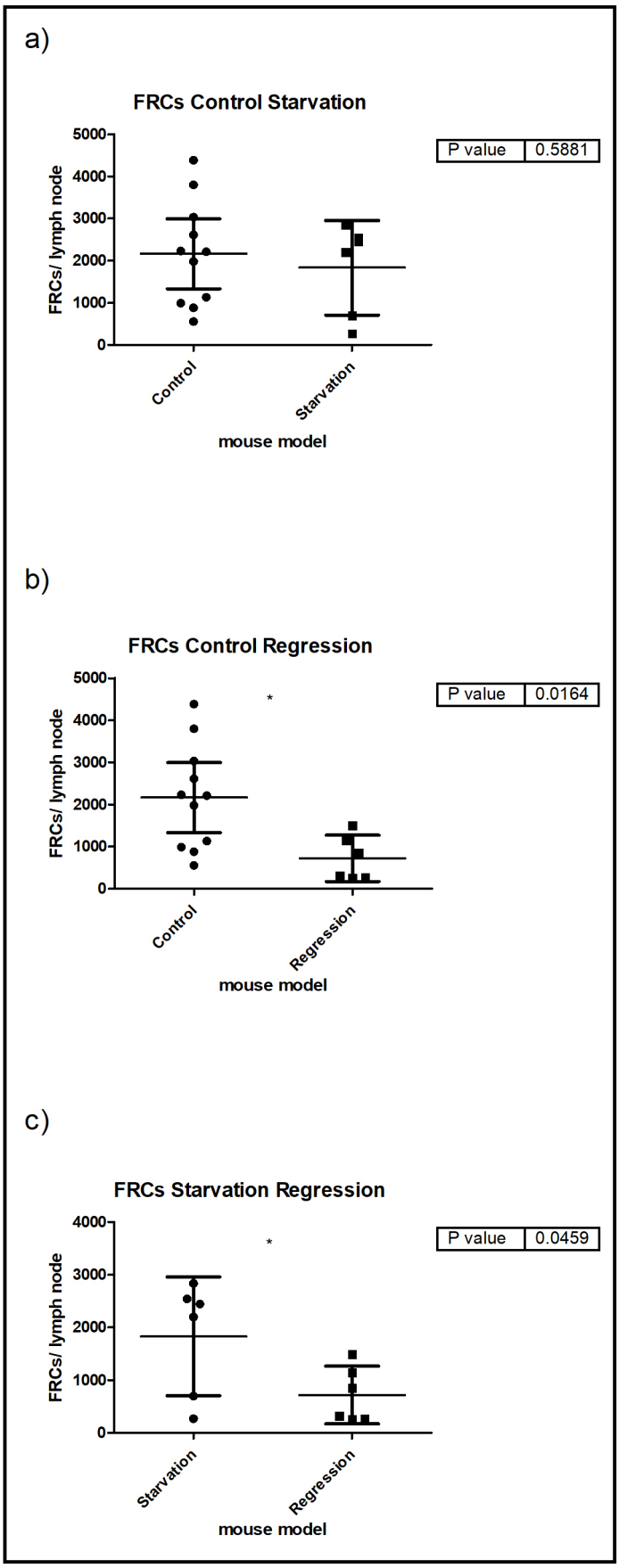
a)
FRCs Control Starvation
FRCs/ lymph node
5000
4000
3000
2000
1000
0
P value
0.5881
Control
Starvation
mouse model
b)
FRCs Control Regression
FRCs/ lymph node
5000
4000
3000
2000
1000
0
*
P value
0.0164
Control
Regression
mouse model
c)
FRCs Starvation Regression
FRCs/ lymph node
4000
3000
2000
1000
0
*
P value
0.0459
Starvation
Regression
mouse model

Figure 9: Distribution of FRCs: In this figure the distribution of FRCs per lymph node is illustrated. The medium bar represents the mean of the given values whereas the lower and upper bar include the 95% confidence interval. a) The comparison of the amount of FRCs per lymph node in healthy control mice (n=11; mean=2163,36 cells/ lymph node) and mice in the state of starvation (n=6; mean=1830,83 FRCs/lymph node) does neither show a significant difference on the 5% significance level (p=0,5881) nor a tendency towards any direction. The highest values in cell count though belong to the control model. b) However if the FRCs of the control group (n=11; mean=2163,36 FRCs/ lymph node) are compared to the group of mice recovering from starvation (n=6; mean=719.333 FRCs/ lymph node), a significant change between two groups is attestable (p=0,0164) in respect of reduced numbers of FRCs in the regression model. c) Also among the starvation group (n=6; mean=1830,83 FRCs/ lymph node) and the regression group (n=6; mean=719,333 FRCs/lymph node) there is a significant change in respect of FRCs numbers (p=0,0459), since similar to b), the total number of FRCs shows a drop in the regression model.

a)

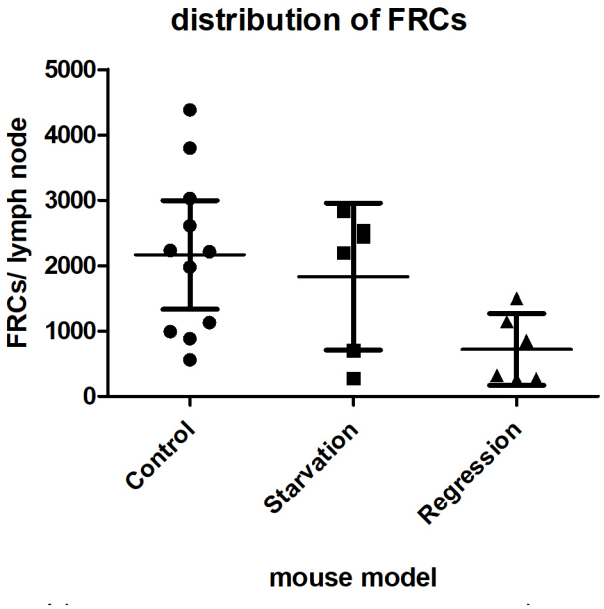

mean of control = 2163,36 FRCs/ lymph node

mean of starvation = 1830,83 FRCs/ lymph node

mean of regression = 719,33 FRCs/ lymph node

b)

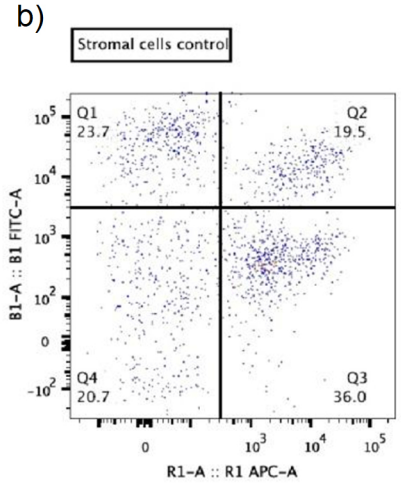

c)

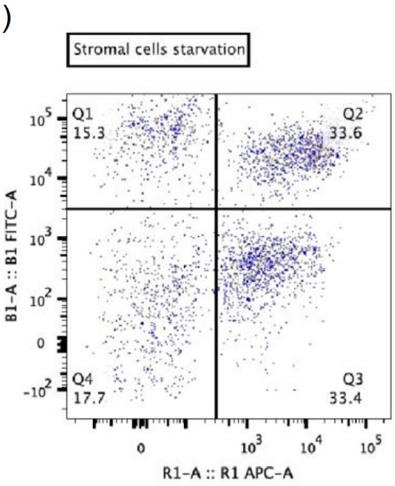

d)

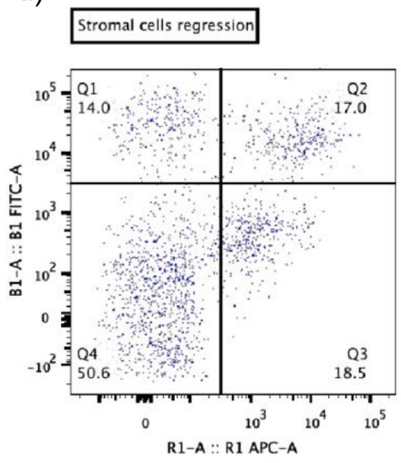

Figure 10: Synopsis of FRC distribution: Figure 10 incorporates the synopsis of figure 9 with an included flow cytometry dot plot example. a) Again plotted on the y-axis is the count of FRCs per lymph node and plotted on the x-axis is the corresponding mouse model. The medium bar shows the mean of the values of each group (mean of control group =2163,36 FRCs per lymph node (n=11); mean of the group of mice in the state of starvation =1830,83 FRCs per lymph node (n=6); mean of the regression group =719,33 FRCs per lymph node (n=6). b) Shows the composition of the stromal cell department after a digest for the production of a single sell suspension with 23,7% BECs, 19,5% LECs, 36% FRCs and 20,7% double negative cells. As in c) and d) in b) on the y-axis is plotted the channel for FITC labeled CD 31 and on the x-axis is plotted the channel for APC labeled gp38. Similar to b) figure 10c) shows the fragmentation of the stromal party in starving mice with 15,3% BECs, 33,6% LECs, 33,4% FRCs and 17,7% double negative cells. d) Introduces the division of the stromal compartment within recovering mice with 14% BECs, 17% LECs, 18,5% FRCs and 50,6% double negative cells.

5.1.2.2 Distribution of lymphatic endothelial cells

Lymphatic endothelial cells, or LECs, are a stromal subset which is characterized by the expression of both, CD31 and gp38, and therefore it is easy to discriminate them from fibroblastic reticular cells and blood endothelial cells. Although they belong to the stromal cell compartment, they fulfill an entirely different tasks than the fibroblastic reticular cells as they are more closely related to blood endothelial cells [195]. LECs build the afferent and efferent lymphatic vessels as their name suggests. The following paragraph deals with the apportionment of these cells in subcutaneous lymph nodes in steady-state situations and in the phase of starvation as well as in the post starvation regression phase. An average of 1633,91 lymphatic endothelial cells populate a subcutaneous lymph node of a C57Bl/6 mouse. But also here, a big variation could be determined, as the values vary from 506 cells per lymph node to 3526 cells per lymph node (see figure 11a)). These values have been determined based on 11 mice/group. The absolute numbers of lymphatic endothelial cells in mice that suffered from 48h starvation showed an analog picture. Averagely 1951 LECs inhabit a single lymph node of starving mice. The range however spans a spectrum from 503 individuals per lymph node to 3974 lymphatic endothelial cells per lymph node. The numbers are alike to those of the control group, hence there is no

significant difference between the two groups (p=0,5835; student t-test)(see figure 11a). Similarly, fibroblastic reticular cells, isolated from mice of the regression group, which suffered 48h from starvation and then had a time span of 72h to recover from the famine, show a massive drop in not just the mean of the cell number, but also the upper range value drastically dropped (see figure 11b). The average amount of lymphatic endothelial cells was an astonishing 601,5 cells in one subcutaneous lymph node, meaning approximately just a third of the mean amount of LECs in the control (mean=1633,91 LECs/ lymph node) and starvation group (mean=1951 LECs/ lymph node). The lowest value counts a total of just 171 lymphatic endothelial cells per lymph node and the highest value is measured with 1317 cells per lymph node. This value is far from the mean of the control group or the mean of the starvation group. Hence it is not surprising that a significant difference can be detected if one compares the values of the regression group to the values of the control group (p=0,0314; student t-test)(see figure 11b)) or of the values of the starvation group (p=0,0416; student t-test)(see figure 11c)). To see what effects the drop in numbers has on the non-hematopoietic compartment as a whole, also the relative amount of the cells within the stromal cell compartment was determined (see figure 16). While in two of the three groups, namely in the control and the regression group, lymphatic endothelial cells are the second biggest stromal subset, in the starvation group, they are the biggest group in respect of sheer numbers and in frequency distribution. In the control and in regression group, they are outnumbered by the fibroblastic reticular cells. While their part in the stromal compartment is averagely 32,754%, that of fibroblastic reticular cells' counts 43,398%. Blood endothelial cells have an average percentage of 23,848% within all stromal cells, however these differences are not significant (p>0,05; 2way ANOVA). As mentioned above, the LECs' compartment is the biggest compared to the other stromal cell populations in the starvation group, counting 39,72%. The LECs outmatch the fibroblastic reticular cells hereby by approximately 3,2%, as the FRCs' average portion is 36,513%. The smallest group is constituted by blood endothelial cells with an average percentage of 23,771%. Also here, the differences between the groups are not significant (p>0,05; 2way ANOVA). The regression group shows again the usual distribution of fibroblastic reticular cells being the biggest subset with 38,275%, followed this time by blood endothelial cells

making up the stromal compartment with 31,931%. The smallest group of stromal cells in the regression group is that of the lymphatic endothelial cells with an average value of 29,794%. The values however do not differ enough to certificate a significant change ($p>0,05$; 2way ANOVA). To take together this data, figure 12 presents a synopsis in which the total values of all three groups are juxtaposed. Also an exemplary gating how the stromal compartment in every model would look like is given. Figure 15 draws a résumé of the position of LECs within the stromal cell compartment.

a)

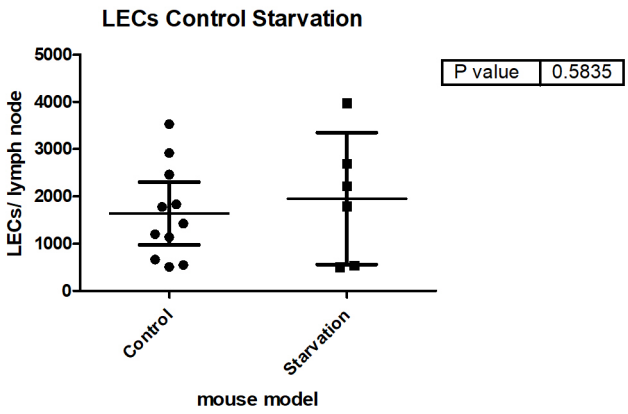
LECs Control Starvation
P value
0.5835
LECs/ lymph node
5000
4000
3000
2000
1000
0
Control
Starvation
mouse model

b)

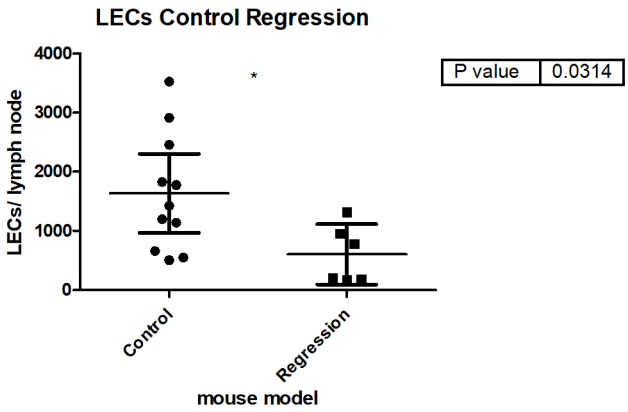
LECs Control Regression
P value
0.0314
*
LECs/ lymph node
4000
3000
2000
1000
0
Control
Regression
mouse model

c)

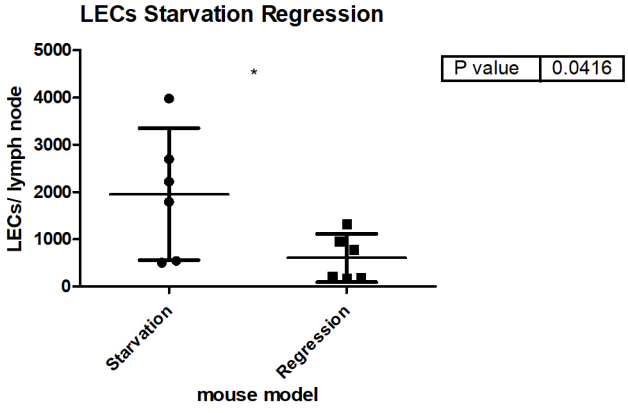
LECs Starvation Regression
P value
0.0416
*
LECs/ lymph node
5000
4000
3000
2000
1000
0
Starvation
Regression
mouse model

Figure 11: Distribution of LECs: Figure 11 portrays the comparison of the distribution of LECs within all three groups of mice. Whereas the number of LECs per lymph node is plotted on the y-axis, the mouse model is shown on the x-axis. The lower and upper bar include the 95% confidence interval, the central bar marks the mean value. a) Presents the amount of LECs in control mice (n=11; mean=1633,91 LECs/ lymph node) and starving mice (n=6; mean=1951 LECs/ lymph node), neither a significant change nor a tendency towards any direction can be proven here (p=0,5835). b) However highlights a significant loss of LECs populating the lymph node of the regression group (n=6; mean= 601,5 LECs/ lymph node) compared to the control group (n=11; mean=1636,82 LECs/ lymph node) (p=0,0314). Alike b), c) shows significantly less LECs again in the regression group by contrast with the starvation group (p=0,0416).

a)

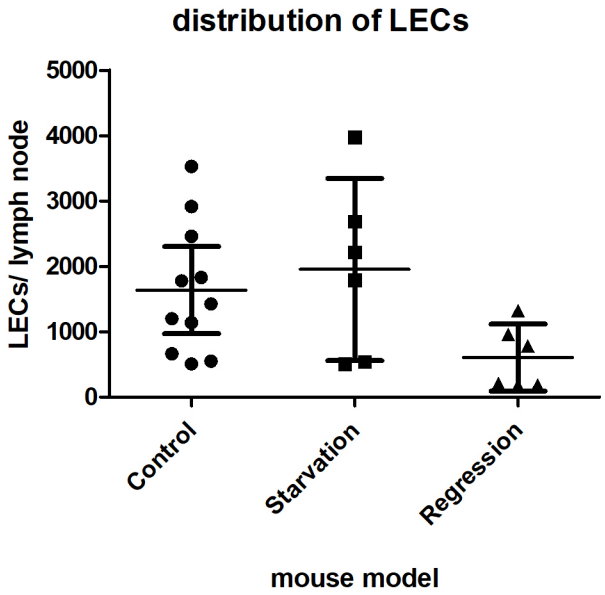

mean of control = 1633,91 LECs/ lymph node

mean of starvation = 1951 LECs/ lymph node

mean of regression = 601,5 LECs/ lymph node

b)

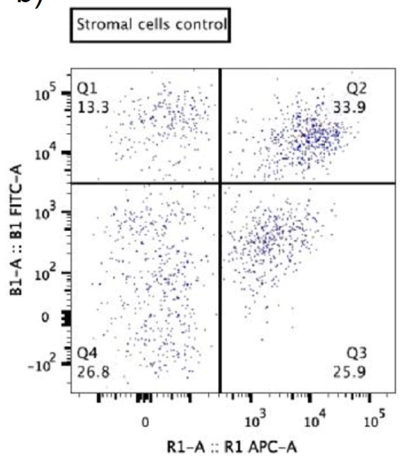

c)

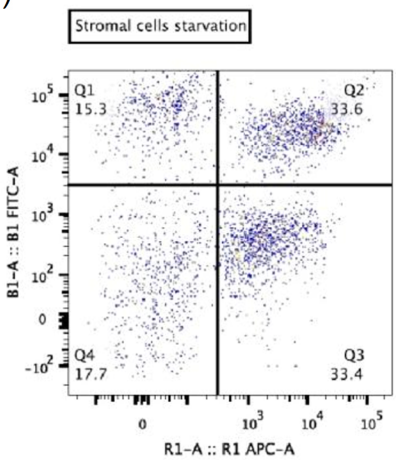

d)

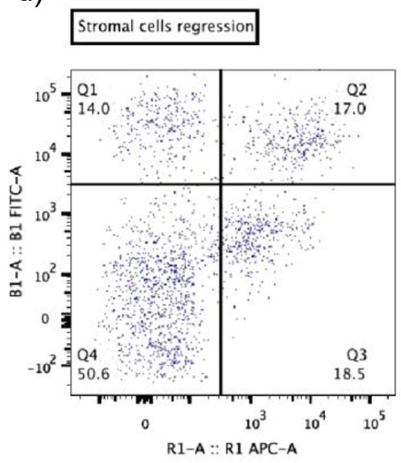

Figure 12: Synopsis of LEC distribution: This data represents a clear view of the preceding figure and an exemplary gate showing the stromal compartment. a) Again the ordinate shows the number of LECs per lymph node and the points on the abscissa stand for the used mouse models. The loss of LECs in the regression model compared to the other models becomes obvious looking at this graph (mean value of control group =1633,91 LECs per lymph node; mean of starvation group =1951 LECs per lymph node; mean of regression group =601,5 LECs per lymph node). Analog to figure 10b), c) and d) have plotted on the y-axis the channel for FITC labeled CD31 and on the x-axis the channel for APC labeled gp38. Figure 12b) shows the layout of the stromal cell compartment in healthy control mice with 13,3% BECs, 33,9% LECs, 25,9% FRCs and 26,8% double negative cells. c) shows the stromal cell composition of starving mice consisting of 15,3% BECs, 33,6% LECs, 33.4% FRCs and 17,7% double negative cells. d) gives information about stromal cell relations in the regression group, namely 14% BECs, 17% LECs, 18,5% FRCs and 50,6% double negative cells.

5.1.2.3 Distribution of blood endothelial cells

Blood endothelial cells, or BECs, are a stromal cell subset which is characterized by the absence of gp38 and the expression of CD31, thus they can be discriminated from FRCs, LECs and double-negative cells easily. They are closely related to lymphatic endothelial cells [195] and adopt alike tasks. They build up the high endothelial venules, which are crucial for cell migration, especially T- and B-cell homing. The paragraph below will elucidate their position within the stromal cell compartment during steady state, starvation and regression. The control group consisted of 11 C57Bl/6 mice which had free access to food and water. The starvation group, consisting of 6 mice has been sacrificed after a 48h period of starvation, in which they still had access to water ad libitum. The last group had 72h time to recover from a 48h starvation phase. In steady-state, an average number of 1122,64 blood endothelial cells has been determined to inhabit a subcutaneous lymph node of a C57Bl/6 mouse, the range however includes values from 405 cells per lymph node to 2227 cells per lymph node (see figure 13a)). They are therefore the smallest stromal cell subset in respect of sheer numbers (see figure 15c)) (due to technical reasons double negative cells have not been included in this consideration). Alike all other stromal populations, their numbers in the starvation model do not differ much from the ones of the control group, for the mean absolute cell number per

lymph node in the starvation model is 908,5. A p value of 0,4071 (student t-test) suggests that there is no significant change in respect of the absolute numbers of blood endothelial cells during starvation (see figure 13b)). Different to the other models, in the regression group again, the number of blood endothelial cells drops critically, resulting in a mean cell number of 517,833 BECs per lymph node, making a significant difference to the control group (p=0,0251; student t-test)(see figure 13b)) and to the starvation group (p=0,0491; student t-test)(see figure 13c)). Figure 16 highlights the relative amount of blood endothelial cells in the stromal compartment of the lymph node. We see that, in the control group and in the starvation group, it is the smallest population, as FRCs in the control group represent 43,398% of the lymph node's stromal cells. The population of FRCs is followed by lymphatic endothelial cells whose part of the stromal division is averagely 32,754% in healthy mice. As stated above, in this model the blood endothelial cells are the smallest population as they build up 23,848% of the lymph node's stroma. Also in starving mice, blood endothelial cells are the smallest of the three stromal subsets, as lymphatic endothelial cells inhabit the lymph node by making 39,72% of the stroma. This time, FRCs are only in the centre span with averagely 36,509%. The remaining 23,771% go to blood endothelial cells. In the last model, the regression model, proportions are different, compared with the control group, fibroblastic reticular cells represent the biggest population with 38,275%, followed this time not by lymphatic endothelial cells, which have this time only an average portion of 29,794%, but by blood endothelial cells, making out 31,931% of the stromal division. 6 mice belonged to the regression group. Figure 14a) juxtaposes the absolute cell numbers of each model for blood endothelial cells to allow direct visual comparison, with the cell number written on the y-axis and the related model on the x-axis. Beyond, representative exemplary gates for every model are given, showing how the stromal subset would presumably look like. A big summary is given in figure 15a)-e) as it shows the position and distribution of blood endothelial cells within the lymph node. While a) and b) incorporate the data of all models and all cell types belonging to the stromal compartment that have been examined, c)-e) give an overview about the cell distribution in distinct models.

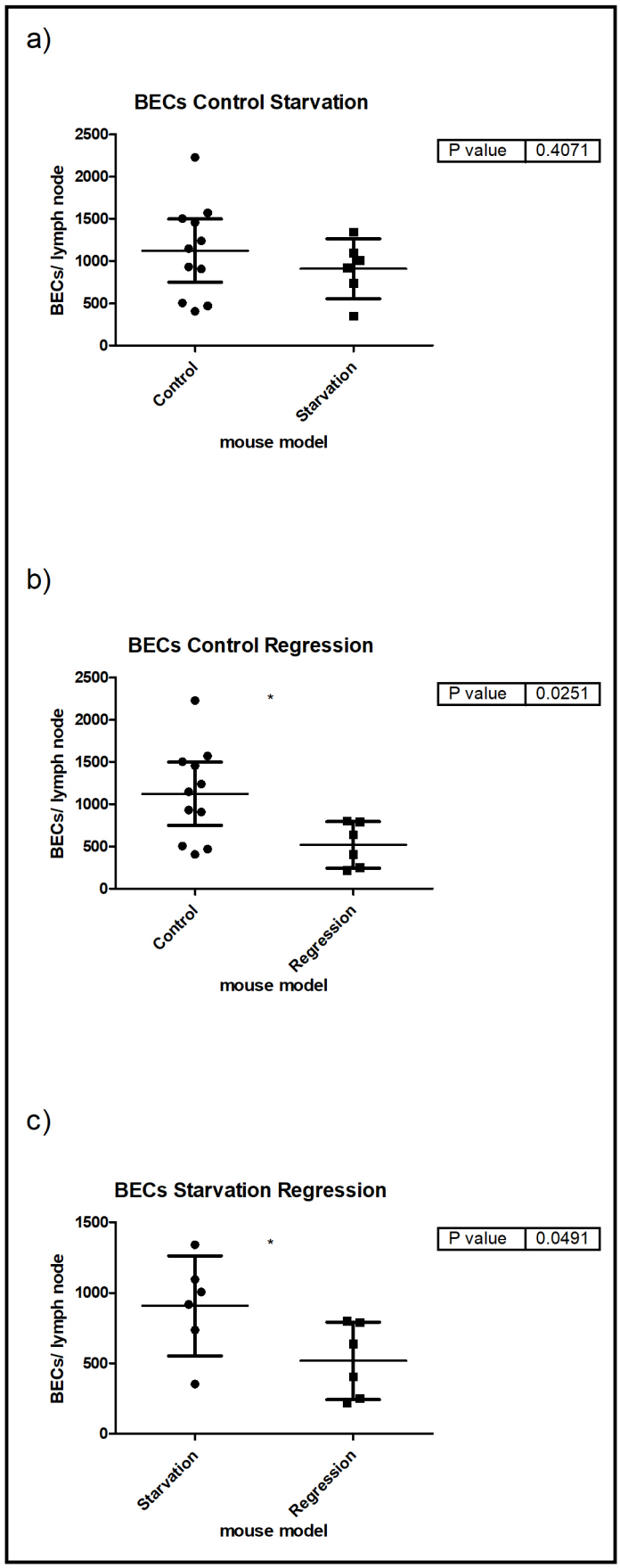
a)
BECs Control Starvation
P value
0.4071
BECs/ lymph node
2500
2000
1500
1000
500
0
Control
Starvation
mouse model
b)
BECs Control Regression
P value
0.0251
*
BECs/ lymph node
2500
2000
1500
1000
500
0
Control
Regression
mouse model
c)
BECs Starvation Regression
P value
0.0491
*
BECs/ lymph node
1500
1000
500
0
Starvation
Regression
mouse model

Figure 13: Distribution of BECs: As we look on blood endothelial cells, figure 13 gives the facts about the amount of those cells per lymph nodes (plotted on the ordinate) regarding the nutrition status (plotted on the abscissa). The bars show the mean and the 95% confidence interval. a) Alike FRCs and LECs there's no significant difference amongst control and starvation group (p=0,4071; student t-test). However b) shows a significantly decreased number of BECs in the lymph nodes of recovering mice, mean(control) =1122,64 BECs per lymph node compared, to mice who didn't hunger, mean(regression) =517,833 BECs per lymph node (p=0,0251; student t-test). c) Indicates that recovering mice also have less BECs than starving mice, mean(stravation) =908,5 BECs per lymph node (p=0,0491; student t-test).

a)

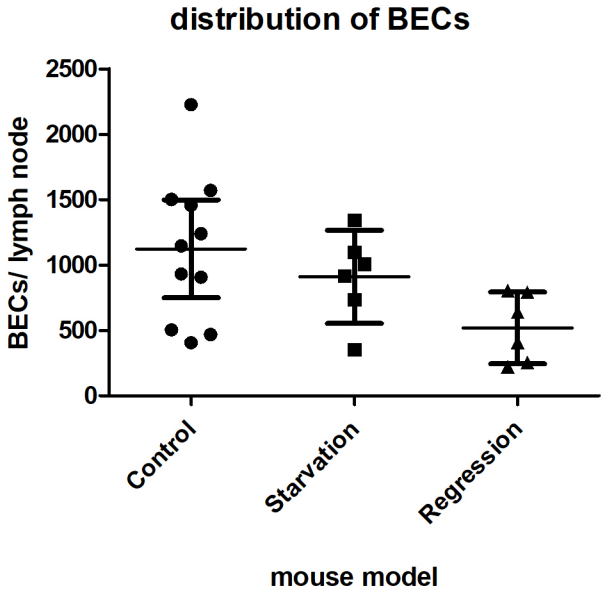

mean of control = 1122,64 BECs/ lymph node

mean of starvation = 908,5 BECs/ lymph node

mean of regression = 517,833 BECs/ lymph node

b)

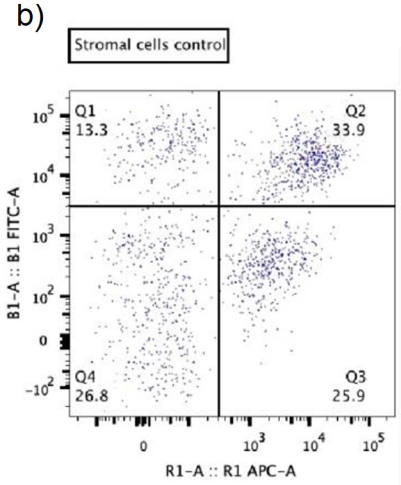

c)

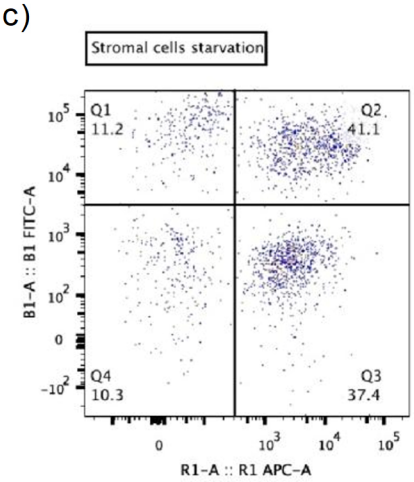

d)

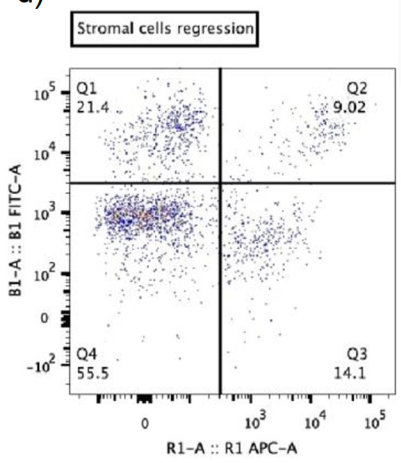

Figure 14: Synopsis of BEC distribution: This figure merges figure 13 and has the same axis labeling concerning a) and again, the graph's bars show mean value and include the 95% confidence interval. The mean values show the decrease of BECs from the control group (n=11) over the starvation group (n=6) down to the regression group (n=6) whereas the difference amongst control and starvation group is not significant, but it is among control and regression group and also between starvation and regression group (mean of control group =1122,64 BECs per lymph node; mean of starvation group =908,5 BECs per lymph node; mean of regression group =517,83 BECs per lymph node). The dot plots in b) c) and d) point out the apportionment of stromal cells in the different mouse models. The detection channel for FITC labeled antibodies on the y-axis is plotted against the detection channel for APC labeled antibodies on the x-axis. For b), which represents the control group, that is 13,3% BECs, 33,9% LECs, 25,9% FRCs and 26,8% double negative cells. The starvation group example, present in c) has approximately the same percentage for BECs as the healthy control, namely 11,2%. The percentage of LECs is with 41,1% higher than in the control group. Also increased is the percentage of FRCs with 37,4% compared to the control group. Only double negative cells with 10,3% have a lower percentage than in healthy control. d) Gives evidence of the stromal compartment in recovering mice with following percentages, BECs 21,4%, LECs 9,02%, FRCs 14,1% and 55,5% double negatives.

a)

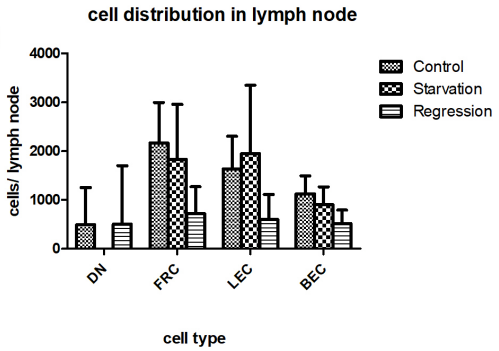

n(Control FRC; LEC; BEC)= 11
n(Control DN)= 3
n(Starvation FRC; LEC; BEC)= 6
n(Regression FRC; LEC; BEC)= 6
n(Regression DN)= 3

b)

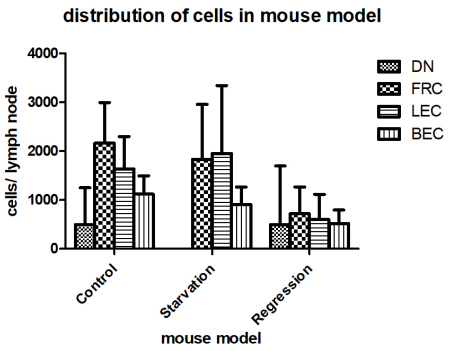

n(Control FRC; LEC; BEC)= 11
n(Control DN)= 3
n(Starvation FRC; LEC; BEC)= 6
n(Regression FRC; LEC; BEC)= 6
n(Regression DN)= 3

c)

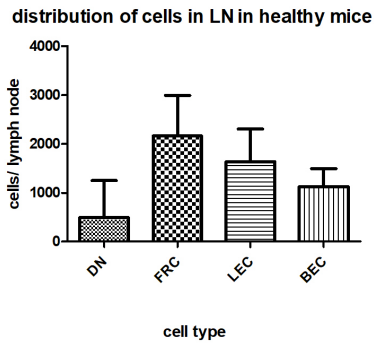

n(FRC; LEC; BEC)=11
n(DN)= 3

d)

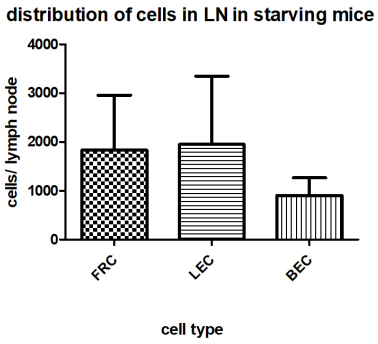

n(FRC, LEC, BEC)=6

e)

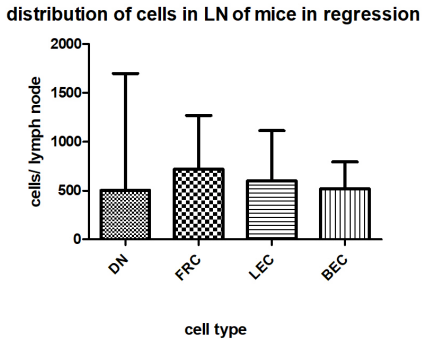

n(FRC; LEC; BEC)=6
n(DN)=3

f)

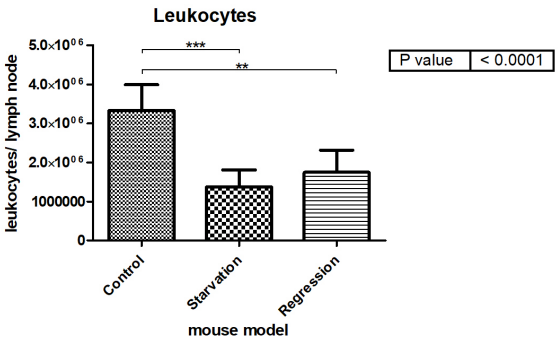

n(Control)= 11
n(Starvation)= 6
n(Regression)= 6

Figure 15: Summary of cellular lymph node composition: The illustration is a summary of the cellular composition of mice's lymph nodes and accounts for stromal cells as well as leukocytes. The y-axis is labeled in a), b), c), d) and e) as cells per lymph node and in f) as leukocytes per lymph node. The x-axis shows in a), c), d) and e) the cell type and in b) and f) the mouse model. In all subfigures the top of the box represents the mean value and the upper bar represents the upper border for the 95% confidence interval. It holds for the control group n(FRCs;LECs;BECs)=11, n(DN)=3, n(leukocytes)=11; for the starvation group n(FRCs;LECs;BECs; leukocytes)=6, for the regression group n(FRCs;LECs;BECs; leukocytes)=6 and n(DN)=3. a) shows each stromal cell population in comparison to the three mouse models as explained in the preceding figures. b) shows the cell composition for each mouse model. c) d) and e) show again the distinct cell numbers for each mouse model in detail, whereas c) shows the healthy control, d) the starvation group and e) the regression group. Subfigure f) shows the difference in leukocyte population amongst the mouse models. Here is to mention that leukocytes in the starvation group are significantly reduced compared to the control group, and the leukocytes in the regression group are also significantly reduced than those in the control group ($p<0,0001$; 1way ANOVA).

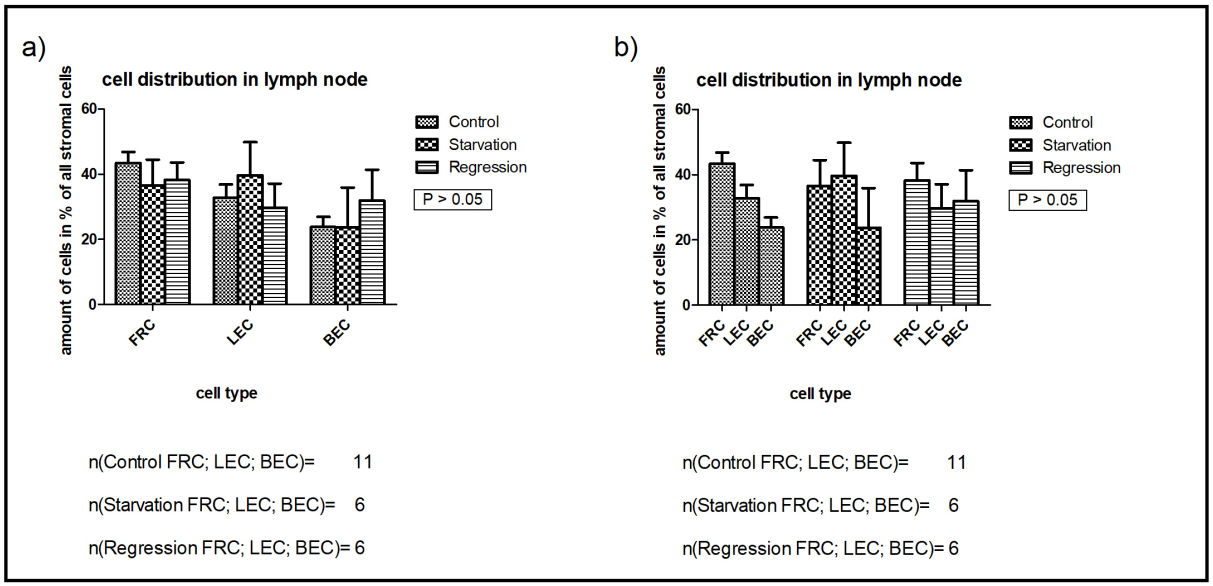

Figure 16: Percentual distribution of stromal cells: The illustration above provides an overview on how the lymph node's stroma is composed. The y-axis shows the percentage of the cell populations. a) Discriminates each cell population (x-axis) in respect of the mouse model, while b) shows each model individually and separates it into stromal subsets. However there are no significant changes detectable in either of the populations ($p>0,05$). While FRCs have together with LECs the highest proportion of the stromal compartment, BECs tend to form the smallest population of all stromal cells.

5.1.2.4 Leukocytes

In this study, leukocytes are defined by CD45 expression, which includes myeloid cells, such as dendritic cells, macrophages, granulocytes on one hand and lymphocytes and innate lymphoid cells on the other. They are an inhomogeneous group of cells, as some of them belong to the innate immune system, some to the acquired immune system and some, such as the dendritic cell, compromise both of them. Dendritic cells, T-cells and B-cells also have been examined separately in the murine blood. The examination of leukocytes led to astonishing results: Before the effect of famine shows in the stromal cell's population, leukocytes already show a massive drop in numbers, indicating a higher sensitivity to starvation. In the phase of regression, one can see that the numbers of leukocytes are still decreased, but, even if not significantly, they have a tendency to regenerate. Figure 15f) illustrates the dynamics of leukocytes during the experiments. As the mice have access ad libitum to water and food, the leukocytes counted 3,331*10^6 cells per lymph node, ranging from 2,053*10^6 cells per lymph node to 4,86*106 cells per lymph node (n=11 mice/ group). As during starvation, the stromal cell compartment, fibroblastic reticular cells, lymphatic endothelial cells or blood endothelial cells, didn't show a significant change in numbers. This is different within the leukocyte's lineage as they drop very significantly in numbers ($p<0,01$; 1way ANOVA), only having left an average of 1,368*10^6 cells per lymph node, which is approximately a third of the output value of the leukocytes in the control group. As one checks on the leukocyte population in the regression model, one can see that the numbers of leukocytes are still decreased if compared to the control group. They count averagely1,745*10^6 cells per lymph node in an individual which has rested and recovered for 72h after starvation. This is a high significant change ($p<0,0001$; 1way ANOVA). However, the numbers of leukocytes in mice that are recovering and the numbers of leukocytes in mice that endured starvation are not significantly different ($p>0,05$; 1way ANOVA), n=6 mice/group.

5.1.2.5 Dendritic cells

Dendritic cells, or DCs, are a subpopulation of leukocytes, which possesses the special property to compromise both, the innate and the acquired immune system, as they modulate immune response of macrophages and lymphocytes. The dendritic cell is a professional antigen-presenting cell [163]. Dendritic cells possess the ability to provide survival signals for FRCs [1, 11], which could be the cause of the massive drop down of FRCs in regression. We can differentiate resident dendritic cells and immigrated dendritic cells in the lymph node, which both have different properties concerning their movement and resting pattern (see 3.1). In this study we define dendritic cells via surface molecules. All cells which are CD45 positive and CD11c positive are considered to be dendritic cells. Within the CD11c positive compartment, we distinguish two different leukocyte populations: CD11c high and a CD11c low population. CD11c high cells represent classical DCs while the CD11c low cells are a mixture of macrophages and DCs. Figure 17 shows an exemplary gating of DCs, which we used in our work. An overview on how the percentual dispersal of the classical dendritic cells in the lymph node looks like is given in figure 18. It is apparent that there is a big gap in respect of absolute numbers between the two described subpopulations (CD11c high and low) as there are more CD11c low+ DCs present in a single lymph node than there are CD11c high+ DCs. Both populations are differently affected by the impact of starvation and the following phase of food reuptake. CD11c high+ DCs seem to be unaffected by the change in nutritional status, the mean of CD11c high+ DCs per lymph node stays almost unaltered ($p=0,8706$; student t-test; n(control; starvation)=3), as in steady state there are averagely 1,452*10^4 of those DCs present per lymph node and in regression this number changes to 1,586*10^4. CD11c low+ cells (mixture of myeloid-lymphoid cells) however are heavily affected by the status of under nutrition, their number drops significantly ($p=0,0463$; student t-test; n(control; starvation)=3) from a mean of 6,002*10^4 cells per lymph node to a mean of 3,236*10^4 cells per lymph node. It has to be mentioned that too few mice have been used to produce these values, so that a valid statistic analysis is not possible here, however it may be possible to see a tendency. Hence the p value is mentioned for the sake of completeness. The results

of this experiment remain to be confirmed by higher numbers of repetitions. As all stromal populations drop in numbers during the regression phase, it has to be examined if cell death is caused by leptin signaling, the loss of dendritic cells or has an unknown origin. As FRCs closely interact with immune cells, the reduced number of CD11clow cells during regression could be a trigger for stromal cell death or alteration. DCs regulate the contractility and survival of FRCs by the help of CLEC-2/Podoplanin interaction. Gp38 or podoplanin controls the contractility of FRCs via actomyosin. During steady state, when not bound by a ligand, gp38 signalling leads to the contraction of the FRC's fiber network. However, during inflammatory conditions, DCs migrate to the lymph node and provide FRCs with CLEC-2, CLEC-2/gp38 binding is critical for the DCs' ability to move along the reticular fiber network, however the ligation of CLEC-2 to gp38 seems to impair the signaling of podoplanin and therefore allows them to expand their reticular fiber network [1, 11, 26]. Furthermore, FRC survival is associated with the elasticity of their surrounding matrix, loss of elasticity will trigger cell death of those stromal cells. In summary, high levels of detectable podoplanin per single cell are an indicator for cell death triggered by the absence of DCs [1, 11]. This is why we examined the expression of APC-labeled gp38 via the mean and median APC fluorescence in FRCs and LECs (see Figure 19 and 20). Both figures show the averaged values of both, the mean and the median APC fluorescence of FRCs and LECs. Each value plotted in this graphic is the mean or median of the APC fluorescence of all single events in a test run. It is obvious, that median and mean show a distinct difference between each other. The mean is prone to outlayers while the median is not, making the median value of APC fluorescence more meaningful than the mean value. In FRCs, the mean value of median and mean APC fluorescence is contradictory, while the average median APC fluorescence drops during regression, the average mean APC fluorescence even rises. Yet the difference between control vs. regression and starvation vs. regression is only significant in the median APC fluorescence of FRCs, see (figure 20a)).

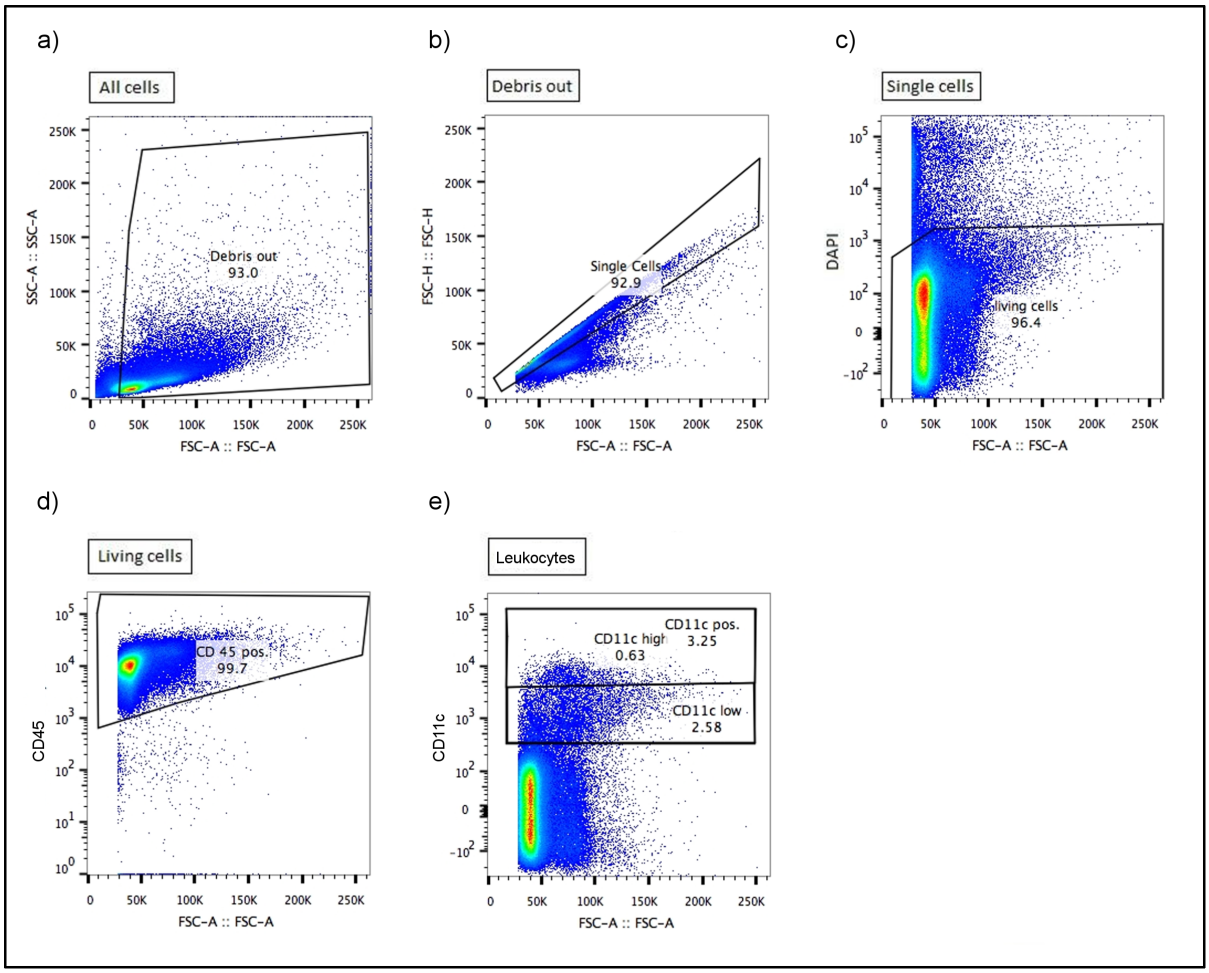

Figure 17: Exemplary gating of DCs: This figure shows an exemplary gating of DCs. a)-c) Are similar to figure 7. As DCs belong to leukocytes, a gate has been drawn around CD45+ cells in d). Subfigure e) shows the differentiation between CD11c high and CD11c low positive DCs within CD45+ cells.

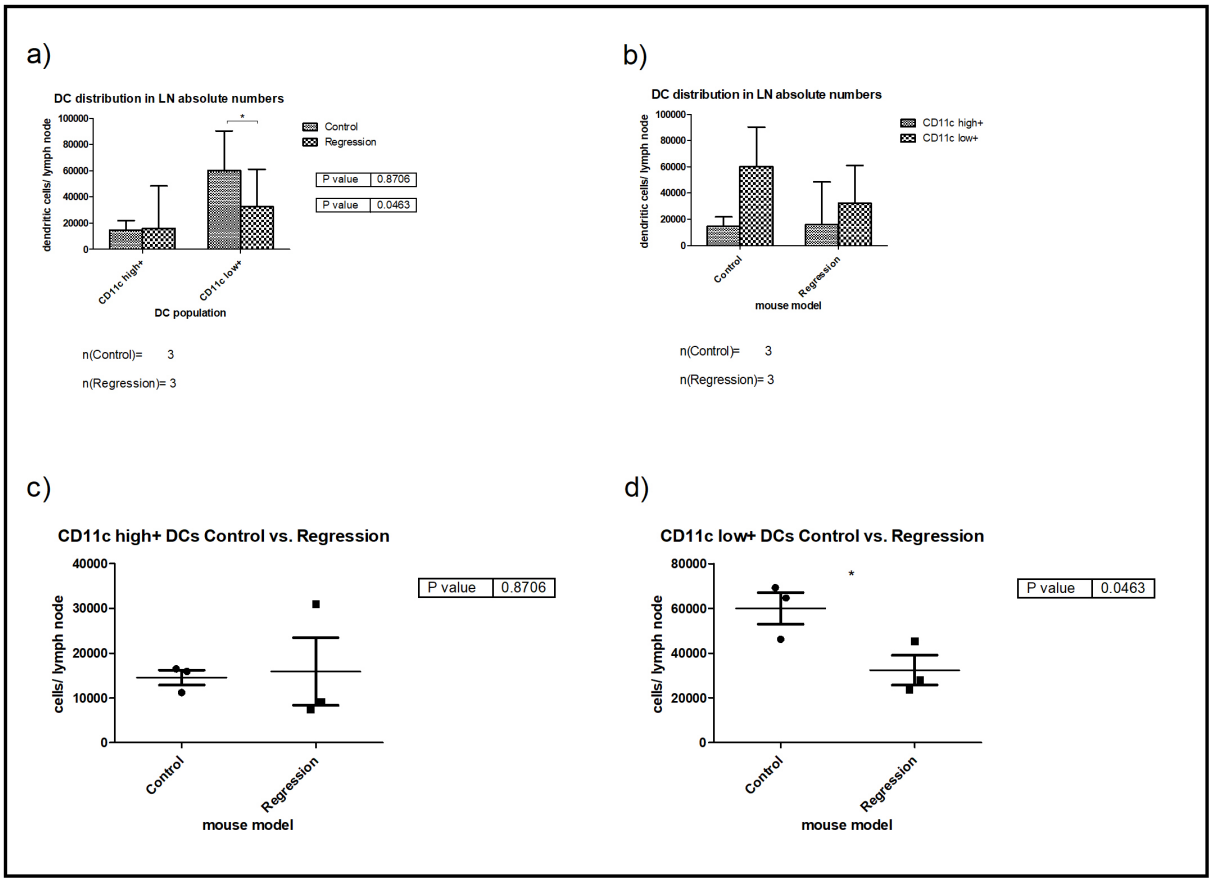

Figure 18: Dendritic cells: An insight on DCs in the mice's lymph nodes during a normal state of nutrition and regression is given here. In this setting, 3 control mice and 3 regression mice were used. Figure 18a) and b) give an overview of the following subfigures. Figure 18a) separates the two populations, shown on the x-axis, while the absolute number of dendritic cells per lymph node is shown on the y-axis. In figure 18b), on the x-axis are listed both mouse models and again the y-axis shows the absolute number of DCs in a lymph node. In all subfigures the mean of the given values is represented by the medium bar, whereas the lower and upper bar include the 95% confidence interval. Both subfigures, a) and b), show that the count of CD11c low+ DCs is much higher than that of CD11c high+ DCs in both, healthy mice and mice in the condition of renutrition. Also, the number of CD11c high+ DCs does not drop during renutrition, in contrast to CD11c low+ DCs, which drop massively in numbers. To break down this figures, c) and d) go into detail. Figure 18c) provides information about CD11b high+ dendritic cells. The y-axis shows again the absolute number of the cells, while the x-axis shows the related mouse model, the mean values do not differ much from each other (mean(control)=14520,3 cells/ lymph node; mean(regression)=15864 cells/ lymph node), so that no significance is measurable (p=0,8706; student t-test n(control; regression)=3). When looking at d), one can see a significant change in numbers. There is a loss of CD11c low+ DCs in the lymph node during the regression phase, their mean number drops from 60020 cells/ lymph node to 32363 cells/ lymph node (p=0,0463; student t-test; n(control; starvation)=3).

a)

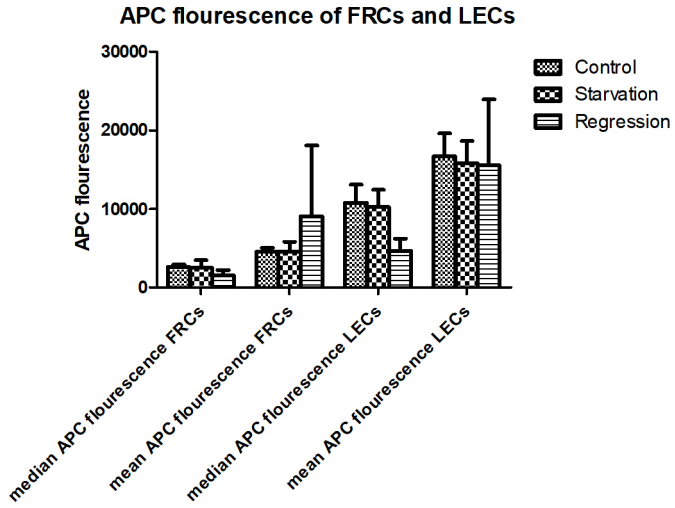

n(Control)= 11

n(Starvation)= 6

n(Regression)= 6

b)

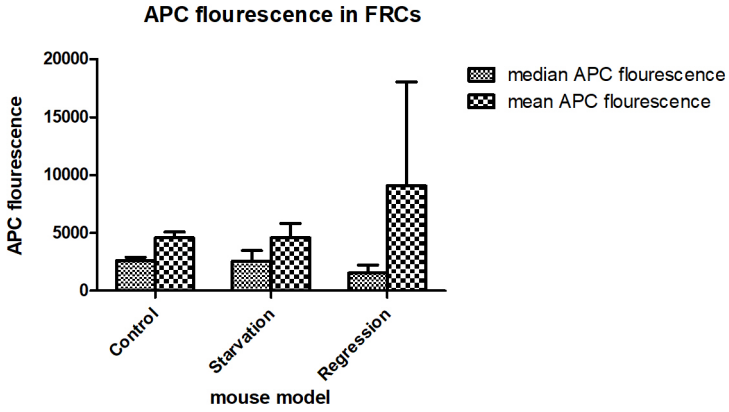

n(Control)= 11

n(Starvation)= 6

n(Regression)= 6

c)

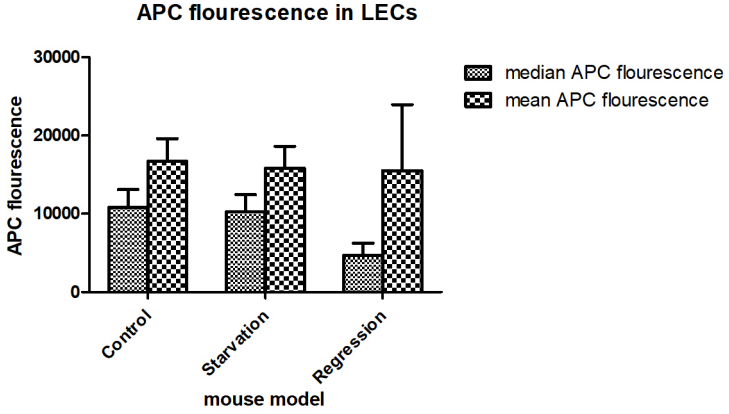

n(Control)= 11

n(Starvation)= 6

n(Regression)= 6

Figure 19: Summarization of APC fluorescence of FRCs and LECs: The APC fluorescence is given on the y-axis on all subfigures. In a) the x-axis shows mean or median APC fluorescence for FRCs or LECs. The same axis shows in b) and c) the experimental system. The top of the box represents the mean value and the upper bar is the upper border of the 95% confidence interval. a) Gives an idea of how mean and median fluorescence in FRCs and LECs looks in the different mouse models. Subfigure b) goes more in detail about mean and median APC fluorescence in the mouse models. Equivalent to b), c) shows the same issue for LECs.

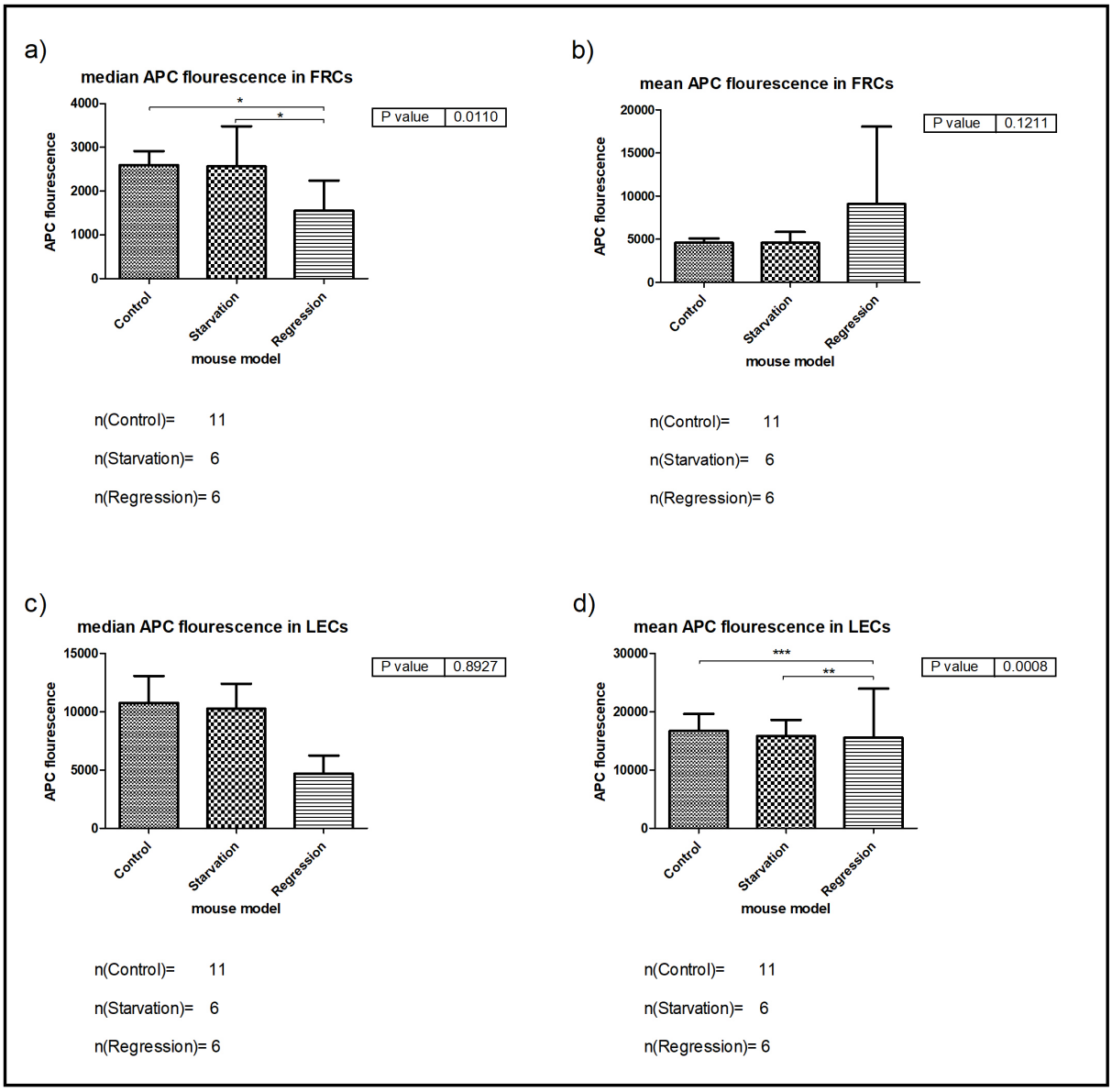

Figure 20: Mean and median APC fluorescence of FRCs and LECs in comparison: This illustration deals with the mean and median APC fluorescence in detail. The APC fluorescence on the ordinate is plotted against the mouse model on the x axis in every subfigure. As in the preceding figure, top row shows the mean value while the upper bar marks the upper border of the 95% confidence interval. a) Pinpoints the median APC fluorescence in FRCs. While the control group (n=11) does not show a significant difference to the starvation group (n=6), both, the control group and the starvation group show a significant difference to the regression group (n=6) which APC fluorescence is lower (p=0,011; 1way ANOVA). b) There are no significant differences within the mean APC fluorescence of the three models detectable (p=0,1211; 1way ANOVA). In contrast to FRCs, the median APC fluorescence of LECs does not change significantly (mean(control)=10769,5; mean(starvation)=10247,2; mean(regression)=4681,5)(p=0,8927, 1way ANOVA, see subfigure c)). Yet d) shows that the mean APC fluorescence in LECs differs between the models. The difference between the mean APC fluorescence of the control group and regression group is very significant

(mean(control)=16679,6; mean(regression)=15511,2), the difference between the starvation group and regression group is very significant (mean(starvation)=15806)(p=0,008; 1way ANOVA).

5.1.3 Steady state and changes in blood

Blood is the main traffic route for hormones, cytokines, chemokines, antigens, catabolic and anabolic molecules, antibodies, complement factors and cells. As there are many cells which migrate between blood and lymph node, the focus in this part of the study lies on T- and B-cells. It is of interest to see how a change in lymph node structure happens during starvation, so we questioned whether these cells are influenced by the effect of a reduced leptin level on FRCs. FRCs provide important homing and survival signals for T-cells, such as CCL21, which is a ligand of CCR7. CCL21 is expressed in a constitutive manner by FRCs. It is not upregulated under inflammatory conditions. Next to cytokines that maintain T-cell homing properties, there are cytokines produced by FRCs which support T-cell survival such as CCL19 [44]. Therefore, it is interesting to see in how far the possibly changed cytokine pattern of FRCs changes the numbers of T- and B-cells in blood. The experimental setting is exactly like the one in the lymph node examination, as blood was taken from the animals that have participated in these experiments, just that no blood has been taken from the regression group due to technical reasons. To generate the blood sample, which was used to check upon lymphocytes, the technique described in 4.5 has been used. Figure 21 gives an exemplary gating of the lymphocyte populations for FACS analysis.

5.1.3.1 T-cells

There are several subtypes of T-cells which fulfill manifold tasks and all of them modulate the immune response. Furthermore these tasks can roughly be grouped in activation of the immune system, or restriction of it, dependent on the type of T-cell. They are characterized by the presence of CD3, which together with the T-cell receptor (TCR) forms the T-cell-receptor-complex [164]. Commonly known T-cell

types are helper T-cells, which are defined by transcription factors and secreted cytokines, cytotoxic T-cells and a plethora of other T-cell-like cells that do show expression of molecules, associated with innate immune responses as well, such as NK-T-cells or gamma/delta-T-cells. In this study however, we examined all T-cells bearing CD3 and did not conduct a further specification. First of all we looked at the absolute number of T-cells in blood. Figure 22a) illustrates the count of described cells in 1ml of mouse blood. In healthy mice, the average number of T-cells per ml blood counts 929,907 cells/ml blood. In the starvation group however, this value almost halves, being 539,946 cells/ml blood, a p value of 0,2279 (student t-test) suggests a missing significance, but as n is only three for both models, the number of used test subjects has to be increased to make a valid statement about the significance of this difference, as a tendency is visible.

5.1.3.2 B-cells

Not as various in their subpopulations as T-cells, but genetically at least as variable, B-cells portray the other significant cell type of lymphocytes. As main actors of the immune system they provide vital support by producing antibodies when activated and differentiated towards a plasma cell. They are typically CD45 positive and exclusively express CD19 and CD20, making it easy to detect those cells with immune stainings, as from a morphological point of view, they very much look alike their CD3 positive counterparts. Figure 22 shows the number of B-cells in blood of mice in the condition of starvation (n=3) and under sufficient nutrition (n=3). As the number of experiments is too low to confirm a significance between both models, there is an obvious trend towards a drop in numbers under starvation visible, for the mean of the control group is 48965 cells/ml blood and for the starvation group 11831 cells/ml blood.

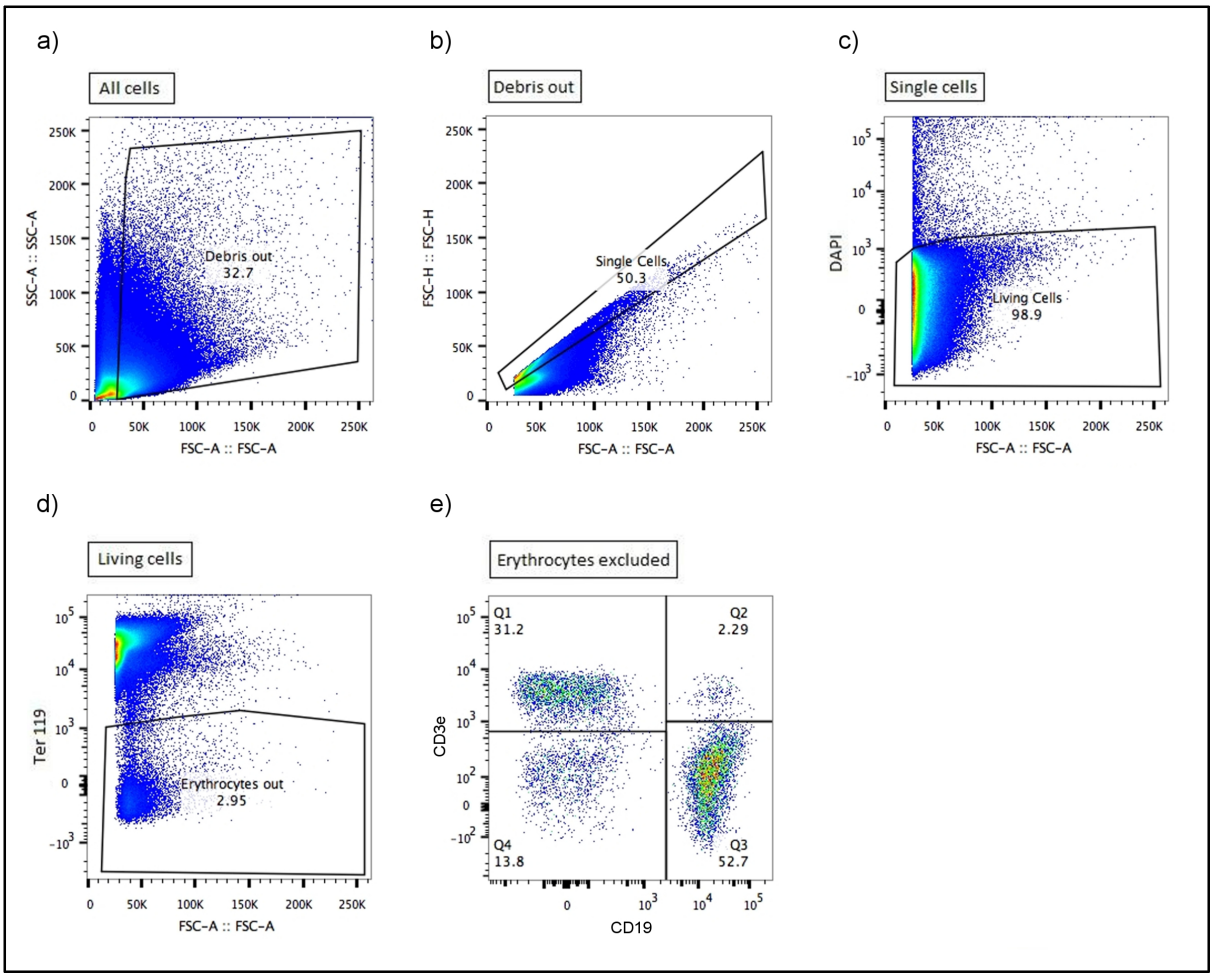

Figure 21: Exemplary gating of lymphocytes: This figure shows an exemplary gating strategy to examine Lymphocytes. a)-d) are similar to figure 7. e) shows the differentiation between T-cells and B-cells. While CD3e, a pan-T-cell-marker is labeled with A488 which appears in the FITC channel, CD19, a marker for B-cells, appears in the PE channel. Next to CD3e+ CD19- T-cells and CD3- CD19+ B-cells, there are double negative and double positive cells.

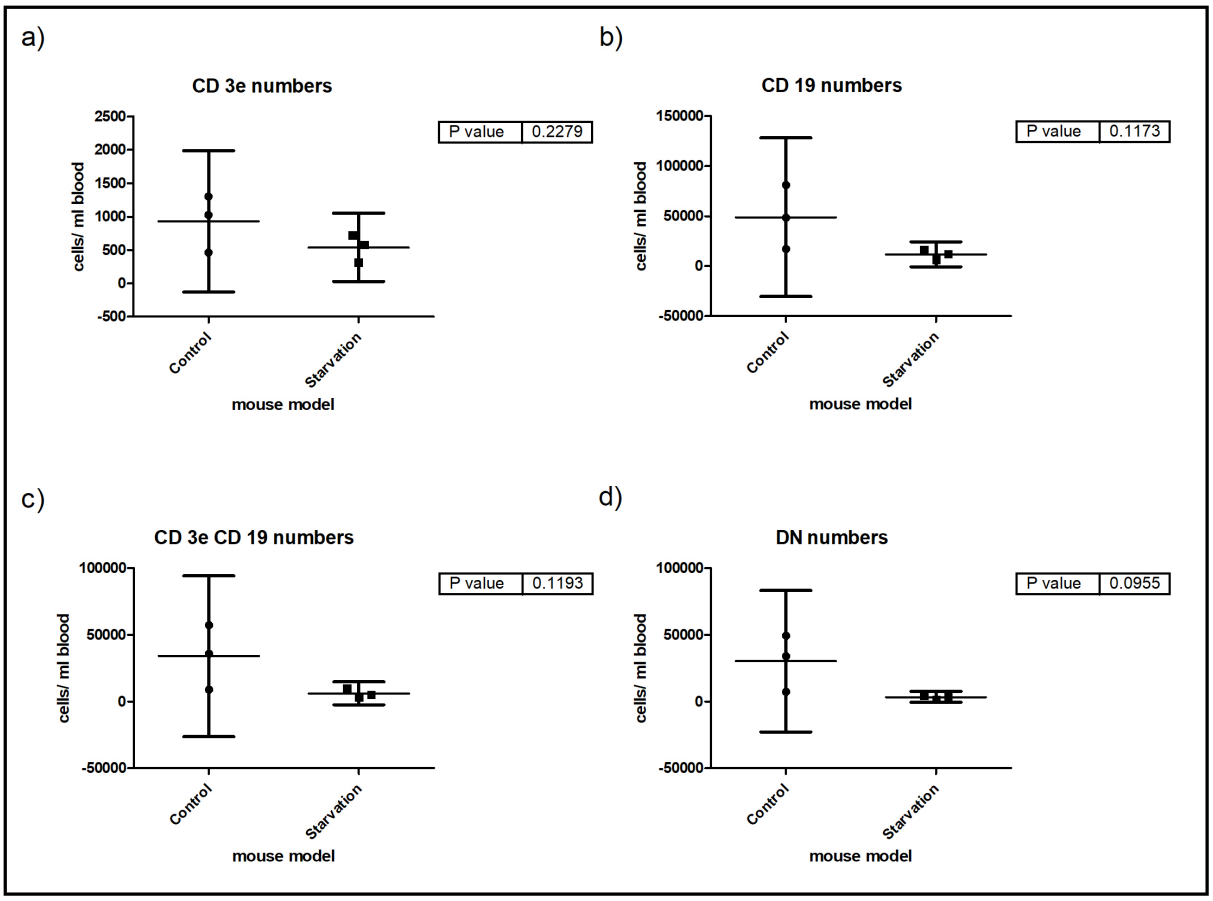

Figure 22: T-cells and B-cells in blood: This figure deals with absolute numbers (cells/ml blood) of T-cells, B-cells, double- positive and double-negative cells. Again the x-axis shows the mouse models, control (n=3) or starvation (n=3), and the bars represent mean and confidence interval, on the y-axis the absolute cell number with cells per ml blood is shown. Even if a tendency to a lower cell number in starvation is visible, these differences are not significant on a 5% significance level. a) T-cell numbers are given here for both, the control and starvation group (CD3e positive CD19 negative). The mean of the T-cell number per ml blood in the control group adds up to 929,907 cells/ml blood, the range spanning a band from 463,287 cells/ml blood to 1303,2 cells/ml blood, while the mean value for the T-cells/ml blood in the starvation group measures 539,946 cells/ml blood, ranging from 316,635 cells/ml blood to 723,261 cells/ml blood, however no significant difference can be found here (p=0,2279; student t-test). b) The B-cell number (CD19 positive CD3e negative) is illustrated in this subfigure, showing again the control and the starvation group. The mean cell amount per ml blood in the control group counts 48965 cells/ml blood, while the values range from 17328,3 cells/ml blood up to 81138,5 cells/ml blood. In the starvation group the mean value, counting 11831 cells/ml blood is lower than in the control group, and ranges from 6552,68 cells/ml blood to 16648,3 cells/ml blood. However this difference is not significant (p=0,1173; student t-test). c) The numbers of CD3e and CD19 positive cells are shown in this subfigure. The control group shows a mean of 34052,2 cells/ml blood, again a lower mean value is presented by the starvation group, which counts only 6099,39 cells/ml blood, the difference is not significant (p=0,1193, student t-test). CD3e/CD19 double positive cells are usually not

existent in living mice, it is supposedly a mere artifact, caused by the process of freezing the mouse blood before processing it, several working groups described this random population [129, 119, 79, 102]. d) Double negative cells are illustrated in this figure. Again the x-axis shows the control and starvation group. While the control group shows a mean value of 30259,2 cells/ml blood, the starvation group's mean is again lower, counting 3474,1 cells/ml blood. However, these differences are not significant for p is 0,0955 (student t-test).

5.2 Function of leptin and its receptor

Leptin is a peptide hormone produced and secreted mainly by white adipocytes but also by many other tissues such as hypothalamus, striped muscle, pituitary gland, ovary, placenta and also in lymphoid organs [139]. Leptin unfolds its effects by binding to the leptin receptor (LepR), which activate several signaling cascades already presented in the introduction. In this part we want to elucidate the type of the receptor present on FRCs and the impact that binding of leptin receptor to its ligand has.

5.2.1 Evidence of leptin receptor on FRCs

As mentioned earlier, we could prove that LepR is present on stromal cells of the lymph node. Figure 23 shows the presence of LepR on FRCs. The approach was similar to that of the establishment of the staining scheme (5.1.1), with the exception that a LepR-antibody and a FITC-related anti-goat-antibody, which binds to the LepR-antibody was added to the staining mix. We can see a shift of the population compared to the isotype control in the histogram, indicating that the whole population is positive for LepR. As this was a qualitative research in the early stages of this work, this gating is not comparable to other examinations performed.

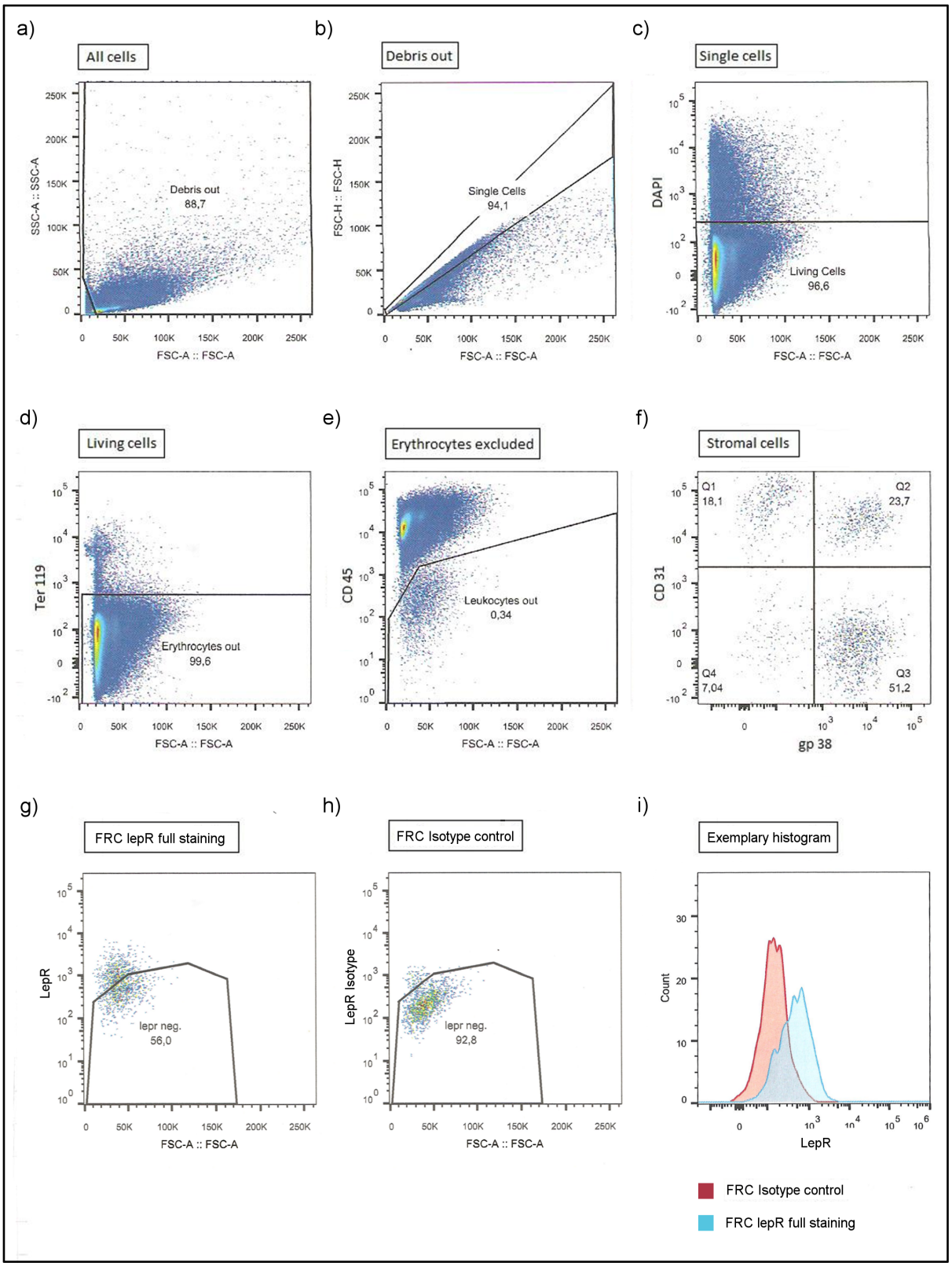
a)
All cells
SSC-A :: SSC-A
Debris out
88,7
FSC-A :: FSC-A
b)
Debris out
FSC-H :: FSC-H
Single Cells
94,1
FSC-A :: FSC-A
c)
Single cells
DAPI
Living Cells
96,6
FSC-A :: FSC-A
d)
Living cells
Ter 119
Erythrocytes out
99,6
FSC-A :: FSC-A
e)
Erythrocytes excluded
CD 45
Leukocytes out
0,34
FSC-A :: FSC-A
f)
Stromal cells
CD 31
Q1
18,1
Q2
23,7
Q4
7,04
Q3
51,2
gp 38
g)
FRC lepR full staining
LepR
lepr neg.
56,0
FSC-A :: FSC-A
h)
FRC Isotype control
LepR Isotype
lepr neg.
92,8
FSC-A :: FSC-A
i)
Exemplary histogram
Count
LepR
FRC Isotype control
FRC lepR full staining

Figure 23: Evidence of leptin receptor on FRCs: a)-f) are steps similar to figure 7. Subfigure g) shows the staining for LepR in the FRC compartment of stromal cells, LepR has been stained with a FITC-related anti-goat-antibody, which binds to the leptin receptor antibody. Subfigure h) is the corresponding isotype control, goat IgG was used as isotype, it was labelled with FITC-related anti-goat-antibody. When consulting i), a exemplary, yet representative histogram, it becomes obvious that all of the FRCs have to bear LepR as the whole population shifts.

5.2.2 Determination of cell culture

In order to determine which type of leptin receptor is present on fibroblastic reticular cells, we decided to use cultured cells, as it would enhance the protein output in comparison to freshly isolated FRCs from mouse lymph node. To see which cell type had the highest level of leptin receptor on their surface, we performed a FACS analysis staining the leptin receptor (see figure 24). As we can see in this figure, the CRL population has with 84,4% of all living single cells the highest number of cells bearing the receptor. FRC-TN and FRC-T have been cultured in RPMI + 10%FBS + 1%P/S + 1/1000 beta-Mercaptoethanol + HEPES (4-(2-hydroxyethyl)-1-piperazineethanesulfonic acid), while CRLs hae been cultured in RPMI + 10%FBS + 1%P/S**.** These findings helped us to decide for the CRL population to extract protein from. In this experiment, we used flow cytometry to evaluate the expression level of LepR, flow cytometry however is not an adequate technique to investigate on protein expression levels, a quantitative ELISA would be appropriate.

a)

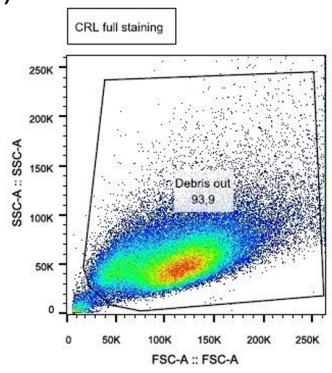

adm2015-04-26.011.fcs
Ungated
80315

b)

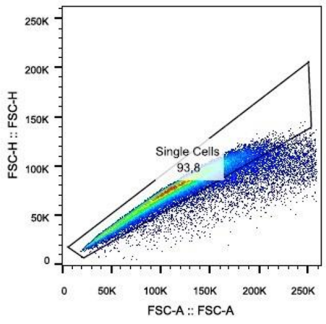

adm2015-04-26.011.fcs
Debris out
75384

c)

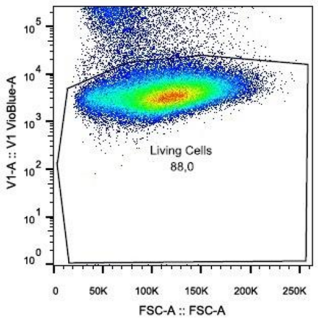

adm2015-04-26.011.fcs
Single Cells
70688

d)

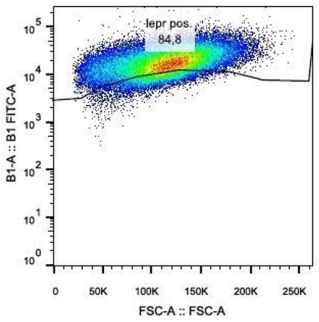

adm2015-04-26.011.fcs
Living Cells
62181

e)

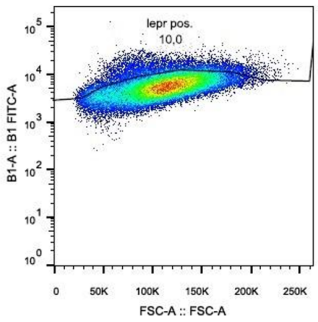

adm2015-04-26.009.fcs
Living Cells
59849

f)

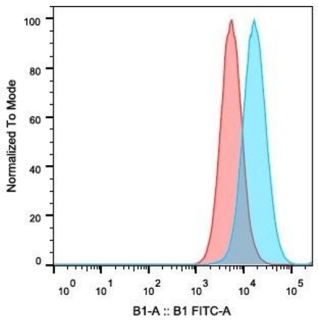

	Sample Name	Count	Workspace Annotation
	adm2015-04-26.011.fcs	62181	full staining
	adm2015-04-26.009.fcs	59849	Isotype Control

g)

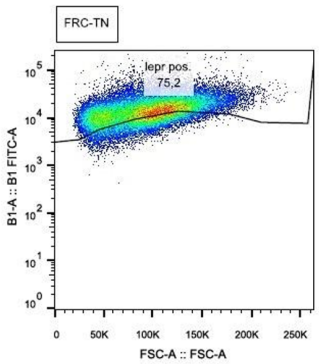

adm2015-04-26.013.fcs
Living Cells
47970

h)

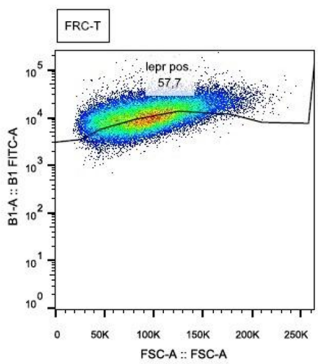

adm2015-04-26.014.fcs
Living Cells
37977

i)

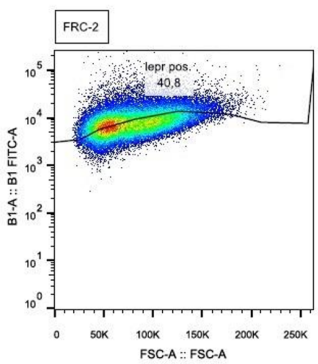

adm2015-04-26.015.fcs
Living Cells
61701

j)

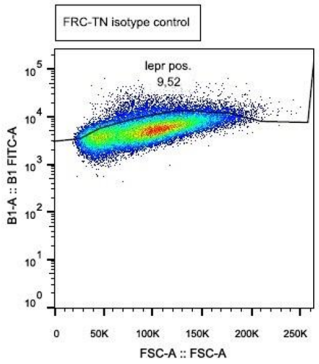

adm2015-04-26.012.fcs
Living Cells
47590

k)

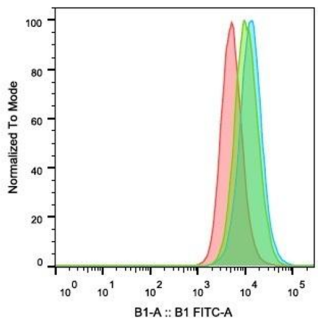

	Sample Name	Count	Workspace Annotation
	adm2015-04-26.014.fcs	37977	FRC-T full staining
	adm2015-04-26.013.fcs	47970	FRC-TN full staining
	adm2015-04-26.012.fcs	47590	Isotype Control

l)

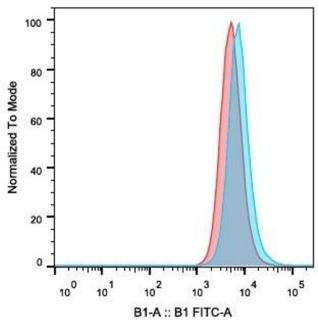

	Sample Name	Count	Workspace Annotation
	adm2015-04-26.015.fcs	61701	FRC-2 full staining
	adm2015-04-26.012.fcs	47590	Isotype Control

Figure 24: Presence of leptin receptor on different cells: Figure 24 shows the presence of leptin receptor on various spleen FRC derived cell lines, namely FRC 2, FRC-T and FRC-TN as well as a bone marrow FRC derived cell line (CRL). Also the gating for this investigation by the example of CRLs is shown. Subfigure a) shows a debris exclusion according to the exemplary gating (figure 7a)). b) Shows the doublets exclusion according to the exemplary gating (figure 7b)). c) Shows the dead cell exclusion via DAPI similar to figure 7c). d) shows the CRLs with an FITC-related anti-goat-antibody, which binds to the LepR-antibody. The FITC channel is plotted on the y-axis whereas the forward scatter is plotted on the x-axis. The leptin receptor positive gate contains 84,8% of the living cells. e) Displays the gating of the isotype control (FITC channel plotted on the y-axis, forward scatter plotted on the x-axis), 10% of the living cells are in the leptin receptor positive gate. The histogram in f) shows a shift of the whole population when the isotype and the full staining are compared (y-axis normalized to mode, x-axis FITC channel). g) Shows the signal for leptin receptor on FRC-TN with 75,2% in the leptin receptor positive gate. j) Represents the FRC-TN isotype control with 9,52% of all living cells in the leptin receptor positive gate. h) 57,7% of the living cells are in the leptin receptor positive gate when looking at FRC-T. i) Also the FRC-2 is checked upon in this subfigure. With 40,8% of all living cells being in the leptin receptor positive gate it is the population with the lowest leptin receptor amount. Subfigure k) shows FRC-T and FRC-TN compared to the FRC-TN isotype control in an histogram (y-axis normalized to mode, x-axis FITC channel). l) shows FRC-2 compared to FRC-TN isotype control in an histogram (y-axis normalized to mode, x-axis FITC channel). In subfigure g)-j) FITC channel is plotted on the y-axis and forward scatter plotted on the x-axis.

5.2.3 Receptor type

As mentioned earlier on, the leptin receptor comes in several isoforms, short ones without an intracellular domain and a long one, which has an intracellular domain. In our study we ruled out which receptor types are present on fibroblastic reticular cells. In order to do so we performed a Western Blot with cell extract of protein which has been extracted from those cultured cells. The Western Blots, both the control and the actual experiment are shown in figure 25. Figure 25a) shows the blot with the leptin receptor and figure 25b) the control, which is gamma-tubulin. We had a protein solution of 1,202 mg protein/ml solution in total and used 754nl of this solution in order to work with 1µg of protein. The left pocket is filled with pre stained dual color marker by Bio-Rad (Bio-Rad Laboratories Inc., Hercules, USA), whereas the following pockets are filled, from left to right, with 5µg, 10µg, 20µg and 30µg of protein. As mentioned earlier, there are several short and a long isoform of the leptin

receptor, the size of the long isoform amounts 132,494 kDa (human) and 130,789 kDa (mouse) and the short forms measure around 100 kDa [208, 209]. For the control we used gamma-tubulin, an ubiquitous protein participating in microtubuli motility, which molecular weight is around 48kDa. In figure 25b) we can clearly see two bands, which lie around the 48kDa mark in all pockets (5µg, 10µg, 20µg and 30µg), hereby proving that the protein isolation and the blotting of the membrane has been successfully performed, making the experimental staining valid. Surprisingly, figure 25a) shows two bands in the pockets filled with 20µg and 30µg of protein, lying approximately on the 130kDa and 100kDa mark [208, 209], which suggests not just the presence of both, the long and the short, or rather several short isoforms of the receptor and the long receptor, but gives also a hint on the amount of receptor in the cell: As in the control staining all pockets showed a signal, it is evident that the concentration of leptin receptor is lower than that of gamma-tubulin.

a)

st 2015-06-30 13hr 39min + test 2015-06-30 13hr 54min white l (Raw 1-D Image)

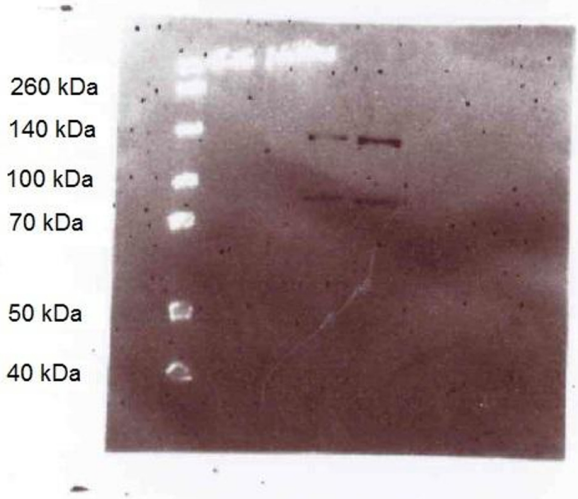

File: test 2015-06-30 13hr 39min + test 2015-06-30 13hr 54min white light.1sc
Low=113 High=198 Gamma=2.5 Exposure: N/A

leptin receptor

b)

test 2015-07-02 13hr 23min (Raw 1-D Image)

γ-Tubulin

Figure 25: Determination of the leptin receptor type: This figure decrypts the type of leptin receptor found on a CRL cell line, it shows a Western Blot membrane with a staining for the extracellular domain of the leptin receptor and γ-tubulin as a control. The molecule weights are shown on the left while the x-axis shows the amount of protein used in the pocket, being from left to right marker, 5µg, 10µg, 20µg and 30µg. The marker, pre stained dual color marker Bio-Rad, is filled into the left pocket and marks the bands for a molecular weight of, from upper to lower, 260kDa, 140kDa, 100kDa, 70kDa, 50kDa and 40kDa. In a) where the leptin receptor is stained, one clearly sees bands at approximately 130kDa and again at approximately 100kDa in the 20µg and 30µg pocket, representing the long and the short isoform of the receptor. b) Represents the gamma-tubulin control with bands in all pockets (5µg, 10µg, 20µg and 30µg) between 50kDa and 40kDa.

5.2.4 Impact of leptin receptor-binding

Leptin, as stated in the introduction, is not just a regulator of the feeling of satiety, but also involved in homeostasis of the immune system, a reasonable suspicion is raised that during starvation and regression, this hormone would have a crucial effect on the structure of the lymph node. Especially as fibroblastic reticular cells interact with the immune system and express LepRb. As leptin is excreted upon feeding and being absent upon famine, we postulated that a resubstitution of leptin during the starvation phase would have a supporting effect on survival of FRCs. To perform this experimental setting, the animals which suffered starvation received daily after the beginning of the starvation phase an intraperitoneal injection of 1µg leptin/g mouse (20µg in 80µl PBS prediluted), as in the preceding experimental settings, they have been killed 48h after the begin of the starvation phase, also a group of mice which suffered starvation, yet didn't receive any leptin injections, served as negative control group and a group of mice on regular diet served as a control group. A regression group couldn't be checked but would surely have been desirable. Only female C57Bl/6 mice aged 7 to 8 weeks have been used. The following part shows the results determined by this experiments. However, this experimental setting only includes the control group and the starvation group. Furthermore, n has been very small, so no valid statistical analysis is possible with this data

5.2.4.1 Impact on fibroblastic reticular cells

Earlier, we described the effects of starvation and regression on the fibroblastic reticular cells. This part sheds light on the effect of additional leptin during the starvation phase. Figure 26 leads us through the results. While figure 26a) and b) give an overview about how the effects of leptin during starvation look like in the different cell types and mouse models by juxtaposing them, c)-f) go more into detail, on their y-axis they show the number of cells per lymph node and on their x-axis the mouse model, the medium bar represents the mean while the upper and lower bar include the 95% confidence interval. c) Broaches the issue of fibroblastic reticular cells. In the control group, which has received a regular diet, the mean of cells per lymph node counts 365 cells per lymph node. The negative control group, comparable to the starvation group in the regular experiments mentioned above, shows a similar result with a slightly higher mean, namely 401,5 cells per lymph node. As it was the case in the control group, also in this group n counted 2 and is therefore not consultable for valid statistical analysis. The last model is the starvation group injected with leptin during starvation. During leptin input, the number of FRCs more than doubles (mean(starvation+leptin)=886,5 cells/ lymph node). Again in the last group, n was 2, therefore forbidding a valid statistical analysis. Yet, if these experiments can be confirmed, this would show that the maintenance of a high leptin level during starvation could prevent FRCs from cell death in the regression phase, as the number of FRC rises during leptin treatment.

5.2.4.2 Impact on lymphatic endothelial cells

Similar to the previous point, this section covers the effects of leptin treatment on lymphatic endothelial cells, again figure 26 will accompany us to depict the happenings during leptin treatment under starvation. Figure 26 covers absolute cell numbers (being written on the y-axis, while the x-axis is showing the mouse model). The medium bar again shows the mean while the upper and the lower bar include the 95% confidence interval. Subfigure 26d) illustrates the happenings in the lymphatic

endothelial cells' fraction. As in the preceding figures, the control group, shown in the first column, has the smallest range of the three groups, enclosing a mean of 232 cells/ lymph node. In the starvation group which didn't receive a leptin injection,the mean undermatches that of the control group (mean(starvation without leptin)=204 cells/ lymph node). The last group is that of the starvation group that was treated with leptin injections during their starvation phase. The mean exceeds the means of the other groups being 455 cells/ lymph node. The number of test subjects used in every group was 2, so statistical analyses are not valid. But again, if these data confirms, a protective effect of leptin on LEC survival can be stated.

5.2.4.3 Impact on blood endothelial cells

Figure 26e) illustrates the impact of leptin treatment during starvation (third column) and also depict a control group (first column) and a negative control group (second column). In the control group, a mean of 240,5 cells/ lymph node is the highest value of the three groups. The control group is followed by the starvation group without leptin injections, the marking points of its range is obviously lower than that of the control group. The mean of this group is the lowest of all three groups with 155 cells/ lymph node. The mean of the starvation group which received leptin treatment lies between the two other groups, being 205,5 cells/ lymph node. In all groups the number of test subjects has been 2. As only two test subjects participated in this experimental setting, a valid statistical statement cannot be given. But again, it seems like leptin treatment stabilizes cell populations during starvation, as cell numbers in the treated group are almost always higher than in the group without treatment.

a)

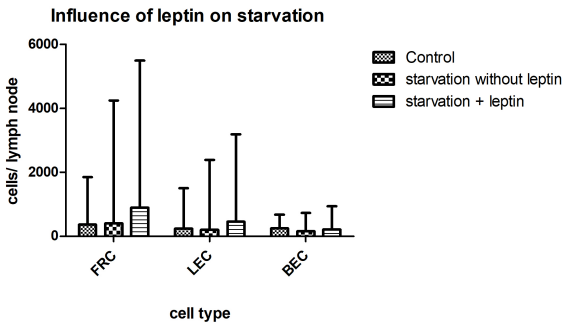
Influence of leptin on starvation
cells/ lymph node
6000
4000
2000
0
FRC
LEC
BEC
cell type
Control
starvation without leptin
starvation + leptin

b)

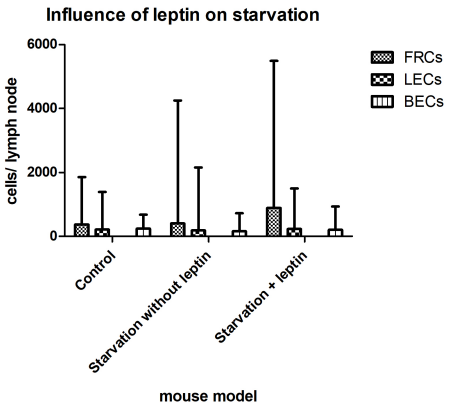
Influence of leptin on starvation
cells/ lymph node
6000
4000
2000
0
Control
Starvation without leptin
Starvation + leptin
mouse model
FRCs
LECs
BECs

c)

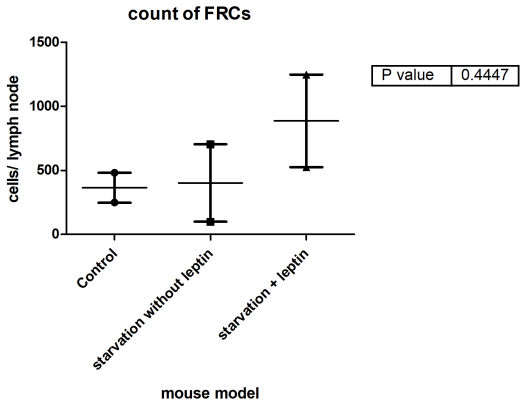
count of FRCs
cells/ lymph node
1500
1000
500
0
Control
starvation without leptin
starvation + leptin
mouse model
P value
0.4447

d)

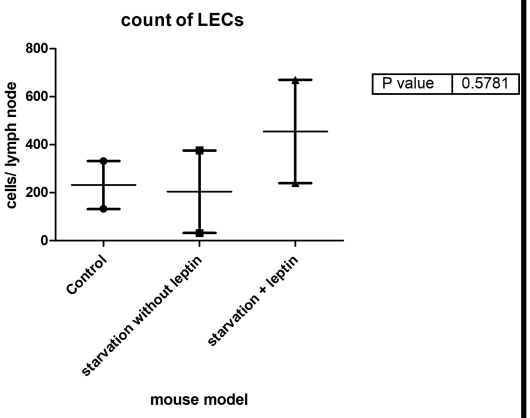
count of LECs
cells/ lymph node
800
600
400
200
0
Control
starvation without leptin
starvation + leptin
mouse model
P value
0.5781

e)

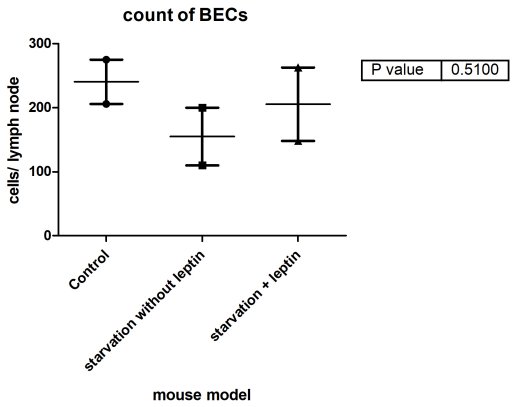
count of BECs
cells/ lymph node
300
200
100
0
Control
starvation without leptin
starvation + leptin
mouse model
P value
0.5100

Figure 26: Effect of leptin on stromal cells: This figure illustrates the effect on leptin on the state of starvation with absolute numbers denoted as cells per lymph node on the ordinate. The abscissa in a) shows the cell type while in all other subfigures it shows the mouse model. Subfigure a) and b) give an overview about the distribution of the cell types within the mouse model. The mean value is given by the medium bar, and the 95% confidence interval is given by the upper and lower bar. Looking at absolute numbers, no significant change in leptin injected animals to starving animals without injection or healthy controls could be verified. N is 2 for all models. c)(p=0,4447; student t-test) d)(p=0,5781; student t-test) e)(p=0,51; student t-test) f)(p=0,4669; student t-test).

5.2.4.4 qPCR

To further understand the FRCs' physiology under the influence of leptin, we tried to analyze the FRCs' expression pattern during different situations. As we know that these cells express LepR, we examined how the addition of leptin would interfere. For this experiment we used a MACSed primary culture of murine lymph node FRCs. We had different experimental setups:
24h incubation with 50ng leptin/ml
24h incubation with 250ng leptin/ml
24h incubation with 1000ng leptin/ml
24h incubation with 50ng leptin/ml + 50ng IFNγ/ml + 50ng TNFα/ml
24h incubation with 250ng leptin/ml + 50ng IFNγ/ml + 50ng TNFα/ml
24h incubation with 1000ng leptin/ml + 50ng IFNγ/ml + 50ng TNFα/ml
24h incubation with 50ng IFNγ/ml + 50ng TNFα/ml as positive control
untreated samples as negative control
After the incubation, mRNA has been isolated and cDNA has been generated. Then a qPCR has been performed to check on different expression patterns. The expression of GAPDH served as control. We hypothesized that leptin itself would change the cellular expression pattern and the addition of leptin to IFNγ and TNFα would neutralize the effect of these proinflammatory cytokines. We checked on the following genes:

1. Col1
2. CXCL-10
3. FLT-3

4. MCSF
5. MMP2
6. MMP9
7. NOS-2
8. SMA
9. TGF-β

However the melting curves of the designed primers were not appropriate and the multiplications were most likely primer dimers, therefore, results of the PCR analysis are not utilizable. Nevertheless a genetic analysis is promising, especially the expression of LepR under different conditions. qPCR could be used to clarify the question in how far the composition of the different LepR isoforms on the FRCs' surface changes under different conditions. Also the effect of gp38 in the regression phase could be investigated by checking again on SMA in the control group and the regression group. An increase in SMA expression would back up the hypothesis that a blockade of podoplanin signaling stimulates the expression of SMA [1, 11, 26] and therefore, promotes the expandability of the reticular fibre network, supporting FRC survival.

6. Discussion

6.1 Lymph node structure

Healthy control mice consisted of female C57BL/6J aged to approximately 9 up to 11 weeks. The mice were provided dry food and water ad libitum. Figure 15 gives an overview about the distribution of stromal cells as well as leukocytes. As one can see, the biggest population in healthy mice's stromal cell compartment is that of FRCs, secondly come the LECs, followed by BECs. The biggest amount of cells is as mentioned earlier build up by leukocytes. The direct comparison between healthy and starving mice on cellular base regarding lymph node structure does not show striking differences between the two models. Surprisingly, during recovery, a massive drop in numbers in all resident lymph node cells occurs, next to the stromal compartment. Also leukocytes and dendritic cells are heavily affected (see figure 15 and 17). Looking at FRCs (see figure 9 and figure 10), there is neither a significant difference nor a tendency towards any direction visible when comparing normal nutritional status with famine. Also the means of both models do not scatter apart and stay closely together. The highest values in cell count though belong to the control group, maybe the phase of starvation is not long enough for any effect to become manifest. After 48h of recovery however, we see a heavy and significant drop in resident FRCs, their number more than halves compared to the control and starvation group. Analog, in the LEC fraction, there are no differences in the arrangement of LECs when looking at the control and starvation model (see figure 11 and figure 12). Also a tendency does not strike the eye as the mean values of both models stay closely together. The previously described cell death during recovery also has its equivalent in this stromal faction, the LECs' population also more than halves during regression compared to the control and starvation group. A similar picture is presented by the BEC partition (see figure 13 and 14) where no evidence of a direct effect of starvation on the absolute cell number compared to the control group is given, the difference between both models is not significant. Alike FRCs and LECs, also here the means do not disperse much when comparing the control group with the starvation group. But even in this small group of stromal cells we can see a significant effect during

reuptake of nutrition, the numbers of BECs fall in lymph nodes. When taking a closer look at figure 15f), we can clearly see that also leukocytes seem to stay unaffected by a phase of reduced food uptake short-term. Again, this status cannot be maintained during nutritional recovery, as the absolute number of leukocytes within the lymph node drops dramatically. Whether leukocytes become the victim of cellular death or just migrate out of the lymph node remains unclear, as we only focused on circulating lymphocytes during starvation, no significant differences between the control group and the starvation group were detectable in this experimental setting. While CD11c high+ DCs stay untouched by famine, CD11c low+ DCs seem to drop in numbers, at least in lymph nodes. To investigate the possible share of FRC and LEC loss caused by dendritic cell death, mean and median APC fluorescence of FRCs and LECs has been looked upon, as gp38 is labeled with a staining that appears in the APC-channel. Acton et al. as well as Astarita et al. state in their paper that DCs are able to support FRC survival by binding the FRCs' podoplanin with their CLEC-2, next to increased FRC survival, the blocking of podoplanin causes the reticular fibre network to become more elastic [1, 11]. As we see in figure 20, the median APC fluorescence of FRCs drops in the regression phase, this could be an adaptation to the cell death of FRCs. As there are less FRCs present in the lymph node, the remaining FRCs are challenged with the maintenance of the reticular fibre network by downregulation of podoplanin. To further develop the idea of Acton et al. and Astarita et al., FRCs are probably able to compensate the lower cell count by stretching their reticular fibre network. In order to confirm this hypothesis, a histological examination with an antibody staining for podoplanin would be necessary. This data contradicts the idea that a decrease in FRC or LEC numbers is owed to DC death or DC emigration, rather would one expect an elevated level of gp38 expression. The contrary is the case, a low g38 signal connected with a low DC count gives a hint on DC emigration due to the downregulation of podoplanin, as the migration of DCs alongside the reticular fibre network is dependent on CLEC-2/gp38 binding [26]. All these findings indicate a severe structural alteration within lymph nodes, at least after the phase of famine. In what exact phase the change happens remains unclear, as well as the time point when the lymph node's structure fully recovers. In order to shed light on

this question, an examination via flow cytometry could be performed 72h after resubstitution of food.

6.2 T-cells and B-cells in blood

As T-cells, B-cells and DCs travel along the reticular fibre network, we hypothesize that this structural change also has a high impact on the homeostasis of cells of the acquired immune system. A flow cytometry analysis has been made to examine the status of B- and T-cells circulating in the mice's blood during steady state and famine. The outcome of this investigation does not show a striking outcome, as both groups show similar results. In the results we can see a special population of cells, CD19/CD3e double positive cells (see figure 21 and figure 22), as mentioned in the legend of figure 22, they are most likely artifacts caused by the storing process, several publications name different reasons for CD19/CD3e double positive cells [129, 119, 79, 102]. However with much higher experimental repetitions and also the inclusion of the regression phase into this research, a significant difference is imaginable.

6.3 Cell culture

Originally, the main task of this research was to study the physiology of the leptin receptor expressed by FRCs (see 5.2.1), this proofed to be harder than expected. First we wanted to set up a FRC primary culture, the material of the digested mouse lymph nodes would be taken into culture. The stromal cells will need 24h to adhere to the bottom of the culture plate, nonadherent cells will be floating in the medium and can be washed out, regular change of medium will eradicate BECs and double negative cells. Next to FRCs, macrophages, dendritic cells and LECs will survive in this culture. Once the culture is fully grown, it can be expanded. When enough cells have been generated, FRCs can be isolated by MACS. After we established several primary cultures, we tried to isolate LepR positive FRCs via cell sorting. This technique proofed to be very error-prone: There are many steps which are sensible

to contamination, as cells are often resuspended and are in contact with many different materials, this also leads to an enormous cellular stress. Regularly, the survival of FRCs due to these conditions was too low to generate a population which is big enough for analysis. As the whole procedure is time consuming and next to it, the output of FRCs is not very high, we distanced from primary cultures. A more reliable and fail-safe source of LepR positive FRCs was the establishment of a cell line. To do so, we first needed to identify the cell line which has the highest expression level of LepR. We used flow cytometry to check on expression levels of LepR, this allowed us to find a suitable population. Figure 24 explains the approach of this procedure. There were four possible FRC-populations: FRC-T, FRC-TN, FRC-2 and CRL. The dot-plots and histograms confirm that the cell line with the highest LepR expression are the CRL cells. However, flow cytometry usually isn't convenient for the detection of expression levels, a better solution would have been a quantitative ELISA. The CRL cells were taken into culture. After expanding and harvesting the cells, they have been used for further experiments. Next to FRCs and CRL cells, many other stromal subsets express LepR, such as thymic stromal cells [136, 73], as well as bone marrow stromal cells [204, 161, 157, 54, 207]. One could say that the expression of LepR is common among stromal cells.

6.4 Leptin receptor

One of the most promising result of our research was the identification of the leptin receptor in FRCs. For there are several isoforms, many short isoforms and one functional long isoform. Most authors share the idea stated by Bjørbaek et al. in 1997, that only the long isoform is functional in vivo [23, 116, 69]. Thus it is of interest to detect which one is present on the FRCs' surface. Normal flow cytometry analysis is not capable to differentiate the isoforms as the leptin receptor antibody binds to the extracellular domain of the receptor which is identical in all isoforms. The difference lays in the intracellular domain. The Western blot technique allowed us to check on the protein's length and, indeed, we discovered two bands when staining for LepR. That means that next to the short isoform, also the long and functional isoform of

LepR is present on FRCs. The short isoform has not been classified in this work. It is however likely that the receptor present on these cells is Ob-Ra, which is widely expressed [60]. The presence of both isoforms, especially the presence of the knock-out receptor raises questions. A hypothetical but possible answer is that the potential of expressing both isoforms enables the cell to autoregulate the effects of leptin: An upregulation of the expression of knock-out LepR and a steady expression, or even downregulation of the expression of functional LepR could impair the effect of leptin on the target cell by raising the probability of leptin/LepR-binding to the knock-out receptor. Similar to that idea, Cao et al. underline the statement of Ahima et al. and Myers et al. based on the findings of Clément et al. as well as Ge et al., that the soluble form of LepR may regulate the concentration of circulating leptin by binding it [30, 4, 127, 42, 68]. Friedman et al. hypothesized 20 years ago, that the short isoform Ob-Ra could be responsible for the transport of leptin beyond the blood-brain barrier and the clearance of leptin, which supports my hypothesis [64, 17, 180]. Yet another possibility is that the short isoforms indeed inhere a signal transducing function: OBRs (this is how Bjørbaek et al. designated the short isoform described in their work) is supposed to be capable of activating signal transduction via JAK2, as well as IRS-1 tyrosine phosphorylation [23, 116]. Bacart et al. attribute a physiological role to Ob-Ra as they showed that in presence of leptin, several LepR isoforms on HEK293T cells form heteromers, in this special case they detected Ob-Ra/b and Ob-Rb/c heteromers. The work group around Bacart et al. suspect that the heteromerization could have an effect on the half-life of Ob-Rb [12]. In order to shed light on that question, a quantitative Western blot or qPCR examination could be performed on leptin-incubated FRCs. A change in the expression pattern of the short isoform LepR would proof this hypothesis.

6.5 Influence of leptin

As we have proven that famine and a follow-up recreation phase heavily changes the murine lymph node's structure, we wanted to investigate whether leptin treatment could slow down, or even prevent these happenings. Leptin is a hormone which

mediates the feeling of saturation, but next to that, it has various influences on the immune system. After famine, the lymph node's cellular structure changes dramatically. As FRCs bear the receptor for leptin on their surface and are closely linked to T-cell maintenance and survival, the supplement of leptin during starvation may reduce cell death or maybe even prevent it. The addition of leptin during starvation seems to have a supportive effect on FRC survival, maybe even the proliferation of these cells is supported by additional leptin: The average count of FRCs per lymph node rises under experimental conditions compared to the starvation only group. A similar effect can be observed when looking at LECs. Their population seems to stay unaffected during famine. Under the influence of leptin though, the number of LECs seems to rise. As already stated above, FRCs support T-cell survival and maintenance. I hypothesize that a drop down in numbers of FRCs during regression or late starvation phase will have a serious influence on T-cell function and therefore cause a heavy impact on an adequate immune response. A stable FRC population during the regression phase or late starvation phase could prevent a negative effect on the immune response. This goal could be reached by the supplementation of leptin during famine. Starvation in general severely affects the immune system by immunosuppressive effects [6]. For instance, Cason et al. described a reduced delayed hypersensitivity reaction as well as a light leucopenia with a reduced T3+ and T4+ count in anorexia nervosa patients [31]. Furthermore, the production of interferon-γ (IFN-γ) by peripheral lymphocytes seems to be impaired in these patients [143]. Lord et al. proved that leptin stimulates proliferation in peripheral blood lymphocytes, their data showed that mainly CD4+ T-cells were affected by the proliferative properties of leptin/LepR signaling. However the effects of leptin on T-cells are ambivalent, as cytokine production of Th1 cytokines, like IL-2 and IFN-γ is enhanced in the presence of leptin, while production of Th2 cytokines such as IL-4 is hampered. Additionally, the impaired delayed type hypersensitivity reaction during starvation could be restored by the supplementation of leptin during the hunger phase [104]. It remains to be investigated whether leptin influences also stromal cell function within SLOs.

6.6 Outlook: Possible clinical connection of stromal leptinR expression in patients

The scenario of the above mentioned settings is not devious: Next to anorexia nervosa patients, a lot of cancer patients suffer from undernutrition caused by their wearing disease. This is a problematic issue during cancer treatment, as this leads to physical katamorphism and increased vulnerability towards infectious diseases. Cancer cachexia is associated with a bad prognosis and higher mortality [55, 197, 181, 158]. Cancer cachexia itself seems not to be mediated by leptin, but somehow by the tumor, the pathogenesis behind this serious complication is not fully understood [55]. Leptin treatment could, next to replenishment of nutrients, be a key player in supportive cancer treatment as it could be protective at least towards infectious diseases such as nosocomial pneumonia. A drawback of additional leptin during cancer treatment could be the inhibition of hungry feeling, as one of the first known effects of leptin is the mediation of the feeling of satiety. This would be counterproductive and even harmful to the patient, as food uptake must be maintained under all circumstances. In a study performed by Demiray et al., leptin levels reciprocally correlate with the overall survival of patients with non-small-cell lung carcinoma (NSCLC) [55]. Serum leptin levels are in general lower in patients with cancer cachexia, this could be linked to a reduced amount of body fat [55, 155], however, Demiray et al. state that overall survival is higher when low levels of circulating leptin are detected [55], which seemingly contradicts the statement that cancer cachexia is one of the main reasons for death during malign disease, as cachexia is supposed to correlate with low levels of leptin. A separation between non-cachexia and cachexia patients did not happen in this study when calculating the overall survival linked to leptin levels. This would have been of interest, as this could show how many of the deceased patients with cachexia had low levels of leptin and how many of these patients had high levels of circulating leptin. As this study only examined a low number of patients, it is possibly not representative. In contrast, Karapanagiotou cannot provide evidence for a drop in leptin levels during weight loss in patients with NSCLC, furthermore they state that overall survival does not correlate with serum leptin level [86]. Studies focussing gastrointestinal malignoma established

a claim that leptin levels drop in patients with gastric and colorectal cancer [24, 57]. Yet another study, performed by Brown et al. on patients with pancreatic cancer showed no significant correlation between cachexia and leptin level or appetite loss and leptin level [25]. Furthermore, Simons et al. underline, that especially high leptin levels are not responsible for cancer cachexia [170]. To further understand the causality and correlation between tumor cachexia and leptin, further studies with a high number of patients have to be performed as literature shows diverging results. This problem probably does not come to full play during intravenous nutrition. However, intravenous nutrition is not an alternative to oral nutrition when the patient does not lack the ability to oral food uptake. Nevertheless, therapeutic addition of leptin is not a novum, it is already state of the art in patients who suffer from congenital leptin deficiency, lipodystrophy and hypothalamic amenorrhea. These diseases are based on a mutated leptin gene [141]. Leptin treatment started in 1997, when congential leptin deficiency was first discovered in humans. The phenotype of these patients resembles is comparable to the phenotype of ob/ob-mice: early obesity, probably caused by the down regulation of the feeling of satiety and resulting hyperphagia due to the low levels of leptin. Also hyperinsulinemia is described in these patients. Treatment of these patients with r-metHuLeptin resulted in the raise of CD4+ naive T-cell numbers. Additionally the treatment also resulted in significant weight loss [140], which is advantageous for the patients described by Paz-Filho et al., however this is not the case in cancer patients, were weight loss would have a dramatic impact. Contrariwise the treatment of common obesity seems not to be possible due to leptin-resistance [141, 175]. Other described side effects of metreleptin (the currently used drug for treatment) include abdominal pain, headache and hypoglycemia [141], whether r-metHuLeptin has these side effects is not mentioned, yet seems likely. Another interesting finding is that in one patient with diabetes mellitus type 2, higher doses of leptin were necessary to achieve positive effects. The explanation could be the leptin resistance caused by diabetes induced obesity [140]. A draw-back of the study of Paz-Filho et al. mentioned in the publication from 2011/2010, is owed to the rareness of this disease, namely the low number of examined cases. Not just the treatment of tumor cachexia is an imaginable scenario, in rodents, leptin deficiency also causes a diabetes type II like

phenotype with insulin resistance and hyperglycemia, treatment with leptin reversed these effects by the reduction of serum glucose and insulin, proving a stabilizing function of leptin in this common metabolic disease [142].

Taken together, it is possible that leptin related changes regarding stromal cell function could add and influence cancer-related cachexia and other nutritional disorders.
Future experiments and clinical studies are necessary to clarify these questions.

8. Bibliography

1. *Acton S, Farrugia A, Astarita J, Mourão-Sá D, Jenkins R, Nye E, Hooper S, van Blijswijk J, Rogers N, Snelgrove K, Rosewell I, Moita L, Stamp G, Turley S, Sahai E, Reis e Sousa C (2014) Dendritic cells control fibroblastic reticular network tension and lymph node expansion. Nature. 514:498–502.*

2. *Acton S, Astarita J, Malhotra D, Lukacs-Kornek V, Franz B, Hess P, Jakus Z, Kuligowski M, Fletcher A, Elpek K, Bellemare-Pelletier A, Sceats L, Reynoso E, Gonzalez S, Graham D, Chang J, Peters A, Woodruff M, Kim Y, Swat W, Morita T, Kuchroo V, Carroll M, Kahn M, Wucherpfennig K, Turley S (2012) Podoplanin-Rich Stromal Networks Induce Dendritic Cell Motility via Activation of the C-type Lectin Receptor CLEC-2. Immunity. 37: 276–289.*

3. *Agrawal S, Gollapudi S, Su H, Gupta S (2018) Leptin Activates Human B Cells to Secrete TNF-α, IL-6, and IL-10 via JAK2/STAT3 and p38MAPK/ERK1/2 Signaling Pathway. Journal of Clinical Immunology. 31(3):472-478.*

4. *Ahima R, Osei S (2004) Leptin signaling. Physiology & Behavior. 81(2):223-241.*

5. *Alvarenga H, Marti L (2014) Multifunctional Roles of Reticular Fibroblastic Cells: More Than Meets the Eye?. Journal of Immunology Research. 2014:402038.*

6. *Alwarawrah Y, Kiernan K, MacIver N (2018) Changes in Nutritional Status Impact Immune Cell Metabolism and Function. Frontiers in Immunology. 9:1055.*

7. *Anderson AO, Anderson ND, White JD, Hay J (ed) (1982) Animal models of immunological processes. London: Academic Press, New York 1982.*

8. *Anderson A, Shaw S (1993) T cell adhesion to endothelium: the FRC conduit system and other anatomic and molecular features which facilitate the adhesion cascade in lymph node. Seminars in Immunology. 5(4):271-282.*

9. *Ansel K, Ngo V, Hyman P, Luther S, Förster R, Sedgwick J, Browning J, Lipp M, Cyster J (2000) A chemokine-driven positive feedback loop organizes lymphoid follicles. Nature. 406(6793):309-314.*

10. *Asperti-Boursin F, Real E, Bismuth G, Trautmann A, Donnadieu E (2007) CCR7 ligands control basal T cell motility within lymph node slices in a phosphoinositide 3–kinase–independent manner. The Journal of Experimental Medicine. 204(5):1167-1179.*

11. *Astarita J, Cremasco V, Fu J, Darnell M, Peck J, Nieves-Bonilla J, Song K, Kondo Y, Woodruff M, Gogineni A, Onder L, Ludewig B, Weimer R, Carroll M, Mooney D, Xia L, Turley S (2014) The CLEC-2–podoplanin axis controls the contractility of fibroblastic reticular cells and lymph node microarchitecture. Nature Immunology. 16(1):75-84.*

12. *Bacart J, Leloire A, Levoye A, Froguel P, Jockers R, Couturier C (2010) Evidence for leptin receptor isoforms heteromerization at the cell surface. FEBS Letters. 584(11):2213-2217.*

13. *Bajénoff M, Egen J, Koo L, Laugier J, Brau F, Glaichenhaus N, Germain R (2006) Stromal Cell Networks Regulate Lymphocyte Entry, Migration, and Territoriality in Lymph Nodes. Immunity. 25(6):989-1001.*

14. *Bajénoff M, Egen J, Qi H, Huang A, Castellino F, Germain R (2007) Highways, byways and breadcrumbs: directing lymphocyte traffic in the lymph node. Trends in Immunology. 28(8):346-352.*

15. *Bajénoff M, Glaichenhaus N, Germain R (2008) Fibroblastic Reticular Cells Guide T Lymphocyte Entry into and Migration within the Splenic T Cell Zone. The Journal of Immunology. 181(6):3947-3954.*

16. *Bajénoff M, Germain R (2009) B-cell follicle development remodels the conduit system and allows soluble antigen delivery to follicular dendritic cells. Blood. 114(24):4989-4997.*

17. *Banks W, Kastin A, Huang W, Jaspan J, Maness L (1996) Leptin enters the brain by a saturable system independent of insulin. Peptides. 17(2):305-311.*

18. *Barletta K, Cagnina R, Wallace K, Ramos S, Mehrad B, Linden J (2012) Leukocyte compartments in the mouse lung: Distinguishing between marginated, interstitial, and alveolar cells in response to injury. Journal of Immunological Methods. 375(1-2):100-110.*

19. *Batra A, Okur B, Glauben R, Erben U, Ihbe J, Stroh T, Fedke I, Chang H, Zeitz M, Siegmund B (2010) Leptin: A Critical Regulator of CD4+T-cell Polarizationin Vitroandin Vivo. Endocrinology. 151(1):56-62.*

20. *Bénézech C, White A, Mader E, Serre K, Parnell S, Pfeffer K, Ware C, Anderson G, Caamano J (2010) Ontogeny of Stromal Organizer Cells during Lymph Node Development. The Journal of Immunology. 184(8):4521-4530.*

21. *Bénézech C, Mader E, Desanti G, Khan M, Nakamura K, White A, Ware C, Anderson G, Caamaño J (2012) Lymphotoxin-β Receptor Signaling through NF-κB2-RelB Pathway Reprograms Adipocyte Precursors as Lymph Node Stromal Cells. Immunity. 37(4):721-734.*

22. *Bennett B, Solar G, Yuan J, Mathias J, Thomas G, Matthews W (1996) A role for leptin and its cognate receptor in hematopoiesis. Current Biology. 6(9):1170-1180.*

23. *Bjørbæk C, Uotani S, da Silva B, Flier J (1997) Divergent Signaling Capacities of the Long and Short Isoforms of the Leptin Receptor. Journal of Biological Chemistry. 272(51):32686-32695.*

24. *Bolukbas F, Kilic H, Bolukbas C, Gumus M, Horoz M, Turhal N, Kavakli B (2004) Serum leptin concentration and advanced gastrointestinal cancers: a case controlled study. BMC Cancer. 4(1):29.*

25. *Brown D, Berkowitz D, Breslow M (2001) Weight Loss Is Not Associated with Hyperleptinemia in Humans with Pancreatic Cancer. The Journal of Clinical Endocrinology & Metabolism. 86(1):162-166.*

26. *Brown F, Turley S (2015) Fibroblastic Reticular Cells: Organization and Regulation of the T Lymphocyte Life Cycle. The Journal of Immunology. 194(4):1389-1394.*

27. *Bruno A, Conus S, Schmid I, Simon H (2005) Apoptotic Pathways Are Inhibited by Leptin Receptor Activation in Neutrophils. The Journal of Immunology. 174(12):8090-8096.*

28. *Burrell B, Warren K, Nakayama Y, Iwami D, Brinkman C, Bromberg J (2015) Lymph Node Stromal Fiber ER-TR7 Modulates CD4+ T Cell Lymph Node Trafficking and Transplant Tolerance. Transplantation. 99(6):1119-1125.*

29. *Caldefie-Chezet F, Poulin A, Vasson M (2003) Leptin Regulates Functional Capacities of Polymorphonuclear Neutrophils. Free Radical Research. 37(8):809-814.*

30. *Cao Y, Xue J, Wu L, Jiang W, Hu P, Zhu J (2011) The detection of 3 leptin receptor isoforms in crucian carp gill and the influence of fasting and hypoxia on their expression. Domestic Animal Endocrinology. 41(2):74-80.*

31. *Cason J, Ainley C, Wolstencroft R., Norton K, Thompson R (1986) Cell-mediated immunity in anorexia nervosa. Clin. Exp. Immunol. 64:370–375.*

32. *Chang J, Turley S (2015) Stromal infrastructure of the lymph node and coordination of immunity. Trends in Immunology. 36(1):30-39.*

33. *"Characterization of CD31" online, available under: http://www.ncbi.nlm.nih.gov/gene/5175 as at 28.04.2018.*

34. *"Characterization of CD45", online, avialable under: http://www.ncbi.nlm.nih.gov/gene/5788 as at 15.10.2018.*

35. *"Characterization of Podoplanin" online, available under: http://www.ncbi.nlm.nih.gov/gene/10630 as at 28.04.2018.*

36. *Chehab F, Lim M, Lu R (1996) Correction of the sterility defect in homozygous obese female mice by treatment with the human recombinant leptin. Nature Genetics. 12(3):318-320.*

37. *Chen J, Li J, Lim F, Wu Q, Douek D, Scott D, Ravussin E, Hsu H, Jazwinski S, Mountz J (2010) Maintenance of naïve CD8 T cells in nonagenarians by leptin, IGFBP3 and T3. Mechanisms of Ageing and Development. 131(1):29-37.*

38. *Chen L, Adams J, Steinman R (1978) Anatomy of germinal centers in mouse spleen, with special reference to "follicular dendritic cells". The Journal of Cell Biology. 77(1):148-164.*

39. *Chou S, Mantzoros C (2014) 20 YEARS OF LEPTIN: Role of leptin in human reproductive disorders. Journal of Endocrinology. 223(1):T49-T62.*

40. *Clark S (1962) The reticulum of lymph nodes in mice studied with the electron microscope. American Journal of Anatomy. 110(3):217-257.*

41. *Claycombe K, King L, Fraker P (2008) A role for leptin in sustaining lymphopoiesis and myelopoiesis. Proceedings of the National Academy of Sciences. 105(6):2017-2021.*

42. *Clément K, Vaisse C, Lahlou N, Cabrol S, Pelloux V, Cassuto D, Gourmelen M, Dina C, Chambaz J, Lacorte J, Basdevant A, Bougnères P, Lebouc Y, Froguel P, Guy-Grand B (1998) A mutation in the human leptin receptor gene causes obesity and pituitary dysfunction. Nature. 392(6674):398-401.*

43. *Cohen J, Guidi C, Tewalt E, Qiao H, Rouhani S, Ruddell A, Farr A, Tung K, Engelhard V (2010) Lymph node–resident lymphatic endothelial cells mediate peripheral tolerance via Aire-independent direct antigen presentation. The Journal of Experimental Medicine. 207(4):681-688.*

44. *Comerford I, Harata-Lee Y, Bunting M, Gregor C, Kara E, McColl S (2013) A myriad of functions and complex regulation of the CCR7/CCL19/CCL21 chemokine axis in the adaptive immune system. Cytokine & Growth Factor Reviews. 24(3):269-283.*

45. *Conus S, Bruno A, Simon H (2005) Leptin is an eosinophil survival factor. Journal of Allergy and Clinical Immunology. 116(6):1228-1234.*

46. *Cording S, Wahl B, Kulkarni D, Chopra H, Pezoldt J, Buettner M, Dummer A, Hadis U, Heimesaat M, Bereswill S, Falk C, Bode U, Hamann A, Fleissner D, Huehn J, Pabst O (2013) The intestinal micro-environment imprints stromal cells to promote efficient Treg induction in gut-draining lymph nodes. Mucosal Immunology. 7(2):359-368.*

47. *Cremasco V, Woodruff M, Onder L, Cupovic J, Nieves-Bonilla J, Schildberg F, Chang J, Cremasco F, Harvey C, Wucherpfennig K, Ludewig B, Carroll M, Turley S (2014) B cell homeostasis and follicle confines are governed by fibroblastic reticular cells. Nature Immunology. 15(10):973-981.*

48. *Crivellato E, Mallardi F (1997) Stromal cell organisation in the mouse lymph node. A light and electron microscopic investigation using the zinc iodide-osmium technique. Journal of Anatomy. 190(1):85-92.*

49. *Cyster J, Ansel K, Reif K, Ekland E, Hyman P, Tang H, Luther S, Ngo V (2000) Follicular stromal cells and lymphocyte homing to follicles. Immunological Reviews. 176(1):181-193.*

50. *Dalamaga M, Chou S, Shields K, Papageorgiou P, Polyzos S, Mantzoros C (2013) Leptin at the Intersection of Neuroendocrinology and Metabolism: Current Evidence and Therapeutic Perspectives. Cell Metabolism. 2013;18(1):29-42.*

51. *Dardeno T, Chou S, Moon H, Chamberland J, Fiorenza C, Mantzoros C (2010) Leptin in human physiology and therapeutics. Frontiers in Neuroendocrinology. 31(3):377-393.*

52. *Dauncey M (1986) Activity-induced thermogenesis in lean and genetically obese (ob/ob) mice. Experientia. 42(5):547-549.*

53. *Dauncey M, Brown D (1987) Role Of Activity-Induced Thermogenesis In Twenty-Four Hour Energy Expenditure Of Lean And Genetically Obese (Ob/ob) Mice. Quarterly Journal of Experimental Physiology. 72(4):549-559.*

54. *Decker M, Martinez-Morentin L, Wang G, Lee Y, Liu Q, Leslie J, Ding L (2017) Leptin-receptor-expressing bone marrow stromal cells are myofibroblasts in primary myelofibrosis. Nature Cell Biology.19(6):677-688.*

55. *Demiray G, Değirmencioğlu S, Uğurlu E, Yaren A (2017) Effects of Serum Leptin and Resistin Levels on Cancer Cachexia in Patients With Advanced-Stage Non–Small Cell Lung Cancer. Clinical Medicine Insights: Oncology. 11:117955491769014.*

56. *Dubrot J, Duraes F, Potin L, Capotosti F, Brighouse D, Suter T, LeibundGut-Landmann S, Garbi N, Reith W, Swartz M, Hugues S (2014) Lymph node stromal cells acquire peptide–MHCII complexes from dendritic cells and induce antigen-specific CD4+T cell tolerance. The Journal of Experimental Medicine. 211(6):1153-1166.*

57. *Dülger H, Alici S, Ş ekeroĞlu M, Erkog R, Özbek H, Noyan T, Yavuz M (2004) Serum levels of leptin and proinflammatory cytokines in patients with gastrointestinal cancer. International Journal of Clinical Practice. 58(6):545-549.*

58. *Eichmann A, Makinen T, Alitalo K (2005) Neural guidance molecules regulate vascular remodeling and vessel navigation. Genes & Development. 19(9):1013-1021.*

59. *Elgert K. (2009) Immunology: Understanding The Immune System. 2nd ed. Wiley-Blackwell, Hoboken.*

60. *Fei H, Okano H, Li C, Lee G, Zhao C, Darnell R, Friedman J (1997) Anatomic localization of alternatively spliced leptin receptors (Ob-R) in mouse brain and other tissues. Proceedings of the National Academy of Sciences. 94(13):7001-7005.*

61. *Fletcher A, Lukacs-Kornek V, Reynoso E, Pinner S, Bellemare-Pelletier A, Curry M, Collier A, Boyd R, Turley S (2010) Lymph node fibroblastic reticular cells directly present peripheral tissue antigen under steady-state and inflammatory conditions. The Journal of Experimental Medicine. 207(4):689-697.*

62. *Fletcher A, Malhotra D, Acton S, Lukacs-Kornek V, Bellemare-Pelletier A, Curry M, Armant M, Turley S (2011) Reproducible Isolation of Lymph Node Stromal Cells Reveals Site-Dependent Differences in Fibroblastic Reticular Cells. Frontiers in Immunology. 2:35.*

63. *Fletcher A, Malhotra D, Turley S (2011) Lymph node stroma broaden the peripheral tolerance paradigm. Trends in Immunology. 32(1):12-18.*

64. *Friedman J, Halaas J (1998) Leptin and the regulation of body weight in mammals. Nature. 395(6704):763-770.*

65. *Frühbeck G (2006) Intracellular signalling pathways activated by leptin. Biochemical Journal. 393(1):7-20.*

66. *Gabay C, Dreyer M, Pellegrinelli N, Chicheportiche R, Meier C (2001) Leptin Directly Induces the Secretion of Interleukin 1 Receptor Antagonist in Human Monocytes. The Journal of Clinical Endocrinology & Metabolism. 86(2):783-791.*

67. *Gardner J, DeVoss J, Friedman R, Wong D, Tan Y, Zhou X, Johannes K, Su M, Chang H, Krummel M, Anderson M (2008) Deletional Tolerance Mediated by Extrathymic Aire-Expressing Cells. Science. 321(5890):843-847.*

68. *Ge H, Huang L, Pourbahrami T, Li C (2002) Generation of Soluble Leptin Receptor by Ectodomain Shedding of Membrane-spanning Receptorsin Vitroandin Vivo. Journal of Biological Chemistry. 277(48):45898-45903.*

69. *Ghilardi N, Ziegler S, Wiestner A, Stoffel R, Heim M, Skoda R (1996) Defective STAT signaling by the leptin receptor in diabetic mice. Proceedings of the National Academy of Sciences. 93(13):6231-6235.*

70. *Giampaolo S, Wójcik G, Klein-Hessling S, Serfling E, Patra A (2017) NFAT-mediated defects in erythropoiesis cause anemia in Il2−/− mice. Oncotarget. 9(11):9632-9644.*

71. *Gretz J, Anderson A, Shaw S (1997) Cords, channels, corridors and conduits: critical architectural elements facilitating cell interactions in the lymph node cortex. Immunological Reviews. 156(1):11-24.*

72. *Gruen M, Hao M, Piston D, Hasty A (2007) Leptin requires canonical migratory signaling pathways for induction of monocyte and macrophage chemotaxis. American Journal of Physiology-Cell Physiology. 293(5):C1481-C1488.*

73. *Gruver A, Ventevogel M, Sempowski G (2009) Leptin receptor is expressed in thymus medulla and leptin protects against thymic remodeling during endotoxemia-induced thymus involution. Journal of Endocrinology. 203(1):75-85.*

74. *Halaas J, Boozer C, Blair-West J, Fidahusein N, Denton D, Friedman J (1997) Physiological response to long-term peripheral and central leptin infusion in lean and obese mice. Proceedings of the National Academy of Sciences. 94(16):8878-8883.*

75. *Hardie D (2003) Minireview: The AMP-Activated Protein Kinase Cascade: The Key Sensor of Cellular Energy Status. Endocrinology. 144(12):5179-5183.*

76. *Havel P (2001) Peripheral Signals Conveying Metabolic Information to the Brain: Short-Term and Long-Term Regulation of Food Intake and Energy Homeostasis. Experimental Biology and Medicine. 226(11):963-977.*

77. *Hayakawa M, Kobayashi M, Hoshino T (1988) Direct Contact between Reticular Fibers and Migratory Cells in the Paracortex of Mouse Lymph Nodes: A Morphological and Quantitative Study. Archives of Histology and Cytology. 51(3):223-240.*

78. *Hess E, Duheron V, Decossas M, Lezot F, Berdal A, Chea S, Golub R, Bosisio M, Bridal S, Choi Y, Yagita H, Mueller C (2011) RANKL Induces Organized Lymph Node Growth by Stromal Cell Proliferation. The Journal of Immunology. 188(3):1245-1254.*

79. *Hoffmann P, Hofmeister R, Brischwein K, Brandl C, Crommer S, Bargou R, Itin C, Prang N, Baeuerle P (2005) Serial killing of tumor cells by cytotoxic T cells redirected with a CD19-/CD3-bispecific single-chain antibody construct. International Journal of Cancer. 115(1):98-104.*

80. *Itano A, Jenkins M (2003) Antigen presentation to naive CD4 T cells in the lymph node. Nature Immunology. 4(8):733-739.*

81. *Itano A, McSorley S, Reinhardt R, Ehst B, Ingulli E, Rudensky A, Jenkins M (2003) Distinct Dendritic Cell Populations Sequentially Present Antigen to CD4 T Cells and Stimulate Different Aspects of Cell-Mediated Immunity. Immunity. 19(1):47-57.*

82. *Janeway CA Jr, Travers P, Walport M et al. (2001). Immunobiology: The Immune System in Health and Disease. 5th ed. Garland Science, New York.*

83. *Jung C, Kim M (2013) Molecular mechanisms of central leptin resistance in obesity. Archives of Pharmacal Research. 36(2):201-207.*

84. *Junt T, Scandella E, Ludewig B (2008) Form follows function: lymphoid tissue microarchitecture in antimicrobial immune defence. Nature Reviews Immunology. 8(10):764-775.*

85. *Khan O, Headley M, Gerard A, Wei W, Liu L, Krummel M (2011) Regulation of T Cell Priming by Lymphoid Stroma. PLoS ONE. 6(11):e26138.*

86. *Karapanagiotou E, Tsochatzis E, Dilana K, Tourkantonis I, Gratsias I, Syrigos K (2008) The significance of leptin, adiponectin, and resistin serum levels in non-small cell lung cancer (NSCLC). Lung Cancer. 61(3):391-397.*

87. *Katakai T, Hara T, Sugai M, Gonda H, Shimizu A (2004) Lymph Node Fibroblastic Reticular Cells Construct the Stromal Reticulum via Contact with Lymphocytes. The Journal of Experimental Medicine. 200(6):783-795.*

88. *Katakai T, Suto H, Sugai M, Gonda H, Togawa A, Suematsu S, Ebisuno Y, Katagiri K, Kinashi T, Shimizu A (2008) Organizer-Like Reticular Stromal Cell Layer Common to Adult Secondary Lymphoid Organs. The Journal of Immunology. 181(9):6189-6200.*

89. *Kato H, Ueki S, Kamada R, Kihara J, Yamauchi Y, Suzuki T, Takeda M, Itoga M, Chihara M, Ito W, Kayaba H, Chihara J (2011) Leptin Has a Priming Effect on Eotaxin-Induced Human Eosinophil Chemotaxis. International Archives of Allergy and Immunology. 155(4):335-344.*

90. *Kelesidis T, Kelesidis I, Chou S, Mantzoros C (2010) Narrative Review: The Role of Leptin in Human Physiology: Emerging Clinical Applications. Annals of Internal Medicine. 152(2):93.*

91. *Kelly R (1975) Functional Anatomy of Lymph Nodes. I. The Paracortical Cords. International Archives of Allergy and Immunology. 48(6):836-849.*

92. *Knight S (2008) Specialized Perinodal Fat Fuels and Fashions Immunity. Immunity. 28(2):135-138.*

93. *Koning J, Mebius R (2012) Interdependence of stromal and immune cells for lymph node function. Trends in Immunology. 33(6):264-270.*

94. *Kratzsch J, Lammert A, Bottner A, Seidel B, Mueller G, Thiery J, Hebebrand J, Kiess W (2008) Circulating Soluble Leptin Receptor and Free Leptin Index during Childhood, Puberty, and Adolescence. The Journal of Clinical Endocrinology & Metabolism. 87(10):4587-4594.*

95. *Lam Q, Wang S, Ko O, Kincade P, Lu L (2010) Leptin signaling maintains B-cell homeostasis via induction of Bcl-2 and Cyclin D1. Proceedings of the National Academy of Sciences. 107(31):13812-13817.*

96. *Lämmermann T, Sixt M (2008) The microanatomy of T-cell responses. Immunological Reviews. 221(1):26-43.*

97. *Lee G, Proenca R, Montez J, Carroll K, Darvishzadeh J, Lee J, Friedman J (1996) Abnormal splicing of the leptin receptor in diabetic mice. Nature. 379(6566):632-635.*

98. *Lee J, Epardaud M, Sun J, Becker J, Cheng A, Yonekura A, Heath J, Turley S (2006) Peripheral antigen display by lymph node stroma promotes T cell tolerance to intestinal self. Nature Immunology. 8(2):181-190.*

99. *Lertkiatmongkol P, Liao D, Mei H, Hu Y, Newman P (2016) Endothelial functions of platelet/endothelial cell adhesion molecule-1 (CD31). Current Opinion in Hematology. 23(3):253-259.*

100. *Link A, Vogt T, Favre S, Britschgi M, Acha-Orbea H, Hinz B, Cyster J, Luther S (2007) Fibroblastic reticular cells in lymph nodes regulate the homeostasis of naive T cells. Nature Immunology. 8(11):1255-1265.*

101. *Link A, Hardie D, Favre S, Britschgi M, Adams D, Sixt M, Cyster J, Buckley C, Luther S (2011) Association of T-Zone Reticular Networks and Conduits with Ectopic Lymphoid Tissues in Mice and Humans. The American Journal of Pathology. 178(4):1662-1675.*

102. *Liwski R, Gasparotto A, Bahuschewskyj C, Montagner J, Neumann J (2017) P173 The ART(EFACT) of multicolor flow cytometry. A case of mysterious CD3/CD19 double*

positive lymphocytes in the flow cytometry crossmatch (FCXM) assay. Human Immunology. 78:187.

103. *Loffreda S, Yang S, Lin H, Karp C, Brengman M, Wang D, Klein A, Bulkley G, Bao C, Noble P, Lane M, Diehl A (1998) Leptin regulates proinflammatory immune responses. The FASEB Journal. 12(1):57-65.*

104. *Lord G, Matarese G, Howard J, Baker R, Bloom S, Lechler R (1998) Leptin modulates the T-cell immune response and reverses starvation-induced immunosuppression. Nature. 394(6696):897-901.*

105. *Lord G, Matarese G, Howard J, Lechler R (2001) The Bioenergetics of the Immune System. Science. 292(5518):855-856.*

106. *Lukacs-Kornek V, Malhotra D, Fletcher A, Acton S, Elpek K, Tayalia P, Collier A, Turley S (2011) Regulated release of nitric oxide by nonhematopoietic stroma controls expansion of the activated T cell pool in lymph nodes. Nature Immunology. 12(11):1096-1104.*

107. *Lüllmann-Rauch R (2009) Taschenlehrbuch Histologie. 3rd ed. Georg Thieme Verlag KG, Stuttgart.*

108. *Luo S, Zhang D, Qin Q, Lu L, Luo M, Guo F, Shi H, Jiang L, Shao B, Li M, Yang H, Wei Y (2017) The Promotion of Erythropoiesis via the Regulation of Reactive Oxygen Species by Lactic Acid. Scientific Reports. 7:38105.*

109. *Luther S, Tang H, Hyman P, Farr A, Cyster J (2000) Coexpression of the chemokines ELC and SLC by T zone stromal cells and deletion of the ELC gene in the plt/plt mouse. Proceedings of the National Academy of Sciences. 97(23):12694-12699.*

110. *Luther S, Vogt T, Siegert S (2011) Guiding blind T cells and dendritic cells: A closer look at fibroblastic reticular cells found within lymph node T zones. Immunology Letters. 138(1):9-11.*

111. *Mabbott N, Kenneth Baillie J, Kobayashi A, Donaldson D, Ohmori H, Yoon S, Freedman A, Freeman T, Summers K (2011) Expression of mesenchyme-specific gene signatures by follicular dendritic cells: insights from the meta-analysis of microarray data from multiple mouse cell populations. Immunology. 133(4):482-498.*

112. *Macia L, Delacre M, Abboud G, Ouk T, Delanoye A, Verwaerde C, Saule P, Wolowczuk I (2006) Impairment of Dendritic Cell Functionality and Steady-State Number in Obese Mice. The Journal of Immunology. 177(9):5997-6006.*

113. *Magnusson F, Liblau R, von Boehmer H, Pittet M, Lee J, Turley S, Khazaie K (2008) Direct Presentation of Antigen by Lymph Node Stromal Cells Protects Against CD8 T-Cell-Mediated Intestinal Autoimmunity. Gastroenterology. 134(4):1028-1037.*

114. *Malhotra D, Fletcher A, Astarita J, Lukacs-Kornek V, Tayalia P, Gonzalez S, Elpek K, Chang S, Knoblich K, Hemler M, Brenner M, Carroll M, Mooney D, Turley S, Immunological Genome Project Consortium (2012) Transcriptional profiling of stroma from inflamed and resting lymph nodes defines immunological hallmarks. Nature Immunology. 3(5):499-510.*

115. *Masuzaki H, Ogawa Y, Aizawa-Abe M, Hosoda K, Suga J, Ebihara K, Satoh N, Iwai H, Inoue G, Nishimura H, Yoshimasa Y, Nakao K (1999) Glucose metabolism and insulin sensitivity in transgenic mice overexpressing leptin with lethal yellow agouti mutation: usefulness of leptin for the treatment of obesity-associated diabetes. Diabetes. 48(8):1615-1622.*

116. *Matarese G (2000) Leptin and the immune system: how nutritional status influences the immune response. European Cytokine Network. 11(1):7-14.*

117. *Mebius R (2003) Organogenesis of lymphoid tissues. Nature Reviews Immunology. 3(4):292-303.*

118. *Meier U, Gressner A (2004) Endocrine Regulation of Energy Metabolism: Review of Pathobiochemical and Clinical Chemical Aspects of Leptin, Ghrelin, Adiponectin, and Resistin. Clinical Chemistry. 50(9):1511-1525.*

119. *"FlowSight FS Measuring Immunological Synapse Using the FlowSight Imaging Flow Cytometer" by Merck KGaA, online, available under https://www.amnis.com/documents/notes/12-007-apn%20FS%20ImmuneSynapse.pdf as at 29.04.2018*

120. *Moe R (1963) Fine structure of the reticulum and sinuses of lymph nodes. American Journal of Anatomy. 112(3):311-335.*

121. *Moon H, Dalamaga M, Kim S, Polyzos S, Hamnvik O, Magkos F, Paruthi J, Mantzoros C (2013) Leptin's Role in Lipodystrophic and Nonlipodystrophic Insulin-Resistant and Diabetic Individuals. Endocrine Reviews. 34(3):377-412.*

122. *Moore S, Huffnagle G, Chen G, White E, Mancuso P (2003) Leptin Modulates Neutrophil Phagocytosis of Klebsiella pneumoniae. Infection and Immunity. 71(7):4182-4185.*

123. *Mosna F, Sensebé L, Krampera M (2010) Human Bone Marrow and Adipose Tissue Mesenchymal Stem Cells: A User's Guide. Stem Cells and Development. 19(10):1449-1470.*

124. *Mueller S, Germain R (2009) Stromal cell contributions to the homeostasis and functionality of the immune system. Nature Reviews Immunology. 9(9):618-629.*

125. *Muñoz-Fernández R, Blanco F, Frecha C, Martin F, Kimatrai M, Abadía-Molina A, Garcia-Pacheco J, Olivares E (2006) Follicular Dendritic Cells Are Related to Bone Marrow Stromal Cell Progenitors and to Myofibroblasts. The Journal of Immunology. 177(1):280-289.*

126. *Muoio D, Dohm G, Fiedorek F, Tapscott E, Coleman R (1997) Leptin Directly Alters Lipid Partitioning in Skeletal Muscle. Diabetes. 46(8):1360-1363.*

127. *Myers M, Cowley M, Münzberg H (2008) Mechanisms of Leptin Action and Leptin Resistance. Annual Review of Physiology. 70(1):537-556.*

128. *Myers M, Heymsfield S, Haft C, Kahn B, Laughlin M, Leibel R, Tschöp M, Yanovski J (2012) Challenges and Opportunities of Defining Clinical Leptin Resistance. Cell Metabolism. 15(2):150-156.*

129. *Nagel A, Möbs C, Raifer H, Wiendl H, Hertl M, Eming R (2014) CD3-Positive B Cells: A Storage-Dependent Phenomenon. PLoS ONE. 9(10):e110138.*

130. *Nichols L, Chen Y, Colella T, Bennett C, Clausen B, Engelhard V (2007) Deletional Self-Tolerance to a Melanocyte/Melanoma Antigen Derived from Tyrosinase Is Mediated by a Radio-Resistant Cell in Peripheral and Mesenteric Lymph Nodes. The Journal of Immunology. 179(2):993-1003.*

131. *Niedbala W, Cai B, Liu H, Pitman N, Chang L, Liew F (2007) Nitric oxide induces CD4+CD25+ Foxp3 regulatory T cells from CD4+CD25 T cells via p53, IL-2, and OX40. Proceedings of the National Academy of Sciences. 104(39):15478-15483.*

132. *Niedbala W, Besnard A, Jiang H, Alves-Filho J, Fukada S, Nascimento D, Mitani A, Pushparaj P, Alqahtani M, Liew F (2013) Nitric Oxide-Induced Regulatory T Cells Inhibit Th17 but Not Th1 Cell Differentiation and Function. The Journal of Immunology. 191(1):164-170.*

133. *Nolte M, Beliën J, Schadee-Eestermans I, Jansen W, Unger W, van Rooijen N, Kraal G, Mebius R (2003) A Conduit System Distributes Chemokines and Small Blood-borne Molecules through the Splenic White Pulp. The Journal of Experimental Medicine. 198(3):505-512.*

134. *Oláh I, Röhlich P, Törő I (1975) Ultrastructure of lymphoid organs: An Electron Microscopic Atlas. Lippincott, Philadelphia*

135. *Pabst R, Binns R (1989) Heterogeneity of Lymphocyte Homing Physiology: Several Mechanisms Operate in the Control of Migration to Lymphoid and Non-Lymphoid Organs In Vivo. Immunological Reviews. 108(1):83-109.*

136. *Palmer G, Aurrand-Lions M, Contassot E, Talabot-Ayer D, Ducrest-Gay D, Vesin C, Chobaz-Peclat V, Busso N, Gabay C (2006) Indirect Effects of Leptin Receptor Deficiency on Lymphocyte Populations and Immune Response in db/db Mice. The Journal of Immunology. 177(5):2899-2907.*

137. *Papathanassoglou E, El-Haschimi K, Li X, Matarese G, Strom T, Mantzoros C (2006) Leptin Receptor Expression and Signaling in Lymphocytes: Kinetics During Lymphocyte Activation, Role in Lymphocyte Survival, and Response to High Fat Diet in Mice. The Journal of Immunology. 176(12):7745-7752.*

138. *van de Pavert S, Olivier B, Goverse G, Vondenhoff M, Greuter M, Beke P, Kusser K, Höpken U, Lipp M, Niederreither K, Blomhoff R, Sitnik K, Agace W, Randall T, de Jonge W, Mebius R (2009) Chemokine CXCL13 is essential for lymph node initiation and is induced by retinoic acid and neuronal stimulation. Nature Immunology. 10(11):1193-1199.*

139. *Park H, Ahima R (2014) Leptin signaling. F1000Prime Reports. 6(73):1-8.*

140. *Paz-Filho G, Wong M, Licinio J (2011) Ten years of leptin replacement therapy. Obesity Reviews. 12(5):e315-e323.*

141. *Paz-Filho G, Mastronardi C, Licinio J (2015) Leptin treatment: Facts and expectations. Metabolism. 64(1):146-156.*

142. *Pelleymounter M, Cullen M, Baker M, Hecht R, Winters D, Boone T, Collins F (1995) Effects of the obese gene product on body weight regulation in ob/ob mice. Science. 269(5223):540-543.*

143. *Polack E, Nahmod V, Emeric-Sauval E, Bello M, Costas M, Finkielman S, Arzt E (1993) Low lymphocyte interferon-gamma production and variable proliferative response in anorexia nervosa patients. Journal of Clinical Immunology. 13(6):445-451.*

144. *Pond C (2005) Adipose tissue and the immune system. Prostaglandins, Leukotrienes and Essential Fatty Acids. 73(1):17-30.*

145. *Procaccini C, Jirillo E, Matarese G (2012) Leptin as an immunomodulator. Molecular Aspects of Medicine. 33(1):35-45.*

146. *Procaccini C, La Rocca C, Carbone F, De Rosa V, Galgani M, Matarese G (2017) Leptin as immune mediator: Interaction between neuroendocrine and immune system. Developmental & Comparative Immunology. 66:120-129.*

147. *Procaccini C, De Rosa V, Galgani M, Abanni L, Calì G, Porcellini A, Carbone F, Fontana S, Horvath T, La Cava A, Matarese G (2010) An Oscillatory Switch in mTOR Kinase Activity Sets Regulatory T Cell Responsiveness. Immunity. 33(6):929-941.*

148. *"PTPRC protein tyrosine phosphatase in mice", online, available under: https://www.ncbi.nlm.nih.gov/gene/19264 as at 07.11.2018.*

149. *Rassow J, Hauser K, Roland N, Deutzmann R (2012) Duale Reihe Biochemie. 3rd ed. Georg Thieme Verlag KG, Stuttgart.*

150. *Reilly M, Iqbal N, Schutta M, Wolfe M, Scally M, Localio A, Rader D, Kimmel S (2004) Plasma Leptin Levels Are Associated with Coronary Atherosclerosis in Type 2 Diabetes. The Journal of Clinical Endocrinology & Metabolism. 89(8):3872-3878.*

151. *Reis B, Lee K, Fanok M, Mascaraque C, Amoury M, Cohn L, Rogoz A, Dallner O, Moraes-Vieira P, Domingos A, Mucida D (2015) Leptin Receptor Signaling in T Cells Is Required for Th17 Differentiation. The Journal of Immunology. 194(11):5253-5260.*

152. *Roozendaal R, Mebius R, Kraal G (2008) The conduit system of the lymph node. International Immunology. 20(12):1483-1487.*

153. *Roozendaal R, Mebius R (2011) Stromal Cell–Immune Cell Interactions. Annual Review of Immunology. 29(1):23-43.*

154. *De Rosa V, Procaccini C, Calì G, Pirozzi G, Fontana S, Zappacosta S, La Cava A, Matarese G (2007) A Key Role of Leptin in the Control of Regulatory T Cell Proliferation. Immunity. 26(2):241-255.*

155. *Rosenbaum M, Nicolson M, Hirsch J, Heymsfield S, Gallagher D, Chu F, Leibel R (1996) Effects of gender, body composition, and menopause on plasma concentrations of leptin. The Journal of Clinical Endocrinology & Metabolism. 81(9):3424-3427.*

156. *Ruster B, Göttig S, Ludwig R, Bistrian R, Müller S, Seifried E, Gille J, Henschler R (2006) Mesenchymal stem cells display coordinated rolling and adhesion behavior on endothelial cells. Blood. 108(12):3938-3944.*

157. *Rux D, Song J, Swinehart I, Pineault K, Schlientz A, Trulik K, Goldstein S, Kozloff K, Lucas D, Wellik D (2016) Regionally Restricted Hox Function in Adult Bone Marrow Multipotent Mesenchymal Stem/Stromal Cells. Developmental Cell. 39(6):653-666.*

158. *Rydén M, Arner P (2007) Fat loss in cachexia—is there a role for adipocyte lipolysis?. Clinical Nutrition. 26(1):1-6.*

159. *Santos-Alvarez J, Goberna R, Sánchez-Margalet V (1999) Human Leptin Stimulates Proliferation and Activation of Human Circulating Monocytes. Cellular Immunology. 194(1):6-11.*

160. *Scandella E, Bolinger B, Lattmann E, Miller S, Favre S, Littman D, Finke D, Luther S, Junt T, Ludewig B (2008) Restoration of lymphoid organ integrity through the interaction of lymphoid tissue–inducer cells with stroma of the T cell zone. Nature Immunology. 9(6):667-675.*

161. *Scheller E, Song J, Dishowitz M, Soki F, Hankenson K, Krebsbach P (2010) Leptin Functions Peripherally to Regulate Differentiation of Mesenchymal Progenitor Cells. STEM CELLS. 28(6):1071-1080.*

162. *Schumann K, Lämmermann T, Bruckner M, Legler D, Polleux J, Spatz J, Schuler G, Förster R, Lutz M, Sorokin L, Sixt M (2010) Immobilized Chemokine Fields and Soluble Chemokine Gradients Cooperatively Shape Migration Patterns of Dendritic Cells. Immunity. 32(5):703-713.*

163. *Schraml B, Reis e Sousa C (2015) Defining dendritic cells. Current Opinion in Immunology. 32:13-20.*

164. *Sharma S, Juffer A (2013) An Atomistic Model for Assembly of Transmembrane Domain of T cell Receptor Complex. Journal of the American Chemical Society. 135(6):2188-2197.*

165. *Shimabukuro M, Koyama K, Chen G, Wang M, Trieu F, Lee Y, Newgard C, Unger R (1997) Direct antidiabetic effect of leptin through triglyceride depletion of tissues. Proceedings of the National Academy of Sciences. 94(9):4637-4641.*

166. *Siegert S, Huang H, Yang C, Scarpellino L, Carrie L, Essex S, Nelson P, Heikenwalder M, Acha-Orbea H, Buckley C, Marsland B, Zehn D, Luther S (2011) Fibroblastic Reticular Cells From Lymph Nodes Attenuate T Cell Expansion by Producing Nitric Oxide. PLoS ONE. 6(11):e27618.*

167. *Siegert S, Luther S (2012) Positive and negative regulation of T cell responses by fibroblastic reticular cells within paracortical regions of lymph nodes. Frontiers in Immunology. 3:285.*

168. *Sierra-Honigmann M, Nath A, Murakami C, García-Cardeña G, Papapetropoulos A, Sessa W, Madge L, Schechner J, Schwabb M, Polverini P, Flores-Riveros J (1998) Biological Action of Leptin as an Angiogenic Factor. Science. 281(5383):1683-1686.*

169. *da Silva Meirelles L, Chagastelles P, Nardi N (2011) Mesenchymal stem cells reside in virtually all post-natal organs and tissues. Journal of Cell Science. 119(11):2204-2213.*

170. *Simons J, Schols A, Campfield L, Wouters E, Saris W (1997) Plasma Concentration of Total Leptin and Human Lung-Cancer-Associated Cachexia. Clinical Science. 93(3):273-277.*

171. *Sivitz W, Walsh S, Morgan D, Thomas M, Haynes W (1997) Effects of Leptin on Insulin Sensitivity in Normal Rats. Endocrinology. 1997;138(8):3395-3401.*

172. *Sixt M, Kanazawa N, Selg M, Samson T, Roos G, Reinhardt D, Pabst R, Lutz M, Sorokin L (2005) The Conduit System Transports Soluble Antigens from the Afferent Lymph to Resident Dendritic Cells in the T Cell Area of the Lymph Node. Immunity. 22(1):19-29.*

173. *Söderberg S, Ahrén B, Jansson J, Johnson O, Hallmans G, Asplund K, Olsson T (1999) Leptin is associated with increased risk of myocardial infarction. Journal of Internal Medicine. 246(4):409-418.*

174. *Suchting S, Bicknell R, Eichmann A (2006) Neuronal clues to vascular guidance. Experimental Cell Research. 312(5):668-675.*

175. *Sudhakar M, Silambanan S, Chandran A, Prabhakaran A, Ramakrishnan R (2018) C-Reactive Protein (CRP) and Leptin Receptor in Obesity: Binding of Monomeric CRP to Leptin Receptor. Frontiers in Immunology. 9:1167.*

176. *Takada K, Jameson S (2009) Naive T cell homeostasis: from awareness of space to a sense of place. Nature Reviews Immunology. 9(12):823-832.*

177. *Tamburini B, Burchill M, Kedl R (2014) Antigen capture and archiving by lymphatic endothelial cells following vaccination or viral infection. Nature Communications. 5(1):3989.*

178. *Tanaka T, Hidaka S, Masuzaki H, Yasue S, Minokoshi Y, Ebihara K, Chusho H, Ogawa Y, Toyoda T, Sato K, Miyanaga F, Fujimoto M, Tomita T, Kusakabe T, Kobayashi N, Tanioka H, Hayashi T, Hosoda K, Yoshimatsu H, Sakata T, Nakao K (2005) Skeletal Muscle AMP-Activated Protein Kinase Phosphorylation Parallels Metabolic Phenotype in Leptin Transgenic Mice Under Dietary Modification. Diabetes. 54(8):2365-2374.*

179. *Tanaka M, Suganami T, Kim-Saijo M, Toda C, Tsuiji M, Ochi K, Kamei Y, Minokoshi Y, Ogawa Y (2011) Role of Central Leptin Signaling in the Starvation-Induced Alteration of B-Cell Development. Journal of Neuroscience. 31(23):8373-8380.*

180. *Tartaglia L, Dembski M, Weng X, Deng N, Culpepper J, Devos R, Richards G, Campfield L, Clark F, Deeds J, Muir C, Sanker S, Moriarty A, Moore K, Smutko J, Mays G, Wool E, Monroe C, Tepper R (1995) Identification and expression cloning of a leptin receptor, OB-R. Cell. 83(7):1263-1271.*

181. *Tisdale M (2002) Cachexia in cancer patients. Nature Reviews Cancer. 2(11):862-871.*

182. *"Characterization of DAPI" by Thermo Fisher Scientific, online, available under: https://www.thermofisher.com/us/en/home/life-science/cell-analysis/fluorophores/dapi-stain.html?icid=fr-dapi-main as at 15.10.2018.*

183. *"Characterization of PI" by Thermo Fisher Scientific, online, available under: https://www.thermofisher.com/us/en/home/life-science/cell-analysis/fluorophores/propidium-iodide.html as at 26.04.2018.*

184. *"Pierce™ BCA Protein Assay Kit Manual" by Thermo Fisher Scientific, online, available under: https://assets.thermofisher.com/TFS-Assets/LSG/manuals/MAN0011430_Pierce_BCA_Protein_Asy_UG.pdf as at 15.10.2018.*

185. *"Real-time PCR handbook" by Thermo Fisher Scientific, online, available under: https://www.thermofisher.com/content/dam/LifeTech/Documents/PDFs/PG1503-PJ9169-CO019861-Update-qPCR-Handbook-branding-Americas-FLR.pdf as at 15.10.2018.*

186. *"Ter119 Antibody" by Thermo Fisher Scientific, online, available under: https://www.thermofisher.com/order/genome-database/antibody/Erythroid-Cell-Marker-TER-119-Antigen-Antibody-clone-TER-119-Monoclonal/A18417 as at 28.04.2018.*

187. *Trayhurn P, Thurlby P, James W (1977) Thermogenic defect in pre-obese ob/ob mice. Nature. 266(5597):60-62.*

188. *Turley S, Fletcher A, Elpek K (2010) The stromal and haematopoietic antigen-presenting cells that reside in secondary lymphoid organs. Nature Reviews Immunology. 10(12):813-825.*

189. *Ushiki T, Ohtani O, Abe K (1995) Scanning electron microscopic studies of reticular framework in the rat mesenteric lymph node. The Anatomical Record. 241(1):113-122.*

190. *Unger R (2003) Minireview: Weapons of Lean Body Mass Destruction: The Role of Ectopic Lipids in the Metabolic Syndrome. Endocrinology. 144(12):5159-5165.*

191. *Van Vliet E, Melis M, Foidart J, Van Ewijk W (1986) Reticular fibroblasts in peripheral lymphoid organs identified by a monoclonal antibody. Journal of Histochemistry & Cytochemistry. 34(7):883-890.*

192. *Vondenhoff M, Greuter M, Goverse G, Elewaut D, Dewint P, Ware C, Hoorweg K, Kraal G, Mebius R (2009) LTbetaR Signaling Induces Cytokine Expression and Up-Regulates Lymphangiogenic Factors in Lymph Node Anlagen. The Journal of Immunology. 182(9):5439-5445.*

193. *Wallace A, McMahon A, Packard C, Kelly A, Shepherd J, Gaw A, Sattar N (2001) Plasma Leptin and the Risk of Cardiovascular Disease in the West of Scotland Coronary Prevention Study (WOSCOPS). Circulation. 104(25):3052-3056.*

194. *Weber F, Wagner V, Rasmussen S, Hartmann R, Paludan S (2006) Double-Stranded RNA Is Produced by Positive-Strand RNA Viruses and DNA Viruses but Not in Detectable Amounts by Negative-Strand RNA Viruses. Journal of Virology. 80(10):5059-5064.*

195. *Wigle J, Oliver G (1999) Prox1 Function Is Required for the Development of the Murine Lymphatic System. Cell. 98(6):769-778.*

196. *Willard-Mack, C (2006) Normal structure, function, and histology of lymph nodes. Toxicolic Pathology. 34(5): 409–424*

197. *Wolf I, Sadetzki S, Kanety H, Kundel Y, Pariente C, Epstein N, Oberman B, Catane R, Kaufman B, Shimon I (2006) Adiponectin, ghrelin, and leptin in cancer cachexia in breast and colon cancer patients. Cancer. 106(4):966-973.*

198. *Wolk R, Berger P, Lennon R, Brilakis E, Johnson B, Somers V (2004) Plasma leptin level is an important and independent predictor of prognosis in patients with established coronary atherosclerosis. Journal of the American College of Cardiology. 44(9):1819-1824.*

199. *Wong C, Cheung P, Lam C (2007) Leptin-mediated cytokine release and migration of eosinophils: Implications for immunopathophysiology of allergic inflammation. European Journal of Immunology. 37(8):2337-2348.*

200. *Woolf E, Grigorova I, Sagiv A, Grabovsky V, Feigelson S, Shulman Z, Hartmann T, Sixt M, Cyster J, Alon R (2007) Lymph node chemokines promote sustained T lymphocyte motility without triggering stable integrin adhesiveness in the absence of shear forces. Nature Immunology. 8(10):1076-1085.*

201. *Worbs T, Mempel T, Bölter J, von Andrian U, Förster R (2007) CCR7 ligands stimulate the intranodal motility of T lymphocytes in vivo. The Journal of Experimental Medicine. 204(3):489-495.*

202. *Xu Y, Elmquist J, Fukuda M (2011) Central nervous control of energy and glucose balance: focus on the central melanocortin system. Annals of the New York Academy of Sciences. 1243(1):1-14.*

203. *Yoshida H, Naito A, Inoue J, Satoh M, Santee-Cooper S, Ware C, Togawa A, Nishikawa S, Nishikawa S (2002) Different Cytokines Induce Surface Lymphotoxin-αβ on IL-7 Receptor-α Cells that Differentially Engender Lymph Nodes and Peyer's Patches. Immunity. 17(6):823-833.*

204. *Yue R, Zhou B, Shimada I, Zhao Z, Morrison S (2016) Leptin Receptor Promotes Adipogenesis and Reduces Osteogenesis by Regulating Mesenchymal Stromal Cells in Adult Bone Marrow. Cell Stem Cell. 18(6):782-796.*

205. *Zarkesh-Esfahani H, Pockley A, Wu Z, Hellewell P, Weetman A, Ross R (2004) Leptin Indirectly Activates Human Neutrophils via Induction of TNF-. The Journal of Immunology. 172(3):1809-1814.*

206. *Zeng M, Smith A, Wietgrefe S, Southern P, Schacker T, Reilly C, Estes J, Burton G, Silvestri G, Lifson J, Carlis J, Haase A (2011) Cumulative mechanisms of lymphoid tissue fibrosis and T cell depletion in HIV-1 and SIV infections. Journal of Clinical Investigation. 121(3):998-1008.*

207. *Zhou B, Yue R, Murphy M, Peyer J, Morrison S (2014) Leptin-Receptor-Expressing Mesenchymal Stromal Cells Represent the Main Source of Bone Formed by Adult Bone Marrow. Cell Stem Cell. 15(2):154-168.*

208. *"Zoom-in on LepR isoforms in homo sapiens" online, available under:* https://www.uniprot.org/uniprot/P48357#P48357-2 a*s at 02.12.2018*

209. *“Zoom-in on LepR isoforms in mus musculus” online, vailable under:* https://www.uniprot.org/uniprot/P48356 *as at 02.12.2018*

9. Publications

1. *Eckert C, Klein N, Kornek M, Lukacs-Kornek V (2015) The Complex Myeloid Network of the Liver with Diverse Functional Capacity at Steady State and in Inflammation. Frontiers in Immunology. 6:179.*

2. *Eckert C, Kim Y, Julich H, Heier E, Klein N, Krause E, Tschernig T, Kornek M, Lammert F, Schuppan D, Lukacs-Kornek V (2016) Podoplanin discriminates distinct stromal cell populations and a novel progenitor subset in the liver. American Journal of Physiology-Gastrointestinal and Liver Physiology. 310(1):G1-G12.*

3. *Heier E, Borchardt H, Julich H, Eckert C, Klein N, Tschernig T, Lukacs-Kornek V (2015) Alterations in liver dendritic cell subtypes during non-alcoholic steatohepatitis. AASLD Abstract, Hepatology 62(1):850A.*

4. *Julich H, Eckert C, Kim Y, Borchardt H, Klein N, Heier E, Tschernig T, Schuppan D, Lukacs-Kornek V (2015) GP38/PODOPLANIN marks a novel subset of progenitor cells in chronic liver injury. AASLD Abstract, Hepatology. 62(1):888A-889A.*

5. *Willms A, Müller C, Julich H, Schwab R, Schaaf S, Krawczyk M, Klein N, Lukacs-Kornek V, Schuppan D, Kornek M (2015) AnnexinV/EpCAM (CD326) Tumor associated microparticles: a novel tool for carcinoma detection and therapy monitoring. AASLD Abstract, Hepatology. 62(1):229A-230A.*

6. *Wilms A, Müller C, Julich H, Klein N, Schwab R, Richardsen I, Schaaf S, Geis C, Krawczyk M, Krawczyk M, Lammert F, Schuppan D, Lukacs-Kornek V, Kornek M (2016) Tumor-associated circulating microparticles: A novel clinical tool for screening and therapy monitoring of HCC and other epithelial neoplasia. EASL Abstract, Journal of Hepatology. 64:336-337.*

7. *Willms A, Müller C, Julich H, Klein N, Schwab R, Güsgen C, Richardsen I, Schaaf S, Krawczyk M, Krawczyk M, Lammert F, Schuppan D, Lukacs-Kornek V, Kornek M (2016) Tumour-associated circulating microparticles: a novel liquid biopsy tool for screening and therapy monitoring of colorectal carcinoma and other epithelial neoplasia. Oncotarget. 7(21):30867-30875.*

10. Acknowledgement

Zu Beginn möchte ich mich bei jun. Prof. Dr. Dr. Veronika Lukacs-Kornek und Dr. Miroslaw Kornek für die Aufnahme in ihre Arbeitsgruppe, für die Unterstützung, Expertise, Motivation und nicht zuletzt für die enorme Geduld die beide mit mir hatten bedanken. Ich habe in euch nicht nur zwei herausragende Mentoren, sondern auch gute Freunde gefunden.

Ein besonderer Dank sei an meinen besten Freund Christoph Eckert gerichtet. Du standest mir jederzeit und ohne jedes Zögern mit deinem akademischen Talent und genialen Geiste zur Seite. Ohne dich hätte ich das alles nicht geschafft!

Ein Wort des Dankes sei auch an Ann-Kathrin Hopp und Henrike Julich-Haertel für die gute Stimmung im Labor und den fachlichen Rat den ihr mir jederzeit gewährt habt gerichtet.

Für ihre Unterstützung in jeder Lebenslage möchte ich mich bei meiner Partnerin Clara Müller bedanken. Auf das noch viele schöne Jahre folgen mögen!

Auch an Frau Dr. Dalia Alansary möchte ich Worte des Dankes für die Möglichkeit zur Nutzung ihres Labors und die große Hilfe die sie mir dabei gewährt hat richten.

Vielen Dank Herr Dr. Becker für die unterhaltsame Zeit in seiner Praxis und seine (alt)klugen Ratschläge. Es war mir jederzeit eine Freude!

Ich möchte mich auch bei meiner ganzen Familie bedanken, für die Unterstützung und dafür dass sie meinen Werdegang immer aufmerksam verfolgt haben. Einen ganz besonderen Dank möchte ich mit einem Augenzwinkern an meine Eltern Gabriele und Armin Klein richten. Ihr habt keine Gelegenheit ungenutzt gelassen mich an die Fertigstellung meiner akademischen Arbeit zu erinnern.

Zu guter Letzt möchte ich mich bei Oma und Opa bedanken die mich stets ohne die Frage nach dem Warum unterstützt haben. Ich wünschte mir, dass ich auch Opa diese Arbeit hätte zeigen können. Du wirst mir immer fehlen.